

**MICROWAVE-ASSISTED SIMULTANEOUS NOVEL SYNTHESIS OF
POLY(DIBROMOPHENYLENE OXIDE)S, POLY(DIIODOPHENYLENE
OXIDE)S (P), CONDUCTING(CP) AND/OR CROSSLINKED (CLP)
AND/OR RADICAL ION POLYMERS (RIP)**

**A THESIS SUBMITTED TO
THE GRADUATE SCHOOL OF NATURAL AND APPLIED SCIENCES
OF
MIDDLE EAST TECHNICAL UNIVERSITY**

BY

GÜLER (BAYRAKLI) ÇELİK

**IN PARTIAL FULFILLMENT OF THE REQUIREMENTS
FOR
THE DEGREE OF DOCTOR OF PHILOSOPHY
IN
CHEMISTRY**

MARCH 2007

Approval of the Graduate School of Natural and Applied Sciences

Prof.Dr. Canan Özgen
Director

I certify that this thesis satisfies all the requirements as a thesis for the degree of
Doctor of Philosophy.

Prof.Dr. Ahmet M. Önal
Head of Department

This is to certify that we have read this thesis and that in our opinion it is fully
adequate, in scope and quality, as a thesis for the degree of Doctor of
Philosophy.

Prof.Dr. Duygu Kısakürek
Supervisor

Examining Committee Members

Prof. Dr. Leyla Aras (METU,CHEM) _____

Prof. Dr. Duygu Kısakürek (METU,CHEM) _____

Prof. Dr. Ahmet M. Önal (METU CHEM) _____

Prof. Dr. Ali Usanmaz (METU,CHEM) _____

Prof. Dr. Halil İbrahim Ünal (Gazi Unv.,CHEM) _____

I hereby declare that all information in this document has been obtained and presented in accordance with academic rules and ethical conduct. I also declare that, as required by these rules and conduct, I have fully cited and referenced all material and results that are not original to this work.

Name, Last name : Güler (Bayraklı) Çelik

Signature :

ABSTRACT

MICROWAVE-ASSISTED SIMULTANEOUS NOVEL SYNTHESIS OF POLY(DIBROMOPHENYLENE OXIDE)S, POLY(DIIODOPHENYLENE OXIDE)S (P), CONDUCTING(CP) AND/OR CROSSLINKED (CLP) AND/OR RADICAL ION POLYMERS (RIP)

ÇELİK, (BAYRAKLI) Güler

PhD., Department of Chemistry

Supervisor: Prof. Dr. Duygu KISAKÜREK

March 2007, 132 pages

Microwave-assisted novel synthesis of poly(dibromophenylene oxide) or poly(diiodophenylene oxide) (**P**), conducting polymer (**CP**) and/or crosslinked polymer (**CLP**) and/or radical ion polymer (**RIP**) were achieved simultaneously from lithium, sodium or potassium 2,4,6-bromophenolate or sodium 2,4,6-iodophenolate in a very short time interval.

Polymerizations were carried out by constant microwave energy with different time intervals varying from 1 to 20 min; or at constant time intervals with variation of microwave energy from 70 to 900 watt; or varying the water content from 0.5 to 5 ml at constant time intervals and microwave energy. Poly(dihalophenylene oxide) and radical ion polymers were characterized by FTIR (Fourier Transform Infrared), ¹H-NMR (Proton Nuclear Magnetic Resonance), ¹³C-NMR (Carbon-13 Nuclear Magnetic Resonance), TGA/ FTIR (Thermal Gravimetric Analysis / Fourier Transform Infrared), DSC (Differential

Scanning Calorimeter), SEM (Scanning Electron Microscope), ESR (Electron Spin Resonance), GPC (Gel Permeation Chromatography), UV-Vis (UV-Visible Spectroscopy), Light Scattering and Elemental Analysis. Conducting and crosslinked polymers were characterized by FTIR, TGA/ FTIR, DSC, SEM, ESR, XRD (Powder Diffraction X-Ray) and Elemental Analysis.

The effects of heating time, microwave energy and water content on the percent conversion and the polymer synthesis were also investigated.

Keywords: Microwave-assisted polymerization; poly(dihalophenylene oxide); conducting polymer; crosslinked polymer; radical ion polymer.

ÖZ

**POLİ(DİBROMOFENİLEN OKSİT), POLİ(DİİYODOFENİLEN OKSİT)
(P), İLETKEN (CP) VE/VEYA ÇAPRAZ BAĞLI (CLP) VE/VEYA İYON
RADİKAL POLİMERLERİN (RIP) İLK KEZ EŞ ZAMANLI
MİKRODALGA-DESTEKLİ SENTEZİ**

ÇELİK, (BAYRAKLI) Güler

Doktora, Kimya Bölümü

Tez Yöneticisi: Prof. Dr. Duygu KISAKÜREK

Mart 2007, 132 sayfa

2,4,6-tribromofenol veya 2,4,6-triiyodofenol ile poli(dibromofenilen oksit) veya poli(diiyodofenilen oksit) (**P**), iletken polimer (**CP**) ve/veya iyon radikal polimer (**RIP**) ve/veya çapraz bağlı (**CLP**) polimerlerin mikrodalga-destekli sentezi ilk defa eş zamanlı olarak kısa zaman aralığında gerçekleştirildi.

Polimerleşmeler 1 ile 20 dakika arasında değişen zaman aralıklarında, sabit mikrodalga enerjisinde veya 70 ile 900 watt arasında değişen mikrodalga enerjilerinde, sabit zaman aralıklarında veya 0.5 ile 5 ml su miktarları değiştirilerek, sabit zamanda ve mikrodalga enerjisinde yapıldı. Sentezlenen polimerlerden, Poli(dihalofenilen oksit) ve radikal iyon polimerleri FTIR (Fourier Transform Infrared Spektroskopisi), ¹H-NMR (Nükleer Manyetik Rezonans), ¹³C-NMR, TGA/ FTIR (Termogravimetrik Analiz / Fourier Transform Infrared), DSC (Diferansiyel Taramalı Kalorimetri), SEM (Taramalı

Elektron Mikroskop), ESR (Elektron Spin Rezonans), GPC (Jel Geirgen Kromatografisi), UV-Vis (UV-Görünür Bölge Spektroskopisi), Işık Saılması ve Elementel Analiz ile karakterize edilmiştir . İletken ve apraz baėlı polimerler FTIR, TGA/ FTIR, DSC, SEM, ESR, XRD (Toz X-ışınları Kırınımı Spektroskopisi), Elementel Analiz ve İletkenlik Ölçümü ile karakterize edilmiştir.

Isıtma süresinin, mikrodalga enerjisinin ve kullanılan su miktarının yüzde dönüşüm ve polimer sentezine olan etkisinde incelenmiştir.

Anahtar Kelimeler: Mikrodalga-destekli polimerizasyon; poli(dihalofenilen oksit), iletken polimer, apraz baėlı polimer, iyon radikal polimer.

TO MY FAMILY

ACKNOWLEDGEMENTS

I would like to express my sincere gratitude and respect to my supervisors Prof. Dr. Duygu KISAKÜREK for her continuous support, encouragement, and valuable suggestions in every step of my study.

I would like to express my special thanks to all my research group friends Elif GÜNGÖR, Binnur ÖZKAN and Leyla MOLU for their support during the days of my hard study.

I would like to thank to Dr. Ömer Kantođlu for his help and valuable discussions.

My special thanks go my husband Cihan ÇELİK for his patient love endless support and for not leaving me alone in my stressful days. Also great thanks to my daughter Begüm Naz ÇELİK for her patience and understanding my frequent absences. Without them this work could not be accomplished.

I should thank to Sabit, Gönül, İbrahim, Songül and İpek BAYRAKLI for their endless support in every step of my education. Words are incapable to express my appreciation to them.

TABLE OF CONTENTS

ABSTRACT	iv
ÖZ	vi
ACKNOWLEDGEMENTS	ix
TABLE OF CONTENTS	x
LIST OF TABLES	xii
LIST OF FIGURES	xiii
ABBREVIATIONS	xvii

CHAPTER

1 INTRODUCTION	1
1.1 Microwave-assisted Polymerization	1
1.1.1 Nature of Microwave Radiation	1
1.1.2 Microwave Techniques Applied to Chemical Transformations	3
1.1.3 Synthesis and Processing Under Microwave Conditions	5
1.2 Phenols	8
1.3 Poly(phenylene oxide)s	11
1.3.1 Poly(phenylene oxide) Synthesis	11
1.3.2 History of poly(phenylene oxide)s	13
1.4 Conducting Polymer	17
1.4.1 History of Conducting Polymers	18
1.4.2 Conductivity	20
1.4.3 Band Theory	21
1.4.4 Solitons, Polarons and Bipolarons	23
1.4.5 Doping Process	25
1.4.6 Hopping Process	25

1.4.7 Synthesis of Conducting Polymers	26
1.4.8 Applications of Conducting Polymers	27
1.5 Crosslinked Polymers	29
1.5.1 Crosslinking Mechanism	29
1.5.2 Formation of Network Structure	33
1.6 Aim of the Study	34
2. EXPERIMENTAL	35
2.1 Chemicals	35
2.2 Apparatus and Instruments	37
2.3 Procedure	42
2.3.1 Synthesis of Polymers	42
2.3.2 Characterization of the Polymers	43
3. RESULTS AND DISCUSSION	44
3.1 Synthesis of Polymer with TBP and NaOH.....	45
3.1.1 Characterization.....	48
3.2 Synthesis of Polymer with TBP and LiOH	68
3.2.1 Characterization	70
3.3 Synthesis of Polymer with TBP and KOH	86
3.3.1 Characterization	88
3.4 Synthesis of Polymer with TIP and NaOH	101
3.4.1 Characterization	103
4. CONCLUSIONS	113
REFERENCES	117
APPENDIX A	124
VITA	133

LIST OF TABLES

TABLES

3.1.1	The effect of polymerization time, energy and amount of water (w) on the % P , CP and WL (TBP and NaOH).....	47
3.1.2	Elemental analysis results of P , RIP , CLP and CP (TBP and NaOH).....	48
3.2.1	The effect of polymerization time, energy and amount of water (w) on the % P and CP (TBP and LiOH).....	69
3.2.2	Elemental analysis results of P and CP (TBP and LiOH).....	70
3.3.1	The effect of polymerization time, energy and amount of water (w) on the % P and CP (TBP and KOH).....	87
3.3.2	Elemental analysis results of P and CP (TBP and KOH).....	88
3.4.1	The effect of polymerization time, energy and amount of water (w) on the % P , CP and WL synthesis (TIP and NaOH).....	102
3.4.2	Elemental analysis results of P , RIP and CP (TIP and NaOH).....	103
3.4.3	Summary Results of Experiments.....	112

LIST OF FIGURES

FIGURES

1.1	Dipolar molecules which try to align with an oscillating electric field.....	2
1.2	Charged particles in a solution.....	3
1.3	The oxidation products of phenols.....	10
1.4	Possible structures of poly (halogenated phenylene oxide)s (a) 1,4-addition (b) 1,2-addition (c) both 1,4-and 1,2-addition	12
1.5	Oxidative coupling reactions of phenols (a) Carbon-oxygen coupling, poly(phenylene oxide)s, (b) Carbon-carbon coupling, diphenoquinone.....	14
1.6	Conductivity diagram of some conjugated polymers.....	21
1.7	Schematic representation of the band structure of an insulator, semiconductor, and a metal	22
1.8	The structure of a polaron and bipolaron in polyphenylene	24
1.9	Mechanism of Cross-linking	30
1.10	Cross-linked Structure	31
2.1	Four-probe conductivity measurement set up.....	42
3.1.1	FTIR spectrum of (a) P , (b) RIP , (c) CLP , (d) CP and (e) released gases during polymerization (TBP and NaOH).....	50
3.1.2	DSC thermograms of (a) P , (b) CP , (c) RIP and (d) CLP (TBP and NaOH).....	51
3.1.3	TGA thermograms of P (TBP and NaOH)	54

3.1.4	TGA thermograms of RIP (TBP and NaOH).....	54
3.1.5	TGA thermograms of CP (TBP and NaOH)	55
3.1.6	TGA thermograms of CLP (TBP and NaOH)	55
3.1.7	¹ H-NMR spectrum of (a) P and (b) RIP (TBP and NaOH).....	57
3.1.8	Proton-decoupled ¹³ C-NMR spectra of P (TBP and NaOH).....	58
3.1.9	¹³ C-NMR proton shift data of P (TBP and NaOH)	59
3.1.10	X-ray powder diffraction spectrum of (a) unwashed CP and (b) washed CP (TBP and NaOH)	61
3.1.11	ESR spectrum of (a) RIP , (b) CLP and (c) CP at room temperature (TBP and NaOH)	63
3.1.12	UV-Vis spectrum of (a) TBP , (b) P and (c) RIP and (d) soluble part of CLP at room temperature (TBP and NaOH).....	64
3.1.13	SEM micrographs of (a) P at 70 watt, 5min, (b) CP at 70 watt, 5 min, (c) CP at 100 watt (d and e) CP at 350 watt and (f) CP at 700 watt, 1 min in 0.5 ml water (TBP and NaOH).....	66
3.1.14	SEM micrographs of (a, b and c) CP at 70 watt, 5min in 0.5 ml water, (d) CLP at 350 watt and (e) RIP at 700 watt, 1 min in 5 ml water (TBP and NaOH)	67
3.2.1	FTIR spectrum of (a) P , (b) CLP , (c) CP and (d) released gases during polymerization (TBP and LiOH)	72
3.2.2	DSC thermograms of (a) P , (b) CLP and (c) CP (TBP and LiOH)...	73
3.2.3	TGA thermograms of (a) P , (b) CLP and (c) CP (TBP and LiOH) ..	76
3.2.4	¹ H-NMR spectrum of (a) P and (b) RIP (TBP and LiOH).....	77
3.2.5	Proton-decoupled ¹³ C-NMR spectrum of (a) P and (b) RIP (TBP and LiOH)	78

3.2.6	X-ray powder diffraction spectrum of (a) unwashed CP and (b) washed CP (TBP and LiOH)	80
3.2.7	ESR Spectrum of (a) CLP and (b) CP at room temperature (TBP and LiOH)	81
3.2.8	UV-Vis spectrum of (a) P and (b) CLP at room temperature (TBP and LiOH)	82
3.2.9	SEM micrographs of (a) Unwashed P (b) Washed P (c) Unwashed CLP (d, e and f) Washed CLP (g) Unwashed CP (h) Washed CP (TBP and LiOH)	85
3.3.1	FTIR spectrum of (a) P , (b) RIP , (c) CP and (d) evolved gases during polymerization (TBP and KOH).....	89
3.3.2	DSC thermograms of (a) P , (b) RIP and (d) CP (TBP and KOH)	90
3.3.3	TGA thermograms of (a) P (b) RIP and (c) CP (TBP and KOH).....	93
3.3.4	¹ H-NMR spectrum of (a) P and (b) RIP (TBP and KOH).....	94
3.3.5	Proton-decoupled ¹³ C-NMR spectrum of (a) P and (b) RIP (TBP and KOH).....	95
3.3.6	X-ray powder diffraction spectra of (a) unwashed CP and (b) washed CP (TBP and KOH)	96
3.3.7	ESR Spectrum of (a) RIP and (b) CP at room temperature (TBP and KOH).....	98
3.3.8	SEM micrographs of (a) P (b) RIP and (c and d) CP (TBP and KOH)	100
3.4.1	FTIR spectra of (a) P and (b) CP (TIP and NaOH)	104
3.4.2	DSC thermograms of (a) P and (b) CP (TIP and NaOH).....	105
3.4.3	TGA thermograms of (a) P and (b) CP (TIP and NaOH)	106
3.4.4	¹ H-NMR spectrum of P (TIP and NaOH)	108

3.4.5	Proton-decoupled ^{13}C -NMR spectrum of P (TIP and NaOH).....	108
3.4.6	X-ray powder diffraction spectra of CP (TIP and NaOH).....	109
3.4.7	ESR Spectrum of (a) CP at room temperature (TIP and NaOH)	109
3.4.8	SEM micrographs of (a) P and (b, c, d, e) CP (TIP and NaOH)	111
A 1.	In situ FTIR spectrum of evolved volatile components during TGA of P synthesized from sodium 2,4,6-tribromophenolate at (a) 177 °C (b) 497 °C (c) 629 °C (d) 707 °C (e) 805 °C (TBP and NaOH).....	126
A 2.	In situ FTIR spectrum of evolved volatile components during TGA of RIP synthesized from sodium 2,4,6-tribromophenolate at (a) 156 °C (b) 493 °C (c) 594 °C (d) 803 °C (TBP and LiOH)	128
A 3.	In situ FTIR spectrum of evolved volatile components during TGA of CP synthesized from sodium 2,4,6-tribromophenolate at (a) 185 °C (b) 421 °C (c) 664 °C (d) 803 °C (TBP and KOH)	130
A 4.	In situ FTIR spectrum of evolved volatile components during TGA of CLP synthesized from sodium 2,4,6-tribromophenolate at (b) 45 °C (c) 397 °C (d) 562 °C (e) 767 °C (TIP and NaOH)	132

ABBREVIATIONS

- TBP:** Tribromophenol
- TIP:** Triiodophenol
- P:** Poly(dihalophenylene oxide)
- CP:** Conducting Polymer
- RIP:** Radical Ion Polymer
- CLP:** Crosslinked Polymer
- DSC:** Differential Scanning Calorimeter
- TGA:** Thermal Gravimetric Analysis
- NMR:** Nuclear Magnetic Resonance
- FTIR:** Fourier Transform Infrared
- SEM:** Scanning Electron Microscope
- VB:** Valance Band
- CB:** Conduction Band

CHAPTER 1

INTRODUCTION

1.1.Microwave-assisted Polymerization

1.1.1. Nature of Microwave Radiation

In the electromagnetic spectrum, the microwave radiation region is located between infrared radiation and radio waves. Microwaves have wavelengths of 1 mm – 1 m, corresponding to frequencies between 0.3 and 300 GHz [1]. Telecommunication and microwave radar equipment occupy many of the band frequencies in this region. In general, in order to avoid interference, the wavelength at which industrial and domestic microwave apparatus intended for heating operates is regulated to 12.2 cm, corresponding to a frequency of 2.450 (± 0.050) GHz, but other frequency allocations do exist. It has been known for a long time that microwaves can be used to heat materials. In fact, the development of microwave ovens for the heating of food has more than a 50-year history [2].

In microwave oven, a magnetron converts ordinary electrical energy into microwaves, just like radio and television waves, but have shorter wavelengths

and higher frequencies. The absorbed microwave energy causes dipolar molecules to rotate at the rate of 2.45 billion cycles per second [3].

When a piece of material is exposed to microwave irradiation, microwaves can be reflected from its surface (when the surface is conducting as in metals, graphite, etc.), can penetrate the material without absorption (in the case of good insulators), and can be absorbed by the material. Thus, heating in microwave ovens is based upon the ability of some liquids and solids to absorb and to transform electromagnetic energy into heat. Microwave radiation, as every radiation of electromagnetic nature, consists of two components: magnetic and electric fields. The electric field component is responsible for dielectric heating mechanisms since it can cause molecular motion either by migration of ionic species (conduction mechanism) or rotation of dipolar species (dipolar polarization mechanism) [4]. In order to understand working principle, it is necessary to comprehend the underlying mechanisms of microwave dielectric heating.

One of the interactions of the electric field component with the matrix is called the dipolar polarization mechanism. For a substance to generate heat when irradiated with microwaves it must possess a dipole moment, as has a water molecule. A dipole is sensitive to external electric fields and will attempt to align itself with the field by rotation (Figure 1.1).



Figure 1.1 Dipolar molecules which try to align with an oscillating electric field.

The second major interaction of the electric field component with the sample is the conduction mechanism. A solution containing ions, or even a single isolated ion with a hydrogen bonded cluster, in the sample the ions will move through the solution under the influence of an electric field, resulting in expenditure of energy due to an increased collision rate, converting the kinetic energy to heat. Charged particles in a solution will follow the applied electric field (Figure 1.2).



Figure 1.2 Charged particles in a solution.

1.1.2 Microwave Techniques Applied to Chemical Transformations

The simplest method for conducting microwave-assisted reactions involves irradiation of reactants in an open vessel. Such a method, termed “microwave-organic reaction enhancement (MORE)”, was developed by Bose et al. [5]. During the reaction, reactants are heated by microwave irradiation in polar, high boiling solvents so that the temperature of reaction mixture does not reach the boiling point of a solvent. Despite the convenience, a disadvantage of

the MORE technique consists in limitation to high boiling polar solvents such as DMSO, DMF etc. The approach has been adapted to lower-boiling solvents (e.g. toluene), but it generates a potentially serious fire hazard.

For reaction at reflux, domestic microwave ovens have been modified by making a shielded opening to prevent leakage, and through which the reaction vessel has been connected to condenser and spectroscopic analyzer [6].

The pressurized conditions for microwave reactions first reported by the groups of Gedye [7] and Giguere [8] have also been developed. Gedye et al. used a domestic microwave oven, commercially available screw-up pressure vessels made of PET and PTFE (both being microwave transparent). The “bomb” strategy has been successfully applied to a number of syntheses, but it always generates a risk of hazardous explosions. Recently, Majetich and Hicks [9] reported 45 different reactions with a commercial microwave oven and PET vessels designed for acid digestion.

Microwave heating has been proven to be of benefit particularly for the reactions under “dry” media in open vessel system (i.e., in the absence of a solvent, on solid support with or without catalyst) [2]. Reactions under “dry” conditions were originally developed in the late 1980s, but solventless systems under microwave irradiation offer several advantages. The absence of solvent reduces the risk of explosions when the reaction takes place in a closed vessel. Moreover aprotic dipolar solvents with high boiling points are expensive and difficult to remove from the reaction mixtures. During microwave induction of reactions under dry conditions, the reactants adsorbed on the surface of alumina, silica gel, clay and other mineral supports absorb microwaves whereas the support does not, and the transmission of microwave is not restricted. Consequently, supported reagents efficiently induce reactions under safe and simple conditions with domestic microwave ovens instead of expensive specialized commercial microwave systems.

1.1.3. Synthesis and Processing Under Microwave Conditions

The application of microwave energy using a commercial domestic oven to organic synthesis has begun in the mid-1980s. As an alternative to conventional heating techniques, microwave irradiation provides an effective and fast synthetic method by heating molecules directly through the interaction between the microwave energy and molecular dipole moments of the starting materials. This in situ mode of energy conversion has many attractions to the chemists, because its magnitude depends on the properties of the molecules. This allows some control of the materials' properties and may lead to selectivity of the reaction [10-12].

Microwave irradiation is a rapid way of heating materials for domestic, industrial and medical purposes. Microwaves offer a number of advantages over conventional heating such as non-contact heating (reduction of overheating of material surfaces), energy transfer instead of heat transfer (penetrative radiation), material selective and volumetric heating, fast start-up and stopping, and, last but not least, reverse thermal effect, i.e., heat starts from the interior of material body. In the last few years there has been a growing interest in the use of microwave heating in organic synthesis [6 and 13-14]. Most microwave-assisted reactions in organic and polymer synthesis have been carried out in household microwave ovens; however, more recently, the use of microwave reactors for chemical synthesis has become more advocated. The main advantage of household microwave ovens is their low cost and possibility to adjust such ovens to chemical synthesis by drilling shielded outlets in the oven walls for assembling appropriate elements like an upright condenser, stirrer, dropping funnel etc. The disadvantage is a pulsating-mode duty cycle- adjustable power regulation in such cheap microwave ovens in which variable power is always obtained by switching the magnetron off and on. Specialized microwave reactors for chemical synthesis are commercially available which are mostly adjusted

from microwave systems for digestion and ashing of analytical samples. They are equipped with built-in magnetic stirrers and direct temperature control by means of shielded thermocouple or fiber-optical temperature sensor, and continuous power feedback control, which enable one to heat reaction mixture to a desired temperature without thermal runaways. In some cases, it is possible to work under reduced pressure or in pressurized conditions within cavity or reaction vessels.

A large number of reactions, both organic and inorganic, undergo an immense increase in reaction speed under microwave irradiation compared with conventional heating. Apart from this main advantage, significant improvements in yield and selectivity have been observed as a consequence of the fast and direct heating of the reactants themselves. Furthermore, high-pressure synthesis is easily accessible for reactions performed in closed vessels, facilitating the use of low boiling solvents and thereby paving the way to environmentally benign reaction conditions [15]. In the field of polymeric materials, in particular, microwave heating has shown a great potential, still far from being extensively used as it could, for accelerated industrial processing of the entire variety of commercial (both commodity and high-performance) plastics, rubbers, thermosetting resins and related composites [16]. The microwave polymerization technique provides a new way for production of polymers at high rates and conversions [17].

The short reaction times and expanded reaction range that is offered by microwave assisted organic synthesis are suited to the increased demands in industry. In particular, there is a requirement in the pharmaceutical industry for a higher number of novel chemical entities to be produced, which requires chemists to employ a number of resources to reduce the time for the production of compounds. Chemistry databases, software for diversity selection, on-line chemical ordering systems, open-access and high throughput systems for analysis and high-speed, parallel and combinatorial synthesis equipment have all contributed in increasing the throughput. The common factors for these technical

resources are automation and computer-aided control. They do not, however, speed up the chemistry itself. Developments in the chemistry have generally been concerned with novel highly reactive reagents in solution or on solid supports. In general, most organic reactions have been heated using traditional heat transfer equipment such as oil baths, sand baths and heating jackets. These heating techniques are, however, rather slow and a temperature gradient can develop within the sample. In addition, local overheating can lead to product, substrate and reagent decomposition. In contrast, in microwave dielectric heating, the microwave energy is introduced into the chemical reactor remotely and direct access by the energy source to the reaction vessel is obtained. The microwave radiation passes through the walls of the vessel and heats only the reactants and solvent, not the reaction vessel itself. If the apparatus is properly designed, the temperature increase will be uniform throughout the sample, which can lead to less by-products and/or decomposition products. In pressurized systems, it is possible to rapidly increase the temperature far above the conventional boiling point of the solvent used.

In conclusion, polymer synthesis as well as processing can greatly benefit from the unique feature offered by modern microwave technology, which was demonstrated in many successful laboratory-scale applications. These can include such technical issues as shorter processing time, increased process yield, and temperature uniformity during polymerization and crosslinking. Although microwave energy is more expensive than electrical energy due to the low conversion efficiency from electrical energy (50% for 2.45 GHz and 85% for 915 MHz), efficiency of microwave heating is often much higher than conventional heating and more than compensates for the higher energy cost.

The action of microwave irradiation on chemical reactions is still under debate, and some research groups have mentioned the existence of so-called non-thermal microwave effects, i.e., inadequate to the observed reaction temperatures' sudden acceleration of reaction rates [18]. Regardless of the type of activation (thermal) or kind of microwave effects (non-thermal), microwave

energy has its own advantages which are still waiting to be understood fully and applied to chemical processes.

1.2. Phenols

Compounds that have a hydroxyl group directly attached to a benzene ring are called Phenols [19]. They are colorless solids or liquids at 25°C and the presence of hydroxyl group in the molecules of phenols, like alcohols, enables to form strong intermolecular hydrogen bonds. This hydrogen bonding causes phenols to have higher boiling points, melting points and densities than hydrocarbons of the same molecular weight [20]. They are distinguished from alcohols by their weak acidic character because of the resonance effect of hydroxyl group and which is enhanced by substitution of the negative groups as halides or nitro group on the ring and reduced by substitution of the alkyl groups.

Sterically hindered phenols have little or no acidic character. The ability to form strong hydrogen bonds to molecules of water confers on phenols a modest solubility in water [21]. They are also soluble in polar solvents like lower alcohols, ketones, esters, pyridine, etc., but have very limited solubility in nonpolar aliphatic hydrocarbons.

A variety of synthetic polymers can be formed from phenols by reactions at the ortho- and para- positions on the aromatic nucleus and by reaction with hydroxyl group. The phenol molecule has four active sites for reaction and a combination of C-C or C-O coupling reactions or oxygenation reactions where the coupling occurs fastest at the position of highest density of free electrons, except where there is steric hindrance [21].

A variety of synthetic polymers, one of which is polyether, can be formed from phenols by the reactions at three active positions on the aromatic nucleus, namely ortho- and para- and by the reactions with hydroxyl group, powerful activating group and ortho- para- director.

The oxidation of phenols by using a catalyst can result in a variety of products, via proper choice of catalyst, solvent and phenol [22]. For example; tetraalkyldiphenquinones (1), polyphenylene ethers (2) and o-benzoquinone (3) can be prepared from catalyzed auto oxidation of phenol by using different copper salts and amines (Figure 1.3).

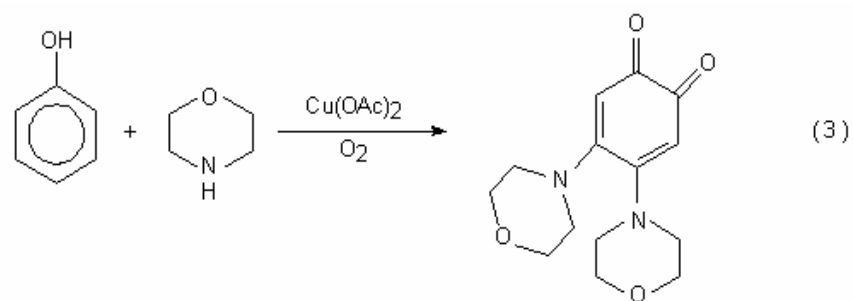
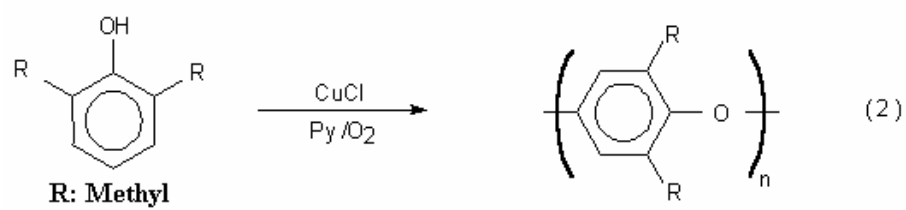
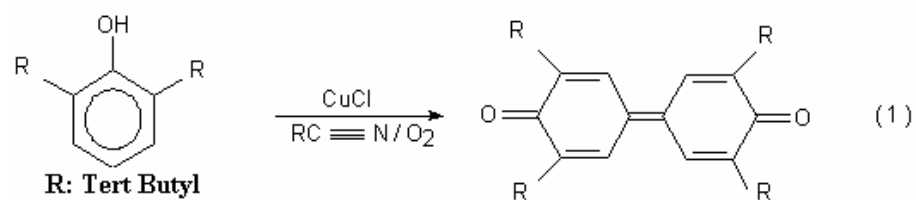


Figure 1.3 The oxidation products of phenols

1.3. Poly(phenylene oxide)s

The discovery of oxidative polymerization of phenols to poly(phenylene oxide)s, permitted the development of an entirely new family of engineering polymers [19]. They are polyether having aromatic groups connected by an oxygen linkage at the backbone. Poly(phenylene oxide)s had been synthesized in various forms since 1916 because of their mechanical, chemical and thermal properties. The largest commercial usage of poly(phenylene oxide)s is in Noryl (General Electric Co.) engineering resin, which are alloys of poly(2,6-dimethyl-1,4-phenylene ether) [23]. Attachment of halogen atoms to the phenyl ring results in poly(halogenated phenylene oxide)s with flame-retarding property in addition to high T_g values. 2,4,6-trihalophenols can be converted to poly(dihalophenylene oxide)s by a reaction that resembles free-radical initiated displacement polymerization.

1.3.1. Poly(phenylene oxide) Synthesis

Poly(dihalophenylene oxide)s can be linear or branched, amorphous or crystalline and have high or low molecular weight depending on the type and the position of the substituent on the starting phenol [24]. Ether linkage is either at ortho- or para- position or both. When it is at para- position the polymer is called poly(1,4-phenylene oxide) (Figure 1.4a) and when it is at ortho-position it is called (1,2-phenylene oxide) (Figure 1.4b) and 1,4 and 1,2 additions may take place at the same monomeric unit (Figure 1.4c).

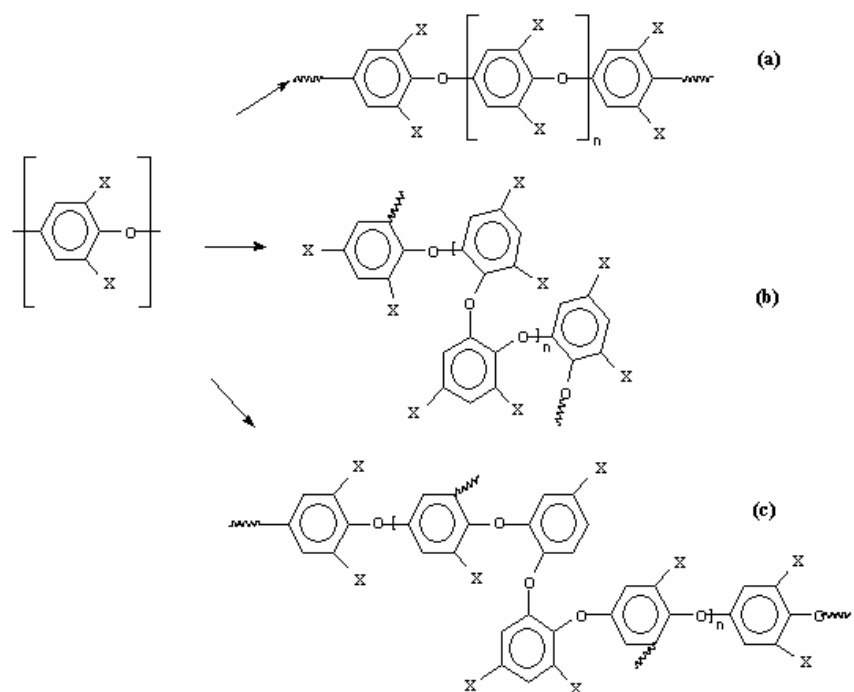
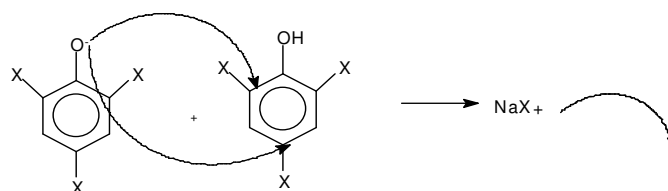
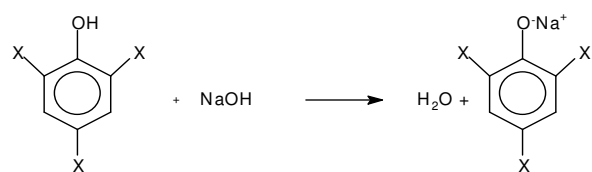
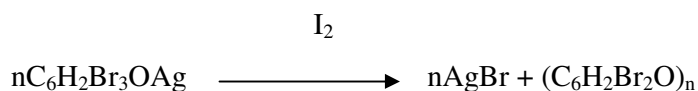


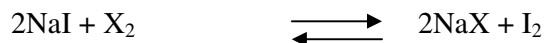
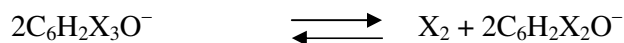
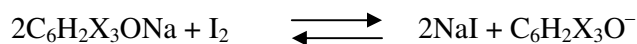
Figure 1.4 Possible structures of poly(halogenated phenylene oxide)s (X: Cl, Br, I) 1,4-addition (b) 1,2-addition (c) both 1,4- and 1,2-addition

1.3.2. History of poly(phenylene oxide)s

In 1916 Hunter [25] was the first to prepare poly(phenylene oxide)s by the ethyl iodide-induced decomposition of anhydrous silver 2,4,6 – tribromophenoxide. The synthesis was achieved from the decomposition of the silver salts or trihalogenated phenols in the presence of ethyl iodide in hot benzene. The polymer is isolated as a white, amorphous powder with a softening point above 300 °C.



In 1917 Hunter reported in a series of papers the polymerization of other trihalophenols and established that iodine was displaced more readily than bromine and the latter more rapidly than chlorine. The p-halogen reacted more readily than the o-chlorine group and only halogen with a free ionizable phenolic group could be displaced [26]. The action of the iodine on polymerization was also investigated by Hunter et. al. [27]. They proposed the following reactions to clear up the effect of iodine:



Where X: halogen

In 1932, Hunter and Dahlen reported that only the halogen in the hydroxyl – bearing nucleus could be displaced in the catalytic decomposition of metallic salts of halogenated phenols [28].

In 1959, Staffin and Price, studied the polymerization of 4-bromo-2,6-disubstituted phenol with several oxidizing agents such as ferricyanide, PbO_2 , I_2 , O_2 and light. They proposed a radicalic mechanism for the polymerization by displacement of bromine by phenoxy radical at the propagation step [29].

Depending on the reaction conditions, two free radicals can undergo oxidative coupling in a variety of ways leading to the formation of carbon-carbon or carbon-oxygen bonds [30] (Figure 1.5). The coupling positions show that a free phenoxy radical is reactive only on oxygen, ortho and para carbon atoms that symbolize the high density of free electrons.

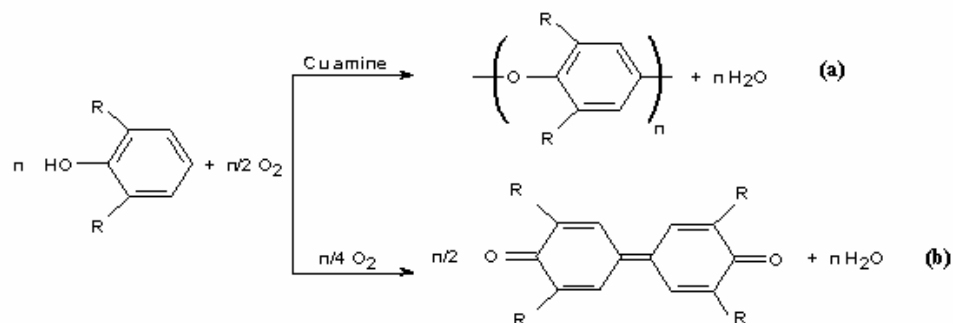


Figure 1.5 Oxidative coupling reactions of phenols

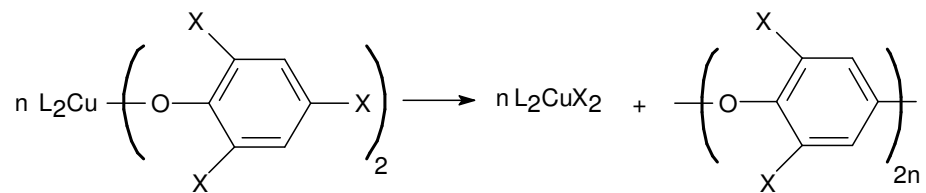
(a) Carbon-oxygen coupling, poly(phenylene oxide)s, $R =$ Unhindered alkyl aryl groups, halogens

(b) Carbon-carbon coupling, diphenylquinone, $R =$ Large and bulky groups

Hay and coworkers concluded that polymer formation readily occurs only if the substituent groups are relatively small and not too electronegative. When the substituents are large and bulky diphenoquinones are formed by tail to tail coupling.

Blanchard et.al. studied the preparation and characterization of bis(phenolato)bis(pyridine)copper(II) complexes [21]. These complexes were decomposed to produce branched polymer under variety of condition. They also proposed a radicalic mechanism for the decomposition.

In 1969, Harrod studied the thermal decomposition of copper (II) complexes containing various amine ligands [31]. They concluded that thermal stability of the complexes depends on the nature of the neutral ligand. The phenoxo complexes with chelating ligands are highly resistant to thermal decomposition compared to non-chelating ligands. The general chemical reaction for the preparation of these polymers was:



Harrod et.al. [32] reported that the molecular weights of poly(phenylene oxide)s increase with the increase in the concentration of bis(2,4,6 – trichlorophenoxy) bis(pyridine) copper(II) complex. They also observed that, observation and changing the solvent from cumene to toluene, to benzene and changing the amine ligand from N,N,N',N'-tetramethyl ethylenediamine to pyridine also increased the \bar{M}_n . The effect of temperature on \bar{M}_n was very small. In 1981 Harrod modified his previously proposed mechanism for the polymerization reaction by performing further studies with ^{13}C -NMR. The results revealed that there is a high density of monomeric branches in the structure of poly(phenylene oxide)s, where this observation cannot be explained on the basis of the mechanism. They proposed ortho substitution occur by an intramolecular process involving two adjacent phenoxy ligands at a single copper center [33].

Since 1980's Kısakürek et.al. made progress in synthesis and characterization of poly(dihalophenylene oxide)s by decomposition of the isolated transition metal complex of different type of phenols with various amine ligands. Various decomposition techniques were employed for polymer synthesis. Electro-initiation in solution [34 - 49], thermal decomposition in solid state [50 - 60] or in solution [61 - 67] and microwave-assisted polymerization [68-70] were investigated. Beside the decomposition method, type of amine ligand and the type of halogen substituted on the phenol ring were found to be effective on the structure, molecular weight and the percent conversion to the polymer. The lowest molecular weight polymers are obtained in electroinitiated polymerization and the highest with thermal decomposition in solution where the solid state polymerization is close to electroinitiation with slightly higher values. Glass transition temperatures (T_g) of the polymers obtained are higher than 160 °C and do not depend on the molecular weight. The nature of the neutral amine ligands also affects the thermal decomposition. The phenoxy complexes with chelating ligand were exceptionally resistant to thermal decomposition compared to non – chelating ligand increasing the induction periods of polymer

formation. The structure of the polymer obtained is also affected by the nature of the ligand. Bromine atom in the para-position of 2,4,6-trihalophenoxides results in polymers with higher linearity being independent of the method of initiation and the type of the ligand substituted. In the case of trichlorophenoxide, 1,2 and 1,4 addition is taking place at equal rates with non-chelating ligand pyridine in thermal polymerization, either in solution or in solid state and in electroinitiation with ligands pyridine and ethylenediamine. However, 1,2 addition is favored over 1,4 catenation in the case of chelating ligands, TMED and ethylenediamine, in thermal polymerization in solution and in electroinitiation. The effect of the type of the transition metal was also examined. Copper, cobalt and nickel were studied as transition metals. It was found that in solid state Cu complexes decompose much more easily than Co and Ni complexes. The type of metal was found to be effective on the structure of the polymer and on the percent conversion.

1.4. Conducting Polymers

An organic polymer that exhibits combination of properties of metal and plastic is termed as conducting polymer (**CP**), more commonly 'synthetic metal'. Interest in conducting polymers is largely due to the wide range of possible applications because of their facile synthesis, good environmental stability and long term stability of electrical conductivity [71, 72]. More recently, polymers with additional intrinsic properties have been developed such as intrinsically conducting polymers exhibiting not only conductivities similar to metals but also the processability of traditional polymers [73].

1.4.1 History of Conducting Polymers

For most the history of polymer technology one of the most valued properties of synthetic polymers has been their ability to act as excellent electrical insulators, both at high voltages and at high frequencies. In spite of this, there has been interest for many years in the possibility of producing electrically conducting polymers [74]. The field of conducting polymers has expanded exponentially since the first discovery of high conductivity in a plastic, doped polyacetylene, in 1977 [75]. This notorious work has spawned an entire arena of scientific research. Fortunately, this massive area has been extensively reviewed [76-80]. Many conducting polymers were known in their nonconducting forms before their conductivity and other properties of interest were discovered. Some of them were also known in their conductive forms, but not well characterized and not much interest paid to their conductivity [78]. For example, poly(p-phenylene sulfide), PPS, has been commercially produced for thermoplastics applications under the brand name Ryton by Philips Chemical Company since the early 1970's, and well-defined synthesis of polyacetylene have been reported since 1971 [81].

The conductive polymers belonging to polyenes or polyaromatics such as polyacetylene, polyaniline, polypyrrole, polythiophene, poly(p-phenylene), poly(phenylene vinylene) classes have been studied extensively. Among all the above classes, the polyaniline family of conjugated polymers is of much interest world wide because of its unique conduction mechanism and good environmental stability in the presence of oxygen and water. Polyaniline is one of the oldest conductive polymers known. It was prepared by Letheby in 1862 by anodic oxidation of aniline in sulphuric acid and described as existing in four different states, each of which was an octamer.

Polyacetylene was initially the most studied conducting polymer from both scientific and practical application point of view. However, due to its high chemical instability in air and related factors, interest in it was confined to its scientific aspects [82]. Polyaniline, polypyrrole, and the polythiophenes remain the most extensively studied conducting polymers to date from both scientific and practical or commercial points of view. In 1970's, the important developments in the field of conducting polymers have showed that they were the potential novel materials with highly promising conductivity, started with the coincidental discovery in a collaborative effort between the Shirakawa and Heeger/McDiarmid groups where polyacetylene exposed to iodine vapors develops very high and well characterized conductivities for an organic material [83]. In the year 2000, twenty-three years after the first experiment demonstrating that certain plastics conduct electricity, the Nobel Prize was awarded to Alan J. Heeger, Alan G. MacDiarmid, and Hideki Shirakawa for "the discovery and development of conducting polymers". In this Nobel Lecture, Alan Heeger offers two brief explanations for the importance of the discovery of conducting polymers: 1. "they didn't exist before," and 2. "they offer a unique combination of properties not available from any other known materials." The first simplistic statement embodies the academic curiosity that has attracted so many researchers in a list of varying disciplines. The second explanation encompasses the potential use of conducting polymers in a vast number of applications by replacing old materials and by developing new technologies based on their unique and unprecedented abilities. The commercialization of conducting polymer technologies has now arrived [84].

1.4.2. Conductivity

In inorganic polymeric materials, conduction may occur through the movement of either electrons or these ions. In each case conductivity σ , is equal to the product of the carrier mobility (μ), its charge (q) and the number of carriers or the concentration (n), so that;

$$\sigma = n q \mu$$

Consequently, doped conjugated polymers, “conducting polymers”, are good conductors for two reasons:

- 1) Doping (through oxidation or reduction) leads to injection of carriers into the π - electron system. Since every monomer is a potential redox site, conjugated polymers can be doped (n-type or p-type) to a relatively high density of charge carriers.
- 2) The π -bonding leads to π -electron delocalization along the polymer chains, and, thereby, to the possibility of charge carrier mobility, which is extended into three dimensional transports by the interchain electron transfer interactions. In principle, the broad π -electron bandwidths can lead to high carrier mobilities.

As a result of the same interchain π -bonding and relatively strong interchain electron transfer interactions, the mechanical properties of conjugated polymers are potentially superior to those of saturated polymers such as polyolefins. Moreover, because of these two features, it may be possible to exceptional mechanical properties with aligned conjugated polymers at lower chain lengths than required for their saturated counterparts [85].

1.4.3. Band Theory

The excitation and/or removal/insertion of electrons in conjugated polymers as a result of electrochemical or photochemical doping processes necessitate discussion of band theory. Solids may be classified in terms of their resistivity or conductivity as conductors, insulators, or semiconductors. These classifications of solid materials can be visualized in terms of the band theory of solids and are strongly correlated with the interatomic spacing in the solid (Figure 1.6). The diagram below shows how the conductivity of conjugated polymers like polyacetylene can vary from being an insulator to a conductor.

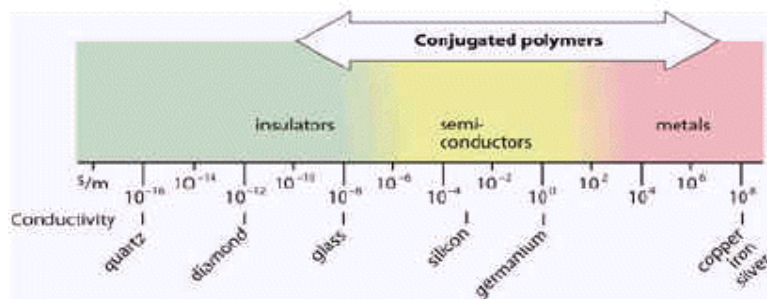


Figure 1.6 Conductivity diagram of various materials.

In all of the above materials, the overlapping of individual molecular electronic states produces electronic bands. Basically, valence electrons overlap to produce a valence band (VB), while electronic levels above these levels also coalesce to produce a conduction band (CB). A gap, called the band gap, generally denoted E_g , exists between these two bands, as shown in Figure 1.7. If

the band gap is large, e.g. 10 eV, it is difficult to excite the electrons into the conduction band, and an insulator results at room temperature. If the gap is small, e.g. 1.0 eV, then electrons may be excited from the valance band into the conduction band by means of several types of excitations such as thermal excitation, vibrational excitation, or excitation by photons. The electrons are then mobile in a sense, and the material is termed as semiconductor. For conduction to take place in conventional, inorganic semiconductors, electrons must generally be excited from the valence band to the conduction band. Normally, thermal excitation at room temperature gives rise to some conductivity in such inorganic semiconductors. “Doped” conducting polymers, when in an appropriate oxidized or reduced state are semiconductors as a result of their unique, extended π -conjugation. Indeed the extended-overlap π -bands become the valence band and the π^* bands become the conduction band in conducting polymers. The band gap is generally greater than 1.0 eV in most conducting polymers. The high conductivity of metals comes from a partially occupied band or zero band gaps [86].

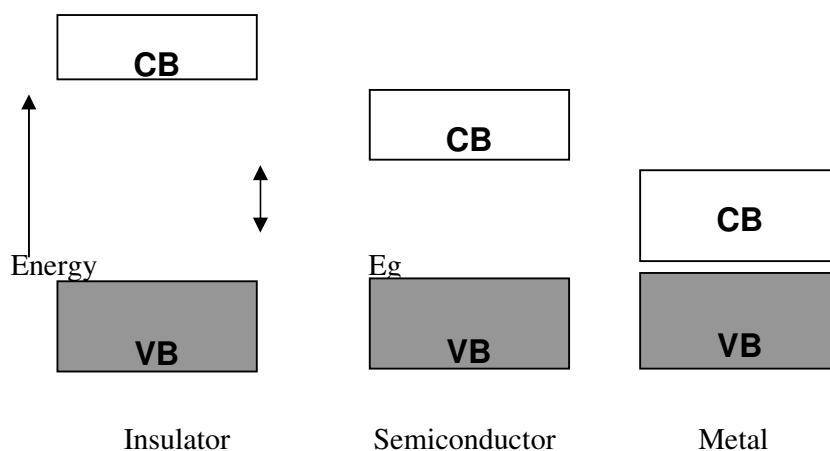


Figure 1.7 Schematic representation of the band structure of an insulator, semiconductor, and a metal

The semi-conducting neutral polymer is converted into an ionic complex consisting of a polymeric cation (or anion) and a counter ion which is the reduced form of the oxidizing agent (or the oxidized form of the reducing agent). The use of an oxidizing agent corresponds to p-type doping and that of a reducing agent to n-type doping.

1.4.4. Solitons, Polarons and Bipolarons

The band theory is not sufficient to explain the electrical behavior of conducting polymers. The concepts of solitons, polarons, and bipolarons have been proposed to get a better understanding on the conduction mechanism of conducting polymers [87].

Solitons and polarons are the structural defects that are highly mobile and may carry the extra charge with them when the system is charged. Therefore, these defects are very important for transport properties of these materials [88].

When the charges (electrons and holes) are added to the polymer chain by chemical doping, photo-excitation, or charge injection, it brings about a reorganization of the π -electron bonding in the vicinity of the charge. Solitons can also be in charged states, that is, with a positive soliton corresponding to a cation and a negative soliton to an anion.

Removal of an electron from the top of the VB of a conjugated polymer, gives rise to a vacancy (radical cation) that is not completely delocalized. Only partial delocalization occurs, which extends over some monomeric units and leads to a lattice distortion. The energy level associated with this radical cation is placed in the band gap (midgap level) [86]. In nondegenerate polymers, the

resonance structures do not have the same energy level in ground state, that is, one structure is more stable than the other structure.

When a second electron is removed from the polymer chain, two polarons are obtained, but if the second electron is extracted from a polaron, a bipolaron (dication) is created. Low doping levels give rise to polarons, whereas higher doping levels produce bipolarons [86]. In an electric field polarons and bipolarons can move along the polymer chain by rearrangement of double and single bonds. As the doping level increases, the energies of bipolarons can overlap and narrow bipolaron bands in the band gap can be created.

A quite unusual conduction mechanism can be envisaged; all bands are either totally filled or empty and mobile bipolarons, instead of electrons, transport the current [89]. The structure of a polaron and bipolaron in polyphenylene are shown in Figure 1.8.

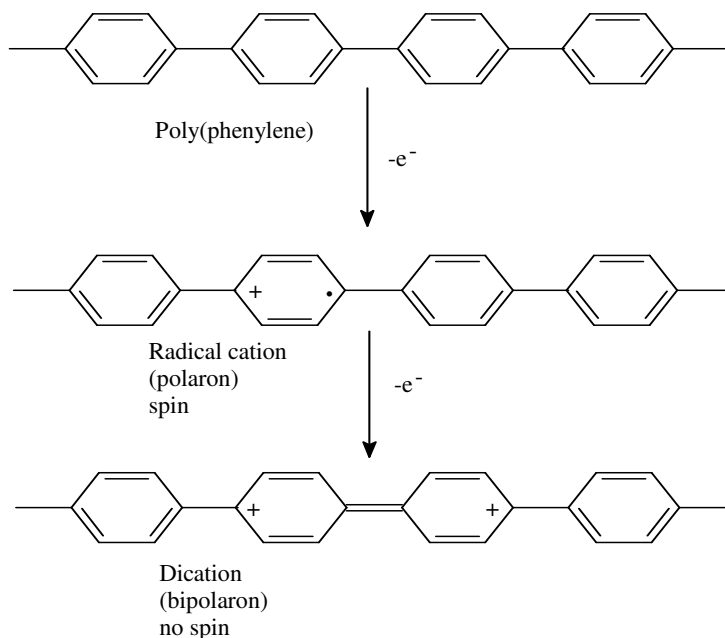


Figure 1.8 The structure of a polaron and bipolaron in polyphenylene.

1.4.5. Doping Process

The conductivity of a polymer can be increased several-fold by doping. It was discovered that doping of polyacetylene with metallic regimes increases its conductivity by 9-13 orders of magnitude [90]. Oxidation caused by chemical species generates a positively charged conducting polymer and an associated anion, similarly reduction generates a negatively charged conducting polymer and an associated cation. Impurities cause the removal or addition of charges from the valence or conduction band and therefore impart higher conductivity. The chemical oxidation of the conducting polymers by anions, or its reduction by cations, was originally called “doping”.

Certain dopants could give rise to magnetic ordering in these polymers along with the electron acceptor e.g. iodine, FeCl_3 , AsF_5 , etc. (p-type) or electron donor such as Na, Li, etc. (n-type) to the polymer which is considered to generate positive carriers (holes) or negative carriers (electrons) in the π -conjugated system [91].

1.4.6. Hopping Process

Carrier mobility is the main reason of electrical transport in conducting polymers. Mobility of the charge carriers can be restricted as the degree of overlapping decreases in molecular or atomic levels. As the electronic states become increasingly localized, transport of the particle occurs through hopping processes. The hopping process produces a generous supply of potential carriers. There are mainly three types of transport for the carrier mobility; single chain or intramolecular transport, interchain transport, interparticle transport [92]. The

intra chain movement depends on the effective conjugation of the polymer, while the inter chain jumping is determined by the stacking of the polymer molecules. The mobility also depends on the movement of electrical charges from particle to particle. These three show a resistive network determining the effective mobility of the carriers. Thus the mobility and therefore conductivity are determined on both a macroscopic (interparticle) and microscopic (intra and interchain) level.

1.4.7. Synthesis of Conducting Polymers

Synthesizing new and novel structures, increasing the order of the polymer backbone (and also conductivity), good processability, easier synthesis, more defined three dimensional structure, stability in both conducting and nonconducting states, solubility in certain solvents such as water and many other application unique properties are some of important targets in conducting polymer synthesis. The synthesis of conducting polymers is divided in two categories: chemical polymerization and electrochemical polymerization. Many conducting polymers can be synthesized by both chemical and electrochemical methods [93, 94].

In chemical synthesis, monomers are polymerized using appropriate catalysis or reagents. The morphological, physical and electrochemical properties are influenced by reaction conditions such as the species and concentrations of catalyst, reagents and solvent, the monomer concentration, the reaction temperature so on. Chemical synthesis is considered to be suitable for producing large amounts of homogeneous polymer [95].

Oxidative chemical polymerization is the least expensive, simple and most widely used chemical synthesis of conducting polymers [96]. In this

method, a stoichiometric amount of oxidizing reagent is used to form polymer that is in its doped or conducting form.

Electrochemical polymerization is an efficient method for synthesizing smooth polymer films on conductive substrates, and it allows for easy probing of electrical and optical properties. It represents one of the simplest and most straight forward methods for elaboration of modified electrodes in which inherent electrochemical and optical properties of the conjugated polymer backbone of polymers are associated with specific properties afforded by covalently.

1.4.8. Applications of Conducting Polymers

The extended π -systems of conjugated polymer are highly susceptible to chemical or electrochemical oxidation or reduction. These alter the electrical and optical properties of the polymer, and by controlling this oxidation and reduction, it is possible to precisely control these properties. Since these reactions are often reversible, it is possible to systematically control the electrical and optical properties with a great deal of precision. It is even possible to switch from a conducting state to an insulating state.

Much research will be needed before many of the above applications will become a reality. The stability and processibility both need to be substantially improved if they are to be used in the market place. The cost of such polymers must also be substantially lowered. However, one must consider that, although conventional polymers were synthesized and studied in laboratories around the world, they did not become widespread until years of research and development had been done. In a way, conducting polymers are at the same stage of development as their insulating brothers were some 50 years

ago. Regardless of the practical applications that are eventually developed for them, they will certainly challenge researchers in the years to come with new and unexpected phenomena. Only time will tell whether the impact of these novel plastics will be as large as their insulating relatives.

The recent developments toward the synthesis of new and processable polymers as well as discovering the broad range of physical phenomena and chemical flexibility opens up opportunities for new technological applications [97]. The higher environmental stability and modification of properties to suit a given end use and processability achieved with the polymers derived from acetylene, pyrrole, thiophene, aniline and their derivatives, polyphenylene, poly(phenylene vinylenes) and poly(p-heterocyclic vinylenes) have emerged as the materials to replace metals and semiconductors in the electrical and electronics industry, as well offering themselves as the materials for the optoelectronic industry.

Among organic materials, **CPs** (or conjugated polymers) have attracted most attention owing to the unique electronic, electrical and optical properties, several potential, technological and commercial applications which can be splitted into three categories. Examples of applications are semiconducting materials for field effect transistor [98] and active material in an electroluminescent device [99, 100]. The second category of applications involves using the polymer in its doped or conducting form, and some representative applications in this category are electrode materials for capacitors [101, 102] and enzyme immobilization [103]. Third category uses the ability of polymer to reversibly switch between its conducting and reduced forms. Upon switching between two states, the polymer undergoes color, conductivity, and volume changes. Applications that use these properties include battery electrodes [104], actuators [105], sensors [106], drug delivery [107] and electrochromics [108-111].

1.5. Crosslinked Polymers

A polymer network may be defined as a structure in which essentially all mers are connected to all other mers and to the macroscopic phase boundary by many paths through the polymer's phase; the number of such paths increases with the average number of intervening bonds and the paths much on the average be co-extensive with the polymer phase [112]. Crosslinked polymers are increasingly used as engineering materials because of their excellent stability toward elevated temperatures and mechanical deformation [113].

Classifying polymer networks according to their end-use properties, the main representatives of crosslinked polymers include vulcanized rubbers, crosslinked thermosetting materials, adhesives, polymeric sorbents, electric and electronics materials, soft gels, etc. Special features of polymer networks in comparison with uncrosslinked polymers include their dimensional stability, increased thermal, physical and chemical stability and ability to store information about their shape and formation history when the gel point is surpassed. Three-dimensional, covalently bonded arrays of atoms, organic or inorganic, rank among the largest molecules known. Their molecular weight is given by the macroscopic size of the object; for instance, a car tire made of vulcanized rubber or a layer of chemically dried (crosslinked) protective coating can be considered a single giant molecule.

1.5.1. Crosslinking Mechanism

The most severe mechanism for decreasing molecular freedom in chemical cross-linking the polymer chains together through covalent or ionic

bonds to form a network. Occasionally the term curing is used to denote cross-linking. There are a number of ways crosslinking can be brought about, but basically they fall into two categories: (1) crosslinking during polymerization by use of polyfunctional instead of difunctional monomers, and (2) cross-linking in a separate processing step after the linear (or branched) polymer is formed.

The mechanism of cross-linking by radiation is either free radical or ionic (Figure 1.9). Cross-linking by interaction with high energy (ionizing) radiation sources occurs through both mechanisms [114].

Cross-linking:

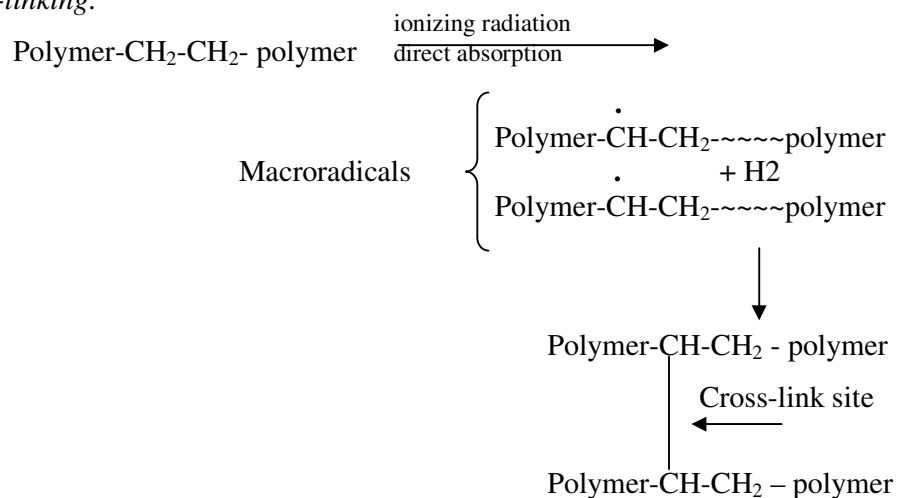


Figure 1.9 Mechanism of Cross-linking

Crosslinking reactions are those that lead to the formation of insoluble and infusible polymers in which chains are joined together to form a three-dimensional network structure. A simple cross-linking reaction is exemplified by polymer chains with several functional groups designated A that are capable of reacting among themselves to form chemical bonds A-A. If these polymer chains are exposed to conditions such that the functional groups do react, then all the

chains in the reaction vessel will be tied to each other through A-A bonds (Figure 1.10). In principle, the polymer molecules in the reaction vessel will have formed one giant molecule.

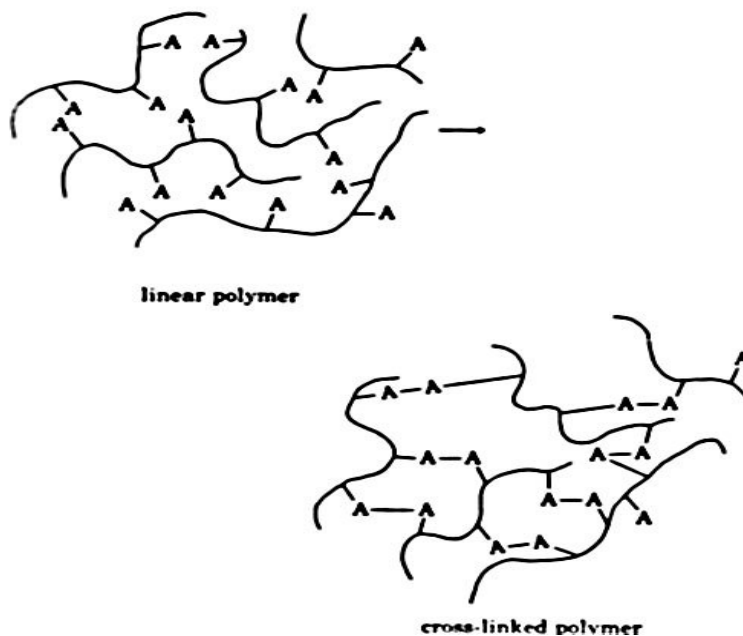


Figure 1.10 Cross-linked structure

An example of cross-linking is the vulcanization process, which makes rubber useful in applications where mechanical strength is important. Other cross-linked polymers are widely used in paints, printing inks, adhesives, sealants, encapsulates and electrical and electronic components. In the example above, the macromolecules were self reacting, but this is not necessary for network formation. Cross-linking can be carried about through the use of a cross-linking agent, a molecule that has two or more groups, capable of reacting with

the functional groups on the polymer chain. Cross-linked polymers can also be prepared by the polymerization of monomers with an average functionality greater than two [115].

A polymer network and a cross-linked polymer need not be the same thing. A polymer may be crosslinked below its gel point, and hence should be considered a branched polymer. The gel point is defined as the state where enough polymer chains are bonded together (either physically or chemically) such that at least one very large molecule is coextensive with the polymer phase. Beyond the gel point, one begins to speak of a polymer network, since increasing fractions of the system are interconnected by more than one bond.

If the polymer network is an amorphous polymer above its glass transition temperature, it usually exhibits rubber elasticity, i.e., it may stretch several hundred percent and essentially recover its original dimensions on release of the stresses. Crystalline or glassy networks do not have this behavior. Linear amorphous polymers above T_g of very high molecular weight may also exhibit rubber elasticity, but the behavior is very much time dependent, as the physical entanglements can relax. It must be noted that all covalently cross-linked polymers also have various physical entanglements. For lightly cross-linked materials, there may be more physical entanglements than covalent (chemical) crosslinks. When polymer chemists use the term crosslinking, they usually mean covalent chemical crosslinking. Covalent cross-linking has certain disadvantages, once cross-linked; a polymer cannot be dissolved or molded hundred percent [116].

1.5.2. Formation of network structure

For the formation of a 3D polymer network, at least one of the starting components must have the number of functional groups per molecule (called component functionality, f) larger than two [117]. This is a necessary but often not sufficient condition. In order that infinite paths of bonds may exist (which is condition for gelation), infinite repetitions of certain sequences of units connected by bonds should be possible. Small molecules carrying functional groups (monomers) or preformed larger molecules carrying functional groups serve as polymer network precursors. There is no straightforward answer of the question if and when an infinite network can be formed. To resolve this problem, one has to recourse to the help of branching theories. The precursors differ in the number of functional groups, nature of the carrier material and equivalent weight per functional group and the architecture of the precursor. The functionality of precursors is important because it determines the conversion or time window of processability of the reacting material (pot life). High-functionality precursors, like primary chains in vulcanization, gel at quite low conversions. Low-functionality precursors can be blended in such a way that the gel point can be adjusted as close to 100% conversion as desired. Even more important than the precursor functionality is the type of the crosslinking reaction: step-wise or chain with fast propagation step. For instance, polycondensation (step-wise reaction) of a blend of tetra- and bifunctional monomers will form gel above 50% conversion, whereas the equivalent blend of monovinyl and divinyl monomers polymerized by free-radical mechanism forms gel in the range of several percent conversions or lower. Moreover, the structure of the product is different as a result of the difference in polymerization mechanisms [118].

1.6. Aim of the study

Microwave-assisted synthesis and characterization of poly(dibromophenylene oxide)s, poly(diiodophenylene oxide)s (**P**) and conducting polymers (**CP**) and/or crosslinked polymers (**CLP**) and/or radical ion polymers (**RIP**) were achieved simultaneously from 2,4,6-bromophenolate or 2,4,6-iodophenolate in a very short time interval.

In this study, the aim is;

To improve a novel polymerization technique for poly(dihalophenylene oxide)s,

To synthesize poly(dibromophenylene oxide)s, poly(diiodophenylene oxide)s by using microwave energy in a very short time interval,

To study the effects of heating time, microwave energy and amount of water on percent conversion, structure and molecular weight of the polymers.

CHAPTER 2

EXPERIMENTAL

2.1. Chemicals

2.1.1. 2,4,6 – Tribromophenol (TBP) and 2,4,6 – Triiodophenol (TIP)

Analytical grade 2,4,6 – Tribromophenol and 2,4,6 – Triiodophenol were provided from Merck and was used without further purification.

2.1.2. Sodium Hydroxide (NaOH), Potassium Hydroxide (KOH) and Lithium Hydroxide (LiOH)

NaOH, KOH and LiOH produced by Merck, were used in the polymerization.

2.1.3. Toluene

Toluene was provided from Merck and used as a solvent for the polymer.

2.1.4. Ethyl Alcohol

Ethyl alcohol was commercially available technical grade and used as non-solvent for the polymers and used as precipitating reagent.

2.1.5. Hydrochloric Acid

It was provided from Merck and used in the precipitation of the synthesized polymers to dissolve the by product salts formed during polymerization.

2.1.6. Deuterated Chloroform (CDCl_3)

CDCl_3 was provided from Merck and was used as a solvent to obtain NMR spectra of the polymers.

2.1.7. Potassium Bromide (KBr)

Spectroscopic grade KBr was provided from Merck and was used to take FTIR spectra of polymers which were dispersed in KBr discs.

2.2. Apparatus and Instruments

2.2.1. Microwave Oven

Domestic microwave oven (BEKO or BOSCH) works at 2.45 MHz and has a period of 10 seconds. It has several time intervals (1-20min) and microwave energies (70-900 watt) and it was used for polymerization.

2.2.2. Differential Scanning Calorimeter (DSC)

Thermal behaviors of the polymers were obtained by using DuPont thermal analyst 2000 DSC 910S model differential scanning calorimeter. In order to obtain thermal behavior of the polymers, in the first run of the DSC analysis both of the samples were heated to 150 °C from room temperature with a heating rate of 10 °C/min then cooled to room temperature with a cooling rate of 10 °C/min to reduce the effect of unwanted contamination. At the second run, polymers were heated to 350 °C by the rate of 10 °C/min under nitrogen atmosphere.

2.2.3. Thermogravimetric Analysis and Fourier – Transform Infrared Spectrophotometer (TGA/FTIR) System

Thermogravimetric analysis (TGA) is a technique that permits the continuous weighing of a sample as a function of temperature and/or as a

function of time at a desired temperature. Weight losses of the polymers due to the increasing temperature were determined by Perkin Elmer Pyris 1 TGA thermogravimetric analyzer coupled to Spectrum 1 FT-IR Spectrometer. Samples were heated from 30 °C to 800 °C with a heating rate of 10 °C/min. under nitrogen atmosphere.

2.2.4. Fourier – Transform Infrared Spectrophotometer (FTIR)

Infrared spectra of the samples were obtained on a Bruker IFS 66/S FTIR spectrometer in the 4000 – 400 cm^{-1} region by dispersing the sample in KBr pellets.

2.2.5. NMR Spectrophotometer

^1H NMR and ^{13}C NMR spectra of poly (dihalophenylene oxide) were recorded on a Bruker Instrument NMR spectrometer (DPX-400) in deuterated chloroform and TMS as an internal reference.

2.2.6. Elemental Analysis (CHNSO) Analyzer

Carbon – hydrogen and oxygen analysis of samples were carried out by means of Leco 932 CHNSO elemental analyzer.

2.2.7. Powder Diffraction X-ray

Powder diffraction X-ray spectra of both washed and unwashed conducting polymer were obtained by using computer controlled automatic Humber-Guinner powder diffractometer with CoK α radiation obtained by using a voltage of 30 kV and a current of 7 mA.

2.2.8. Light Scattering

Molecular weight, radius of gyration, and virial coefficient of polymers were determined at 37 °C by using Multi-angle light scattering spectrometer (Malvern 5000). The ALV/CG-3 Goniometer system is designed to perform dynamic and static light scattering analysis simultaneously.

2.2.9. GPC

$\overline{M}_w/\overline{M}_n$ values were measured with PL-GPC 220 Gel Permeation Chromatography in THF.

2.2.10. ESR

Electron spin resonance has been used as an investigative tool for the study of radicals formed in polymers, since the radicals typically produce an unpaired spin on the molecule from which an electron is removed. ESR spectrums of the products were recorded by Bruker Xepr ELEXSY-580 spectrometer in quartz cell at room temperature where diphenylpicrylhydrazine was the reference.

2.2.11. SEM

Analysis of the surface morphologies of all type polymers were done by using JEOL JSM- 6400 scanning electron microscope.

2.2.12. UV-Vis

UV-Visible spectrums of samples were obtained on Cary 100 UV-Visible Spectrophotometer in the 800 – 200 nm region by dissolving the sample in toluene.

2.2.13. Conductivity Measurement

Conductivity measurements were performed both two and four-probe techniques. The Four Probe Method is one of the standard and most widely used methods for the measurement of conductivity. The four osmium probes aligned in a colinear geometry. The error due to contact resistance, which is significant in the electrical measurement on semiconductors, is avoided by the use of two extra contacts (probes) between the current contacts. In this arrangement the contact resistance may all be high compared to the sample resistance, but as long as the resistance of the sample and contact resistance's are small compared with the effective resistance of the voltage measuring device (potentiometer, electrometer or electronic voltmeter), the measured value will remain unaffected. Because of equal pressure contacts, the arrangement is also especially useful for quick measurement on different samples or sampling different parts of the sample. Figure 2.1 demonstrates a simple four-probe measurement setup. Four equally spaced osmium tips touch the surface of polymer film taped on an insulating substrate. A known steady current is passed through the electrodes 1 and 4 and measured while the potential drop (ΔV) between contacts 2 and 3 assessed.

Conductivity is calculated from the following equation,

$$\sigma = \ln 2 / (\pi R t)$$

where R is the resistance of the sample, and t is the thickness.

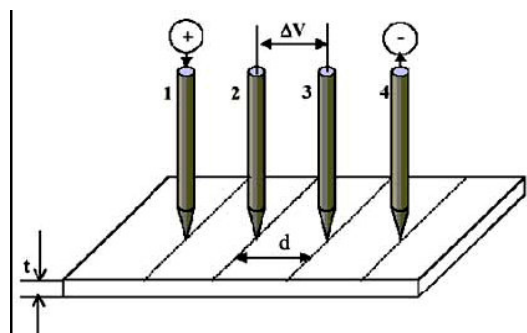


Figure 2.1 Four-probe conductivity measurement set up.

2.3. Procedure

Trihalophenol (tribromophenol (TBP) or triiodophenol (TIP)), sodium hydroxide (NaOH) (or potassium hydroxide (KOH), lithium hydroxide (LiOH)) and water were used as starting material for the microwave-assisted polymerization.

2.3.1. Synthesis of Polymers

Microwave initiated polymerizations were performed at several time intervals (1-20 min), in different ranges of microwave energy (70-900 watt) and in various amounts of water (0.5-5 ml). Trihalophenol and NaOH, KOH or LiOH were mixed by grinding and wetting by deionized water. Polymerization was performed in a Pyrex glass holder, loosely covered with a lid, inserted in a microwave oven working at 2.45 MHz and having a pulse period of 10 s. At the

end of the reaction time intervals, the simultaneously resulting products were dissolved in 100 ml toluene by vigorous stirring. The insoluble black colored conducting polymer (**CP**) or white colored crosslinked polymer (**CLP**) were removed by filtration and washed several times by triple distilled hot water for purification. The toluene soluble poly(dihalophenylene oxide) (**P**) or orange colored radical ion polymer (**RIP**) were precipitated in ethanol. All the recovered precipitates were dried to a constant weight under vacuum.

2.3.2. Characterization of the Polymers

Poly(dihalophenylene oxide) and radical ion polymers were characterized by FTIR, ¹H-NMR, ¹³C-NMR, TGA/ FTIR, DSC, SEM, ESR, GPC, UV-Vis, light scattering and elemental analysis. Conducting and crosslinked polymers were characterized by FTIR, TGA/ FTIR, DSC, SEM, ESR, powder diffraction X-Ray and elemental analysis.

CHAPTER 3

RESULTS AND DISCUSSION

Microwave-assisted polymerizations were carried out with a constant microwave energy and constant amount of water at different time intervals ranging from 1 to 20 min; or at constant time intervals and constant amount of water with variation of microwave energy ranging from 70 to 900 watt or at constant time intervals and constant microwave energy with changing amount of water ranging from 1 to 5 ml.

Percentage conversion values of each product were calculated by using the following equation:

$$\text{Conversions (\%)} = \frac{\text{Weight of product}}{\text{Initial weight of monomer}} \times 100$$

Results will be discussed under four topics. Each topic includes the results related to the synthesis and the characterization of the polymers which were synthesized with different monomers (TBP or TIP) and Metal-hydroxides (NaOH, LiOH or KOH).

3.1. Synthesis of Polymer with TBP with NaOH

Poly(dibromophenylene oxide) (**P**) and conducting polymer (**CP**) and/or crosslinked polymer (**CLP**), and/or radical ion polymers (**RIP**) were synthesized simultaneously from sodium 2,4,6-tribromophenolate with microwave-assisted polymerization in a very short time interval. Polymerizations were performed at several time intervals (1-7 min), in different ranges of microwave energy (70-700 watt) and in various amount of water (0.5-5 ml). The synthesis of **CLP** and **RIP** were achieved in 5 ml water at 350 watt and 700 watt at the end of 1 min, respectively. At the end of the reaction time, the simultaneously resulting products were dissolved in 100 ml toluene by vigorous stirring. The insoluble black colored conducting polymer (**CP**) or white colored crosslinked polymer (**CLP**) were removed by filtration and washed several times by triple distilled hot water for purification. The toluene soluble poly(dihalophenylene oxide) (**P**) or orange colored radical ion polymer (**RIP**) were precipitated in ethanol. All the recovered precipitates were dried to a constant weight under vacuum.

The effect of polymerization time, energy and amount of water on the % conversions and % weight losses (WL) were listed in Table 3.1.1. At 70 watt in 0.5 ml water, the % conversion of **P** showed an increasing trend up to 19.5% followed by a decrease at the end of 7 min to 15.6 %. As the water content increased, the % conversion of **P** increased while **CP** decreased significantly up to 5 ml water. At 70 watt, the synthesis of **P** and **CP** were achieved at the end of 3 min whereas in the range of 100-700 watt, the syntheses were in between 1 to 3 min. In addition, in 5 ml water, only **P** synthesized at the end of 5 min whereas **CLP** an **RIP** synthesis were achieved at 350 watt and 700 watt, respectively at the end of 1 min. In the range of 100-700 watt, generally % conversion slightly increased for **P** and % WL whereas decreased for **CP** as the time increased from 1 to 3 min. On the other hand, % conversion increased slightly for **P** while decreased slightly for **CP** as the amount of water was increased (0.5-5.0 ml).

Hence, the optimum conditions to obtain the highest % conversion of **P** and **CP** were 70 watt for 5 min in 5 ml water and 100 watt for 1 min in 0.5 ml water having maximum values 23.6 and 27.2 % respectively. The % WL generally increased slightly as the time and energy increased and sharply decreased as the amount of water increased reaching to the maximum value at 50.8 % at the end of 1.5 min at 500 watt.

Table 3.1.1 The effect of polymerization time, energy and amount of water (w) on the % **P**, **CP** and **WL** (TBP and NaOH).

70watt	1,5min 0,5 ml w	3 min 0,5 ml w	5 min 0,5 ml w	5 min 1 ml w	7 min 0,5 ml w
%P	-	16.2	19.5	20.2	15.6
%CP	-	20.8	21.0	8.9	22.3
%WL	-	41.0	41.2	29.9	44.1
100watt	1 min 0,5 ml w	1 min 1 ml w	1 min 5 ml w	1.5 min 0,5 ml w	3 min 0,5 ml w
%P	14.1	15.6	15.5	13.7	12.5
%CP	27.2	26.4	22.8	23.1	21.8
%WL	40.0	29.9	27.5	43.2	43.7
350watt	1 min 0,5 ml w	1 min 1 ml w	1 min 5 ml w	1.5 min 0,5 ml w	3 min 0,5 ml w
%P	13.5	14.2	16.7	12.3	11.9
%CP	25.6	25.0	20.1^(a)	24.9	22.4
%WL	46.9	30.4	28.3	42.8	50.4
500watt	1 min 0,5 ml w	1 min 1 ml w	1 min 5 ml w	1.5 min 0,5 ml w	3 min 0,5 ml w
%P	12.0	13.9	15.6	10.8	-
%CP	21.9	26.0	25.8	20.4	-
%WL	47.1	28.2	29.5	50.8	-
700watt	1 min 0,5 ml w	1 min 1 ml w	1 min 5 ml w	1.5 min 0,5 ml w	3 min 0,5 ml w
%P	9.9	10.2	10.5^(b)	6.8	-
%CP	19.5	15.1	-	15.4	-
%WL	45.6	30.1	30.6	51.0	-
(a) CLP synthesized instead of CP					
(b) RIP synthesized instead of P					

3.1.2. Characterization

Elemental analysis results of the polymers correlate perfectly with the written stoichiometries as tabulated in Table 3.1.2.

Table 3.1.2 Elemental analysis results of **P**, **RIP** and **CP** (TBP and NaOH) (experimental errors ± 0.5).

	% C		% H	
	Calc.	Found	Calc.	Found
P	29.12	29.51	1.111	0.986
RIP	29.20	29.26	1.273	1.204
CP	69.60	69.59	2.595	2.199

In the FTIR spectrum of **P** and **RIP** (Figure 3.1.1a and 3.1.1b respectively), the characteristic absorption bands at 955-1040 cm^{-1} arose from C-O-C stretching signifying the formation of poly(phenylene oxide). The bands related to the out of plane C-H bending, C-O stretching and C=C ring stretching were observed at 850 cm^{-1} , 1140-1210 cm^{-1} and 1440 and 1580 cm^{-1} respectively. Also the peaks at 3079 cm^{-1} and 3500 cm^{-1} were related to aromatic C-H stretching and the phenolic end group respectively.

FTIR spectra of **CLP** (Figure 3.1.1c) was similar to FTIR spectra of **P** except the characteristic absorption bands around 955-1040 cm^{-1} (C-O-C stretching bands) were shifted to 1050-1200 cm^{-1} .

FTIR spectra of **CP** exhibited the peaks at 1460-1600 cm^{-1} related to C=C stretching of both benzenoid and quinoid structures. The absorption peaks at 1710 cm^{-1} and 1110-1280 cm^{-1} related to C=O stretching and C-O stretching respectively. The peak around 3050 cm^{-1} was aromatic C-H stretching and 730-760 cm^{-1} was attributed to C-Br stretching (Figure 3.1.1d).

The FTIR spectra of the evolved gas collected in a glass cell during polymerization, exhibited the peak at 2450 cm^{-1} and 1270 cm^{-1} related to CO_2 and C=O stretching respectively (Figure 3.1.1e).

The thermal properties of the synthesized polymers were studied with DSC and TGA. The DSC thermograms of the **P** and **RIP** showed (T_g) glass transition temperature at 194.27, 214.99 $^{\circ}\text{C}$ respectively, indicating high rigidity of polymers (Figures 3.1.2a and 3.1.2c). However, in the case of **CP** and **CLP** the glass transition temperature was not observed (Figures 3.1.2b and 3.1.2d).

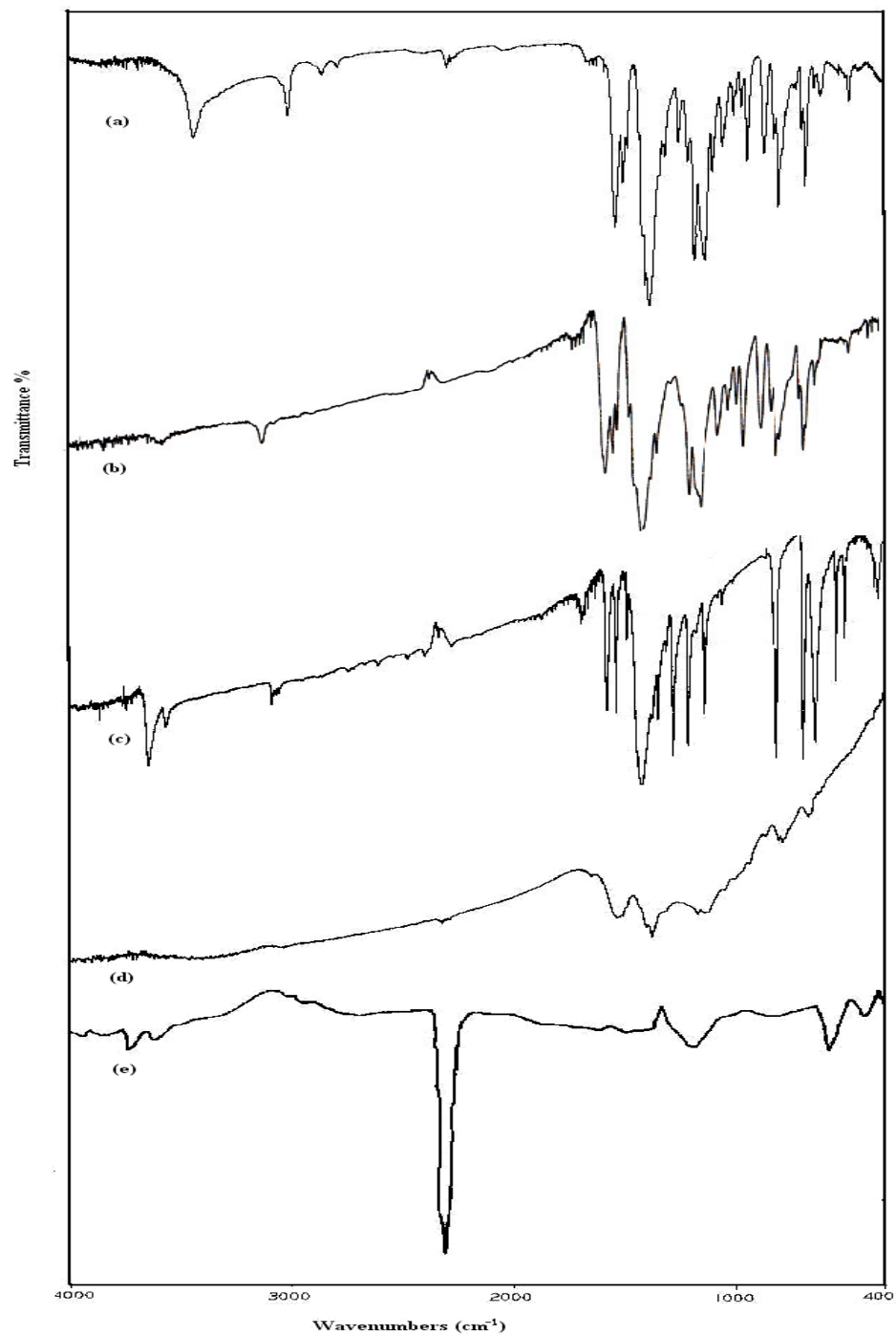


Figure 3.1.1 FTIR spectrum of (a) **P**, (b) **RIP**, (c) **CLP**, (d) **CP** and (e) released gases during polymerization (TBP and NaOH).

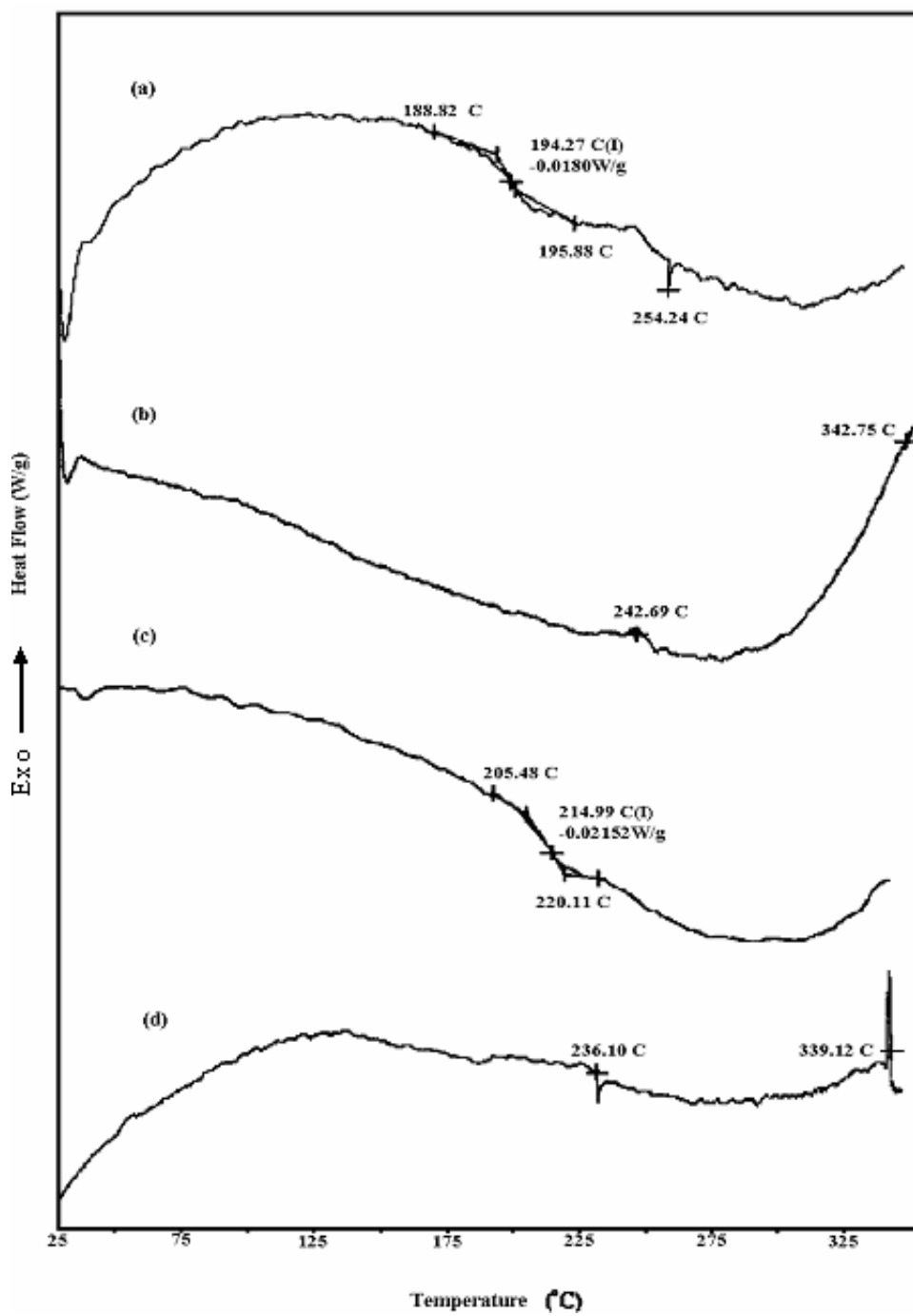


Figure 3.1.2 DSC thermograms of (a) **P**, (b) **CP**, (c) **RIP** and (d) **CLP** (TBP and NaOH).

In the TGA thermogram, the **P** was stable up to nearly 300 °C and then approximately 80 % of sample was lost when the temperature reached to 600 °C. TGA weight loss curve and the corresponding derivative curves (DTG) for **P** is shown in Figure 3.1.3, while FTIR spectrum of the evolved gases during the thermal degradation are displayed in Figure A 1 from a to e. **P** shows no weight loss up to 140 °C and decomposition occurs in four stages with the small weight loss around 170 °C and 380 °C, main degradation around 480 °C and 600 °C at a heating rate of 10 °C. In the first and second stage of degradation with a weight loss of 4% and 6% respectively, the characteristic peaks of an aromatic groups (2974, 2880, 1380 cm^{-1}) were observed. FTIR spectra obtained from main degradation during the third weight loss of polymer show bands of CO_2 (2358 and 2309 cm^{-1}), CO (2100-2200 cm^{-1}), HBr (2300-2700 cm^{-1}), vinyl bromide (1460 and 2950 cm^{-1}). Fourth emission around 600 °C show bands of CO_2 , CO and HBr.

The TGA thermogram of the **RIP** is very similar to the TGA thermogram of **P** (Figure 3.1.4). **RIP** shows no significant weight loss up to 360 °C, and approximately 95 % of sample was lost when the temperature reached to 800 °C. FTIR spectrums of the evolved gases during the thermal degradation are displayed in Figure A 2 from a to d. For **RIP**, decomposition occurs in four stages. In the first and second stage of degradation occur around 180 °C and 380 °C with a small weight loss, the characteristic peaks of an aromatic group were observed. Spectrum obtained from main degradation during the third weight loss of around 500 °C **RIP** shows bands of CO_2 , CO, HBr, vinyl bromide. Fourth emission around 600 °C show bands of CO_2 , CO and HBr (Figure 3.1.4).

The TGA and DTG curves of **CP** are shown in Figure 3.1.5. **CP** shows no significant weight loss up to 500 °C, indicating a higher thermal stability and still having residues less than 30% beyond 800 °C. The main decomposition occurs in two stages with maximum rate of degradation around 600 °C and 800 °C. Figure A 3 from a to d shows the in situ FTIR spectrum of evolved volatile components at each mass loss. This polymer showed in the first emission

around 600 °C with characteristic bands of CO₂, CO. In the second main weight loss which is beyond 700 °C, characteristic peaks of HBr were observed in addition to CO₂ and CO peaks.

The TGA and DTG curves showed the thermal stability of **CLP** in Figure 3.1.6. Figure A 4 from a to d shows the in situ FTIR spectrum of evolved volatile components at each mass loss. The generation of H₂O was observed over the whole range because of the trap water in cross-linked region of polymers. In the beginning stage of degradation, the characteristic peaks of H₂O were observed with a 30% weight loss. In the second stage of degradation shows characteristic peaks of CO₂. Then around 550 °C, peak of CO was evolved. Finally beyond 700 °C, characteristic peaks of HBr started to be observed. It is commonly believed that a crosslinked polymer will be inherently more thermally stable than is the corresponding thermoplastic polymer e.g. polystyrene and cross-linked polystyrene [119].

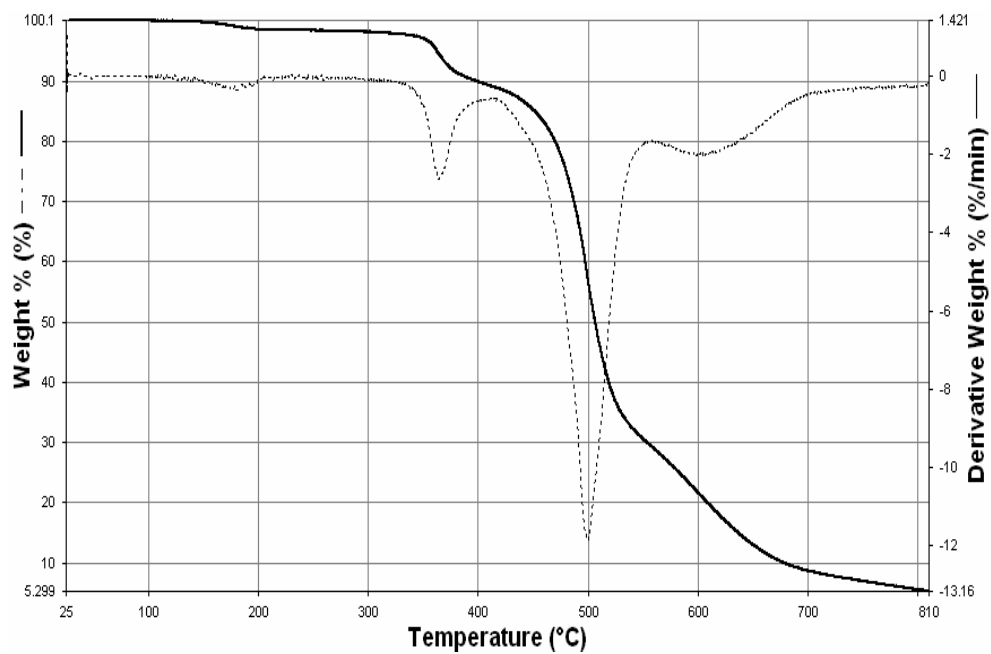


Figure 3.1.3 TGA thermograms of P (TBP and NaOH).

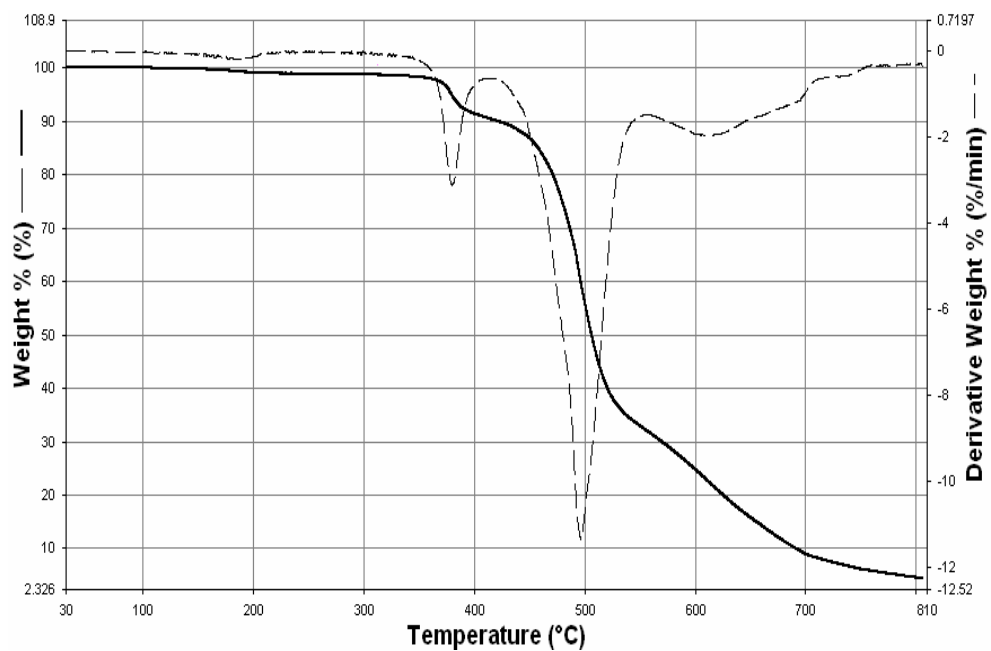


Figure 3.1.4 (a) TGA thermograms of RIP (TBP and NaOH).

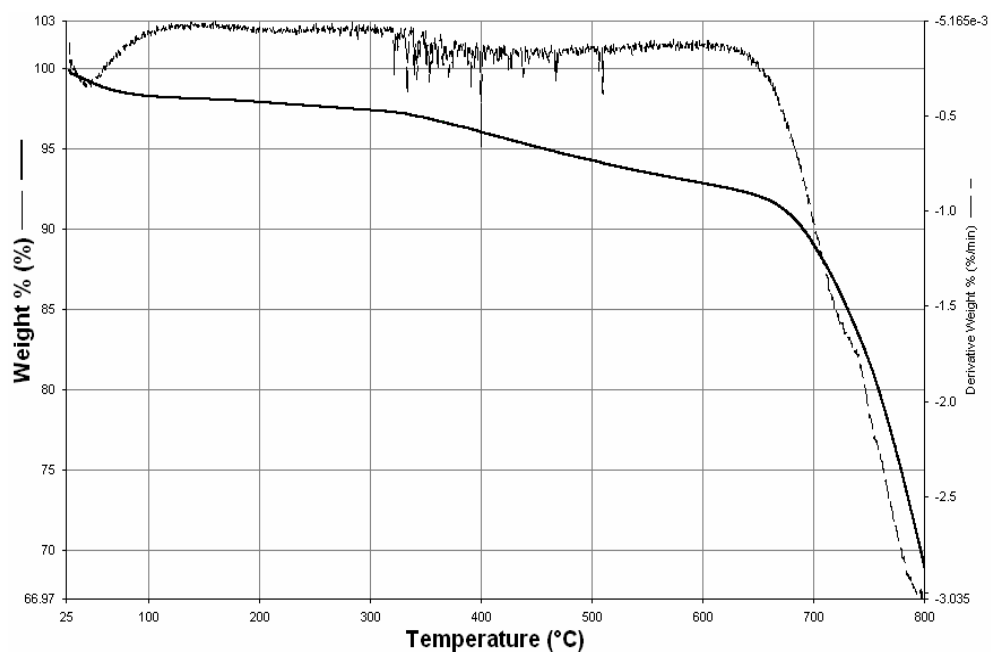


Figure 3.1.5 TGA thermograms of CP (TBP and NaOH).

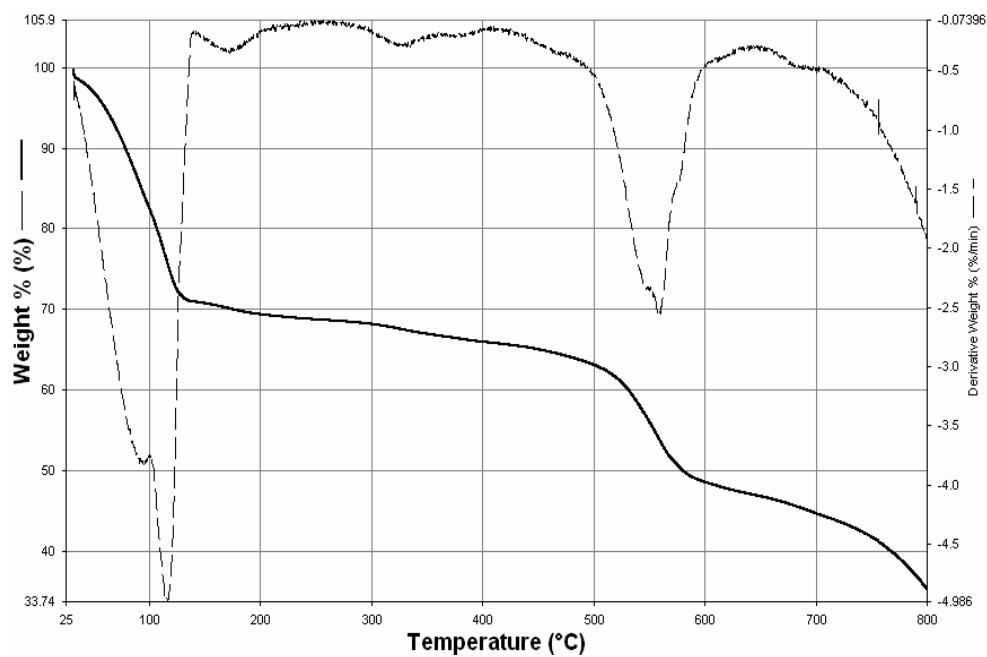
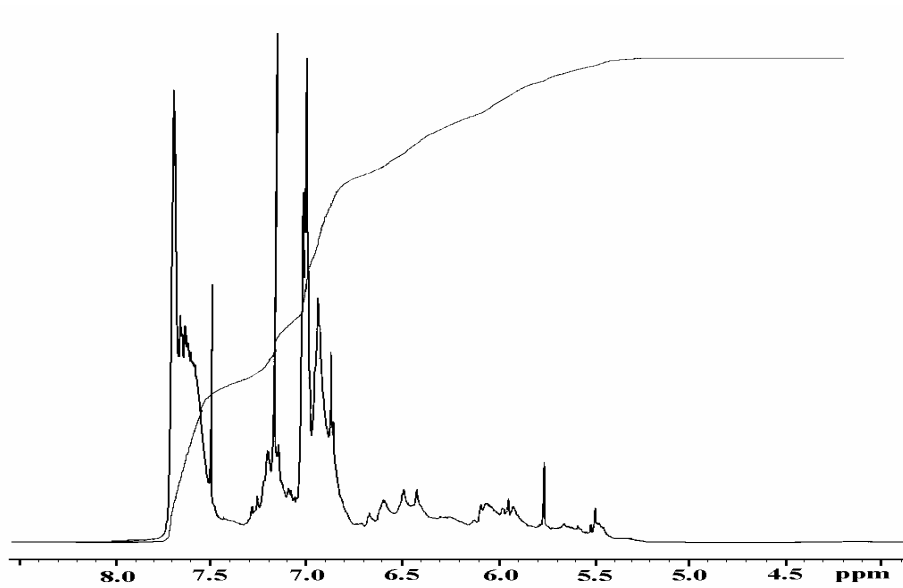


Figure 3.1.6 TGA thermograms of CLP (TBP and NaOH).

The ^1H -NMR spectrum of **P** and **RIP** were characterized by the intense peak at 7.0 ppm due to protons of 2,6-dibromo-1,4-phenylene oxide (1,4-addition) and at 7.6 ppm due to protons of 2,4-dibromo-1,6-phenylene oxide unit (1,2 addition) and the broader peaks at higher field due to the presence of 1,2 and 1,4-addition on the same monomeric unit (Figure 3.1.7).

^{13}C -NMR decoupled spectrum of **P** is displayed in Figure 3.1.8. The theoretical ^{13}C -NMR chemical shift data for five possible addition products were calculated by using appropriate tables [93]. ^{13}C -NMR shift data showed that **P** correlated well with the structure (Figure 3.1.9c and d) indicating 1,2- and 1,4-addition at almost equal rate.

a)



b)

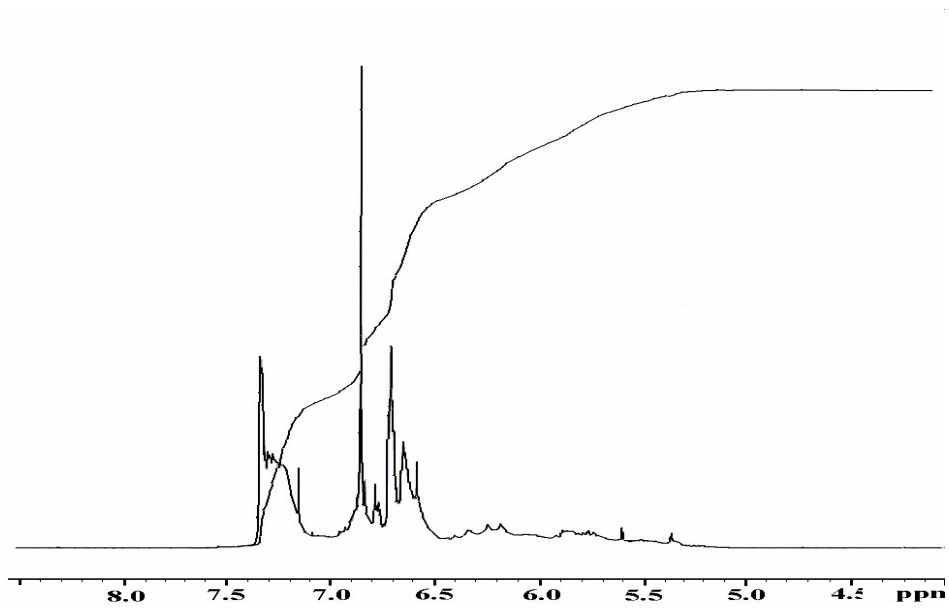


Figure 3.1.7 ¹H-NMR spectrum of (a) **P** and (b) **RIP** (TBP and NaOH).

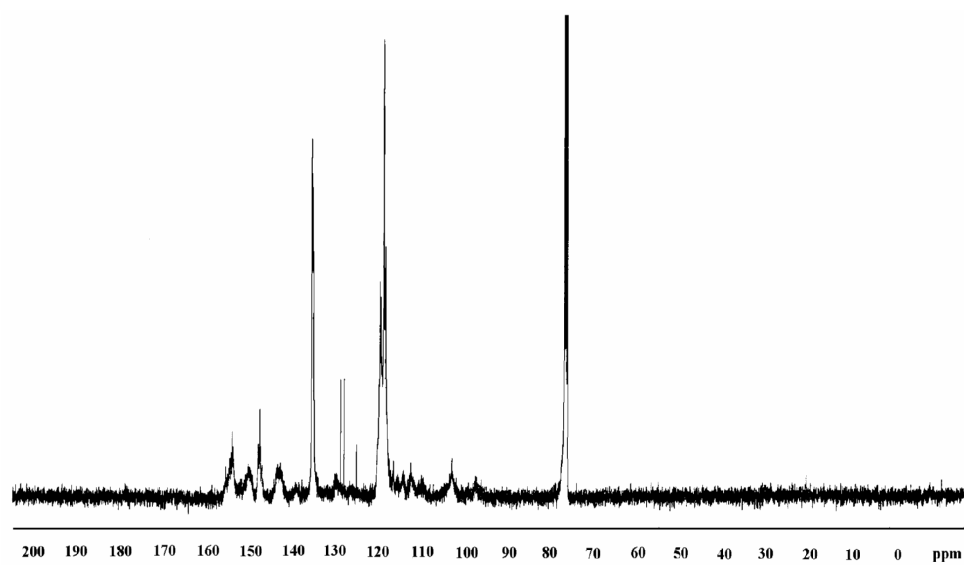


Figure 3.1.8 Proton-decoupled ^{13}C -NMR spectra of **P** (TBP and NaOH).

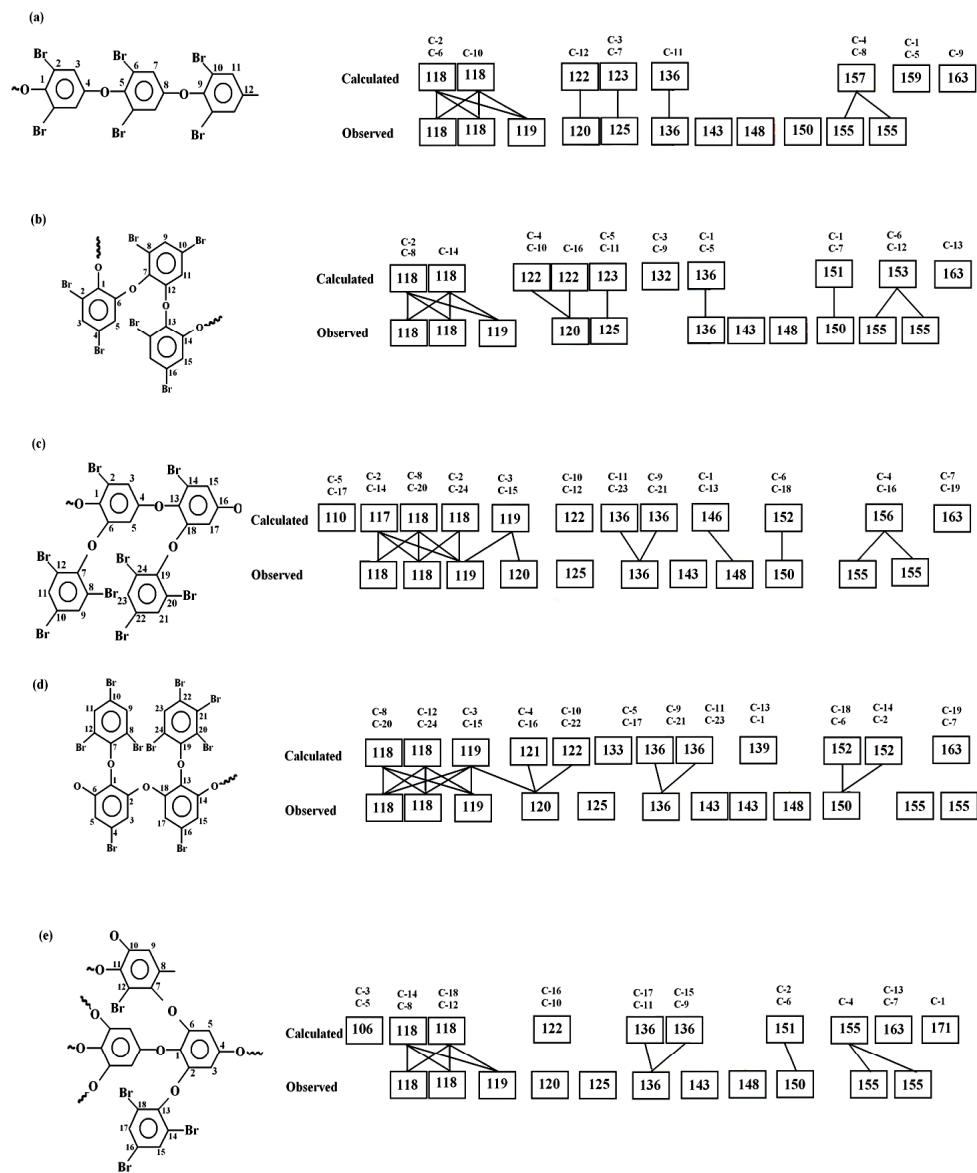


Figure 3.1.9 ^{13}C -NMR proton shift data of **P** (TBP and NaOH).

The powder diffraction X-ray spectrum of unwashed CP contains three strongest line of d-spacing of NaBr (byproduct during the polymer synthesis) (Figure 3.1.10a). Then CP was washed with hot water several times to remove all NaBr. The washed CP having a broad line in the spectrum indicates an amorphous polymer (Figure 3.1.10b).

The direct synthesis of highly conducting polymers was achieved in the absence of applied doping process with microwave-assisted polymerization in a very short time sequence. The electrical conductivities of washed CP, unwashed CP and RIP were measured as 0.1, 1 and 1×10^{-4} S cm⁻¹ respectively whereas CLP and P were insulators. Conductivity of washed CP was higher than unwashed CP, indicating doping effect of NaBr. Very similar conductivity values were observed for CP which was synthesized at different reaction conditions (such as variations in microwave- energy, time and amount of water).

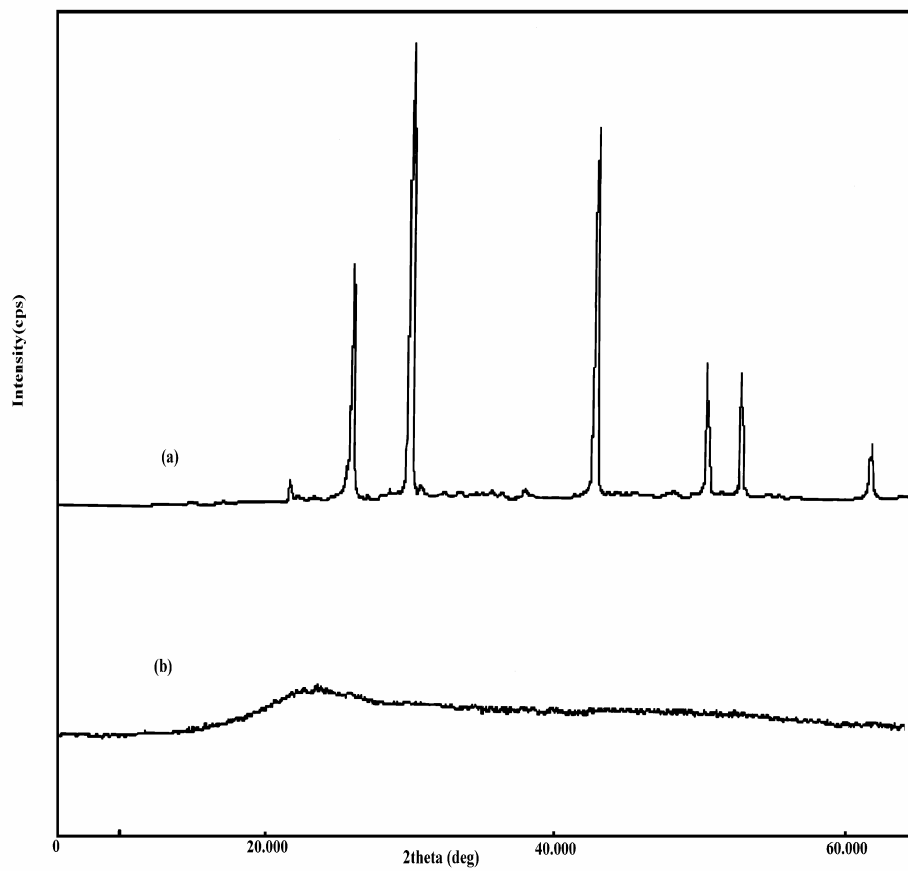


Figure 3.1.10 X-ray powder diffraction spectrum of (a) unwashed **CP** and (b) washed **CP** (TBP and NaOH).

ESR spectrum was used in order to confirm the presence of radicals in synthesized polymers. ESR spectra of polymers were recorded at room temperature. As a result, **RIP**, **CLP** and **CP** presence were revealed by the signals with *g* values of 2.00552, 2.00549 and 2.00294 respectively (Figure 3.1.11 a, b and c) which were very close to the *g* values of free electron (2.0023).

The UV-Visible absorption spectrum of monomer and polymers dissolved in toluene were shown in Figure 3.1.12. The spectrum of monomer (TBP) and **P** showed single absorption maxima around 270 nm which can be correlated to absorption of aromatics (Figure 3.1.12a and b). However, in the spectrum of **RIP** and soluble part of **CLP** - evolution of new broad band located around 470 nm were observed - which can be related to the π - π^* transition and the formation of polarons (Figure 3.1.12c and d).

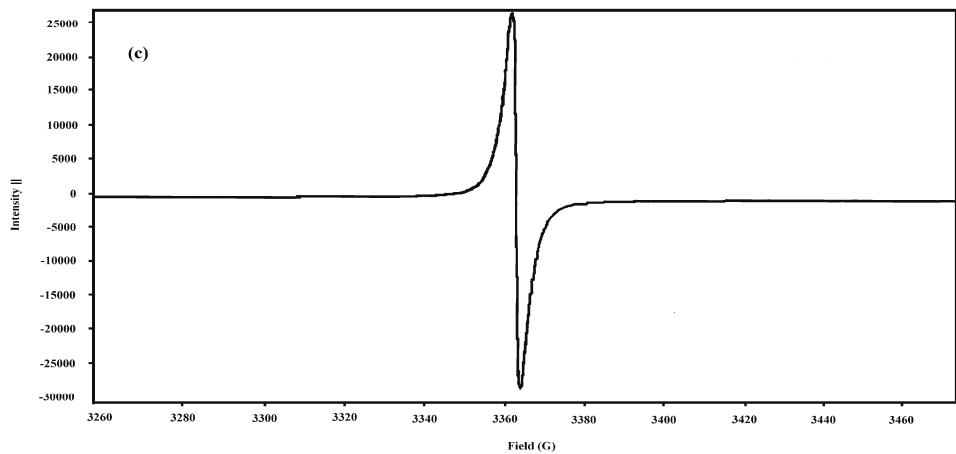
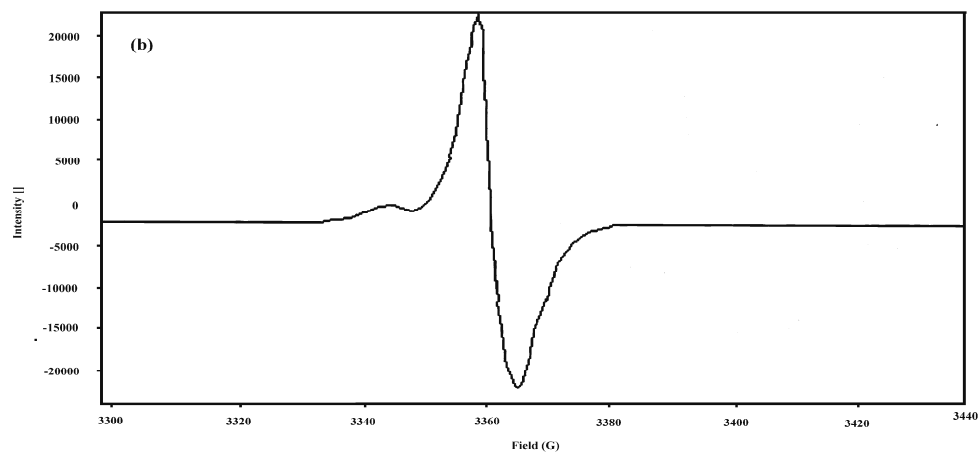
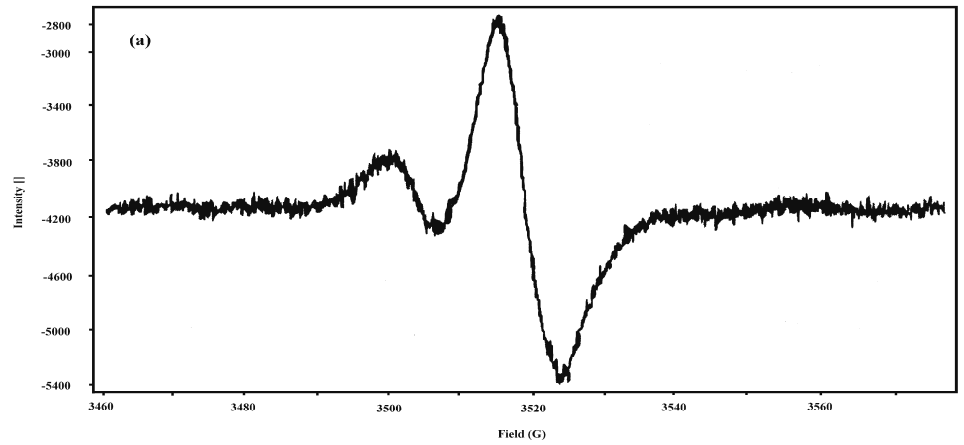


Figure 3.1.11 ESR Spectrum of (a) **RIP**, (b) **CLP** and (c) **CP** (TBP and NaOH).

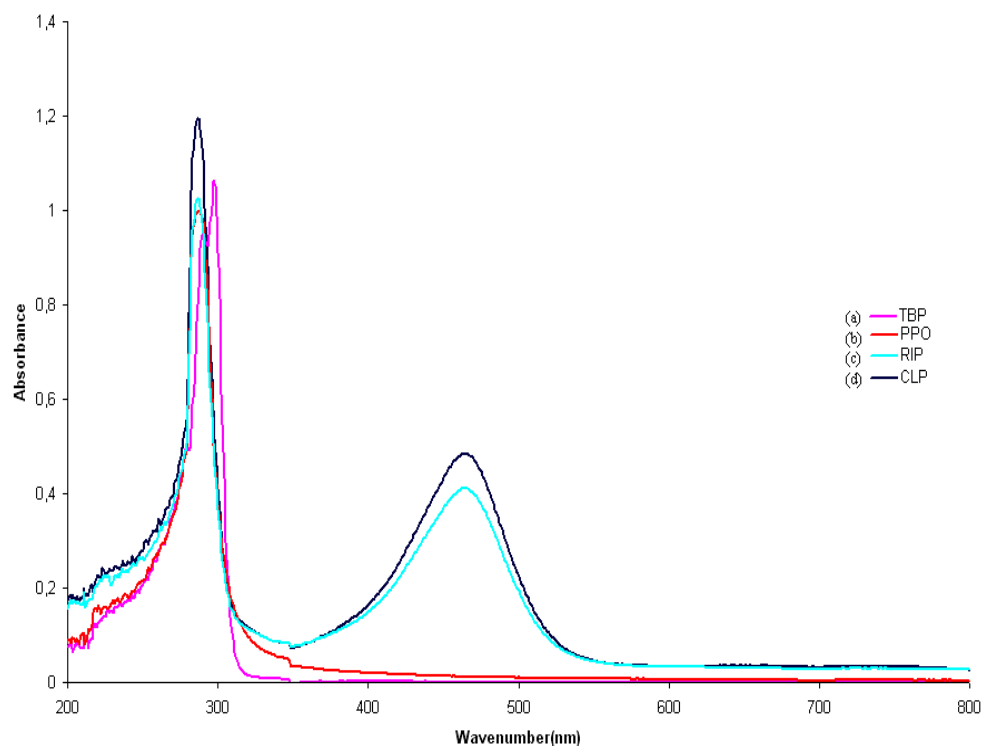
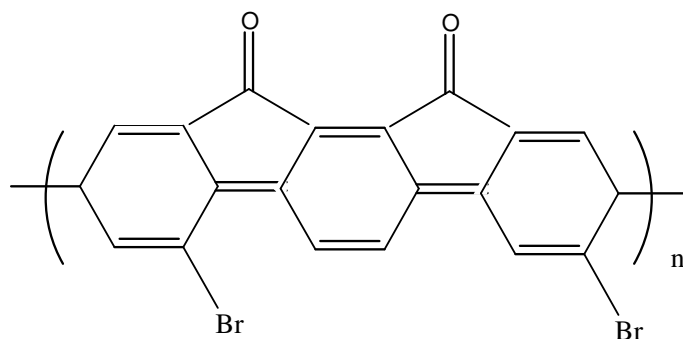


Figure 3.1.12 UV-Vis Spectrum of (a) TBP, (b) **P** and (c) **RIP** and (d) soluble part of **CLP** (TBP and NaOH) at room temperature .

The weight average molecular weight (\overline{M}_w) of the **P** (in 5 ml water, at 70 watt) and **RIP** were determined as 2.97×10^5 g/mol and 1.2×10^4 g/mol by the light scattering respectively. The highest molecular weight among the synthesized poly(dihalophenylene oxide)s was achieved. The radius of gyration and the second virial coefficient for **P** determined as 2.285×10^2 nm and 2.125×10^{-7} mol dm^3/g^2 and for **RIP** 3.619×10^1 nm and 4.119×10^{-7} mol dm^3/g^2 respectively. The observed $\overline{M}_w/\overline{M}_n$ values for **P** and **RIP** are 1.026 and 1.363 respectively by means of GPC.

Analysis of the surface morphologies of all types of polymers were done by scanning electron microscope, (Figure 3.1.13 and 3.1.14). In Figure 3.1.13a, **P** had fine granular structure, significantly different from the **CP** having sponge like structures (Figure 3.1.13b, c and d) and tubular structures (Figure 3.1.13e and f) were observed as the applied energy increased. However, as the amount of water increased (0.5 to 1.0 ml) at 70 watt, the coexistence of spongy and dendrite structures of **CP** and **CLP** was detected, respectively (Figure 3.1.14 a). In Figure 3.1.13b and c, structures of **CP** and **CLP** were more clearly seen when magnified 5000 times. At 350 watt in 1 min, as the amount of water increased (0.5 to 5.0 ml), only dendrite structures of **CLP** was observed (Figure 3.1.14d). By the application of 700 watt for 1 min in 5.0 ml water solution orange colored coarse surface of **RIP** was detected (Figure 3.1.14e). The X-ray microanalysis system detected the existence of O, Br and C on all of **P**, **CP**, **CLP** and **RIP** whereas Na detected on the unwashed **CP**.

From the elemental analysis, powder diffraction X-Ray, TGA, DSC and FTIR results, the following structure was proposed for **CP**:



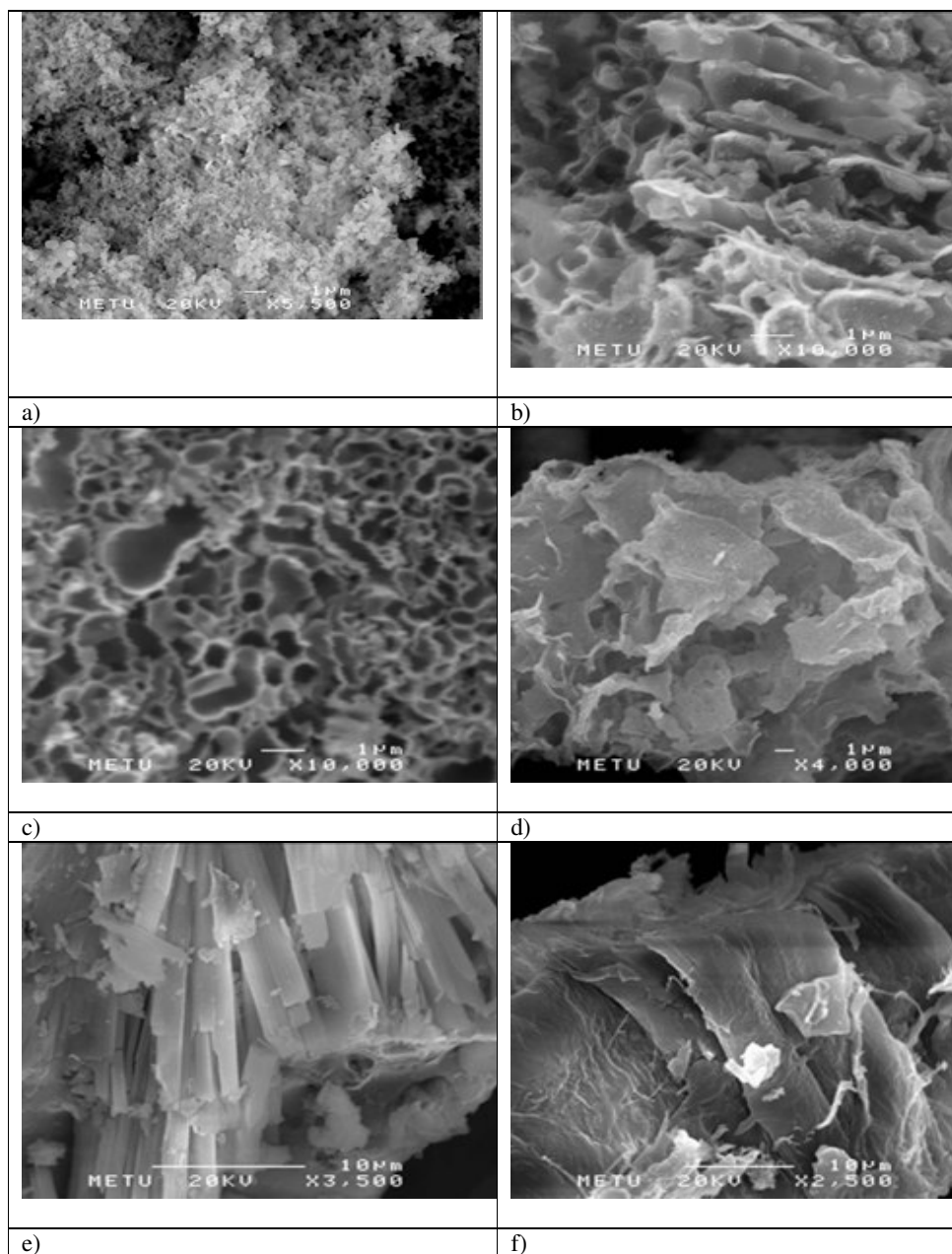


Figure 3.1.13 SEM micrographs of (a) **P** at 70 watt, 5min, (b) **CP** at 70 watt, 5 min, (c) **CP** at 100 watt (d and e) **CP** at 350 watt and (f) **CP** at 700 watt, 1 min in 0.5 ml water (TBP and NaOH).

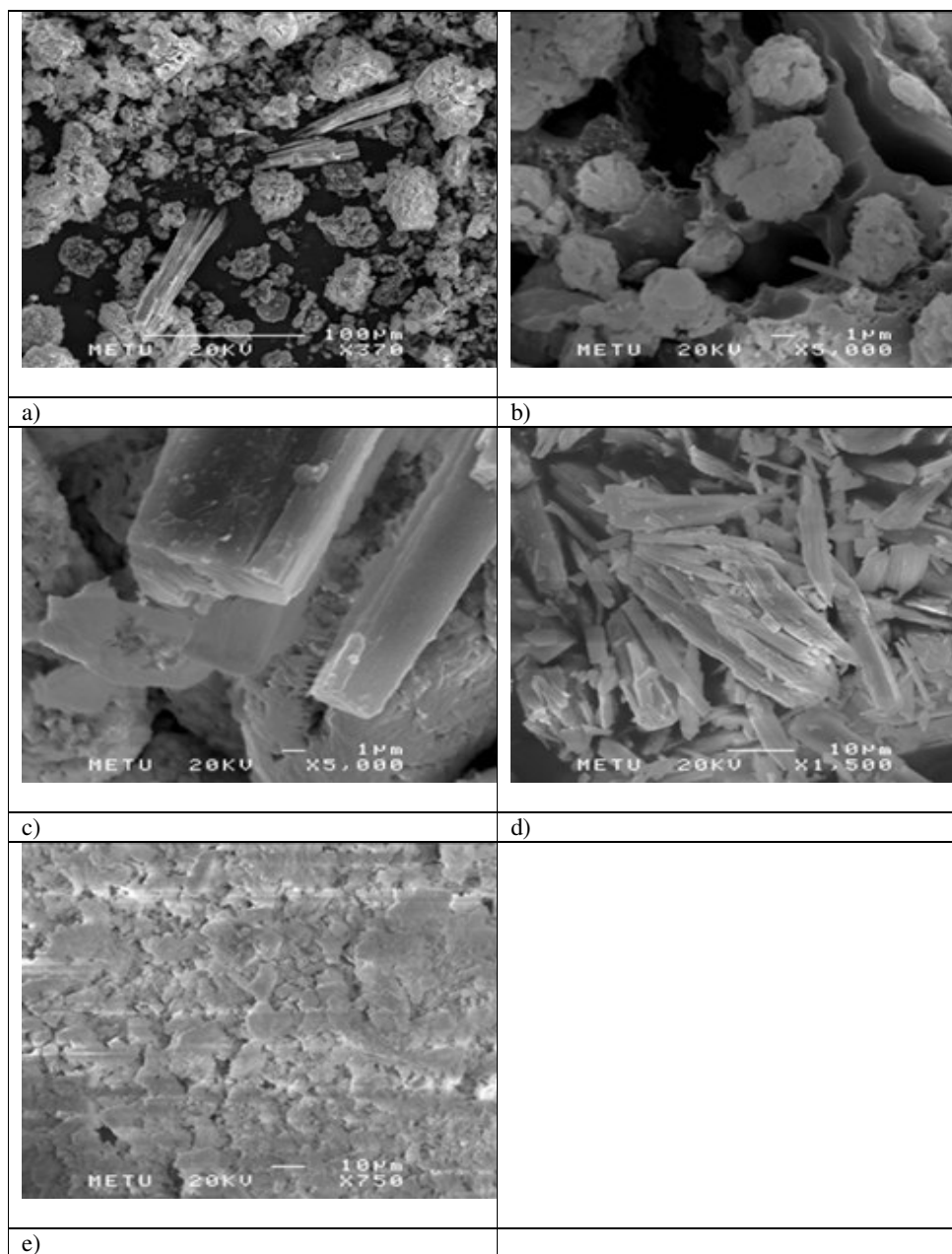


Figure 3.1.14 SEM micrographs of (a, b and c) CP at 70 watt, 5min in 0.5 ml water, (d) CLP at 350 watt and (e) RIP at 700 watt, 1 min in 5 ml water (TBP and NaOH).

3.2. Synthesis of Polymer with TBP and LiOH

A microwave-assisted novel synthesis of poly(dibromophenylene oxide) (**P**) and conducting polymer (**CP**) and/or crosslinked polymer (**CLP**) were achieved simultaneously from lithium 2,4,6-tribromophenolate with microwave energy in a very short time interval.

Table 3.2.1 listed the effect of polymerization time, energy and amount of water on the % conversions and polymerizations. At 90 watt and 180 watt, synthesis of **P** and **CLP**, whereas at 360 watt and 900 watt synthesis of **P** and **CP** were achieved simultaneously in 1 ml water. However, as the amount of water was increased to first 3 ml and then 5 ml, only the synthesis of **CP** and **CLP** were achieved at 360 watt and 900 watt, respectively. At 90 watt, the polymers synthesized at the end of 5 minutes whereas in the range of 180-900 watt, the syntheses were achieved in between 2 minutes. % conversion of **CP** and **CLP** showed an increasing trend as microwave energy increased from 90 to 900 watt. On the other hand, % conversion increased slightly for **P** up to 24.5% followed by a decrease to 12.1% at 900 watt. Hence, the optimum condition for synthesis of **P**, **CP** and **CLP** were at 180 watt for 2 min in 1 ml water, 900 watt for 5 min in 3 ml water, 900 watt for 10 min in 5 ml water having maximum % conversion values 24.5, 53.1 and 80.8 % respectively.

Table 3.2.1 The effect of polymerization time, energy and amount of water (w)

on the % **P**, **CP** and **CLP** (TBP and LiOH).

90 watt	5 min 1 ml water	10 min 3 ml water	20 min 5 ml water
%P	21,6	16,6	-
%CP	-	51,1	-
%CLP	45,3	-	59,3
180 watt	2 min 1 ml water	5 min 3 ml water	20 min 5 ml water
%P	24,5	13,9	-
%CP	-	48,3	-
%CLP	43,9	-	66,7
360 watt	2 min 1 ml water	5 min 3 ml water	5 min 5 ml water
%P	15,4	-	-
%CP	29,9	50,6	-
%CLP	-	-	79,2
900 watt	2 min 1 ml water	5 min 3 ml water	10 min 5 ml water
%P	12,1	-	-
%CP	35,6	53,1	-
%CLP	-	-	80,8

3.2.1 Characterization

The results of the elemental analysis of all polymers correlate perfectly with the written stoichiometries given in Table 3.2.2.

Table 3.2.2 Elemental analysis results of **P**, **CLP** and **CP** (TBP and LiOH) (experimental errors ± 0.5).

	% C		% H	
	Calc.	Found	Calc.	Found
P	31.72	31.19	1.31	1.34
CLP	-	24.14	-	1.62
CP	-	25.31	-	0.48

FTIR spectra of **P** exhibited the characteristic absorptions at 850 cm^{-1} (out of plane C-H bending), $955\text{-}1040\text{ cm}^{-1}$ (C-O-C stretching), $1140\text{-}1210\text{ cm}^{-1}$ (C-O stretching), 1440 and 1580 cm^{-1} (C=C ring stretching), 3079 cm^{-1} (aromatic C-H stretching) and 3500 cm^{-1} (the phenolic end group) (Figure 3.2.1a).

FTIR spectra of **CLP** (Figure 3.2.1b) was similar to FTIR spectra of **P** except $955\text{-}1040\text{ cm}^{-1}$ (C-O-C stretching) was shifted to $1050\text{-}1200\text{ cm}^{-1}$.

FTIR spectra of **CP** exhibits the peaks at 1460-1600 cm^{-1} (C=C stretching of both benzenoid and quinoid structures), 1710 cm^{-1} (C=O stretching), 1110-1280 cm^{-1} (C-O stretching), 3050 cm^{-1} (aromatic C-H stretching) and 730-760 cm^{-1} (C-Br stretching) (Figure 3.2.1c).

FTIR spectra of the evolved gas collected in a glass cell during polymerization, exhibits the peak at 2450 cm^{-1} (CO_2) and 1270 cm^{-1} (C=O stretching) (Figure 3.2.1d).

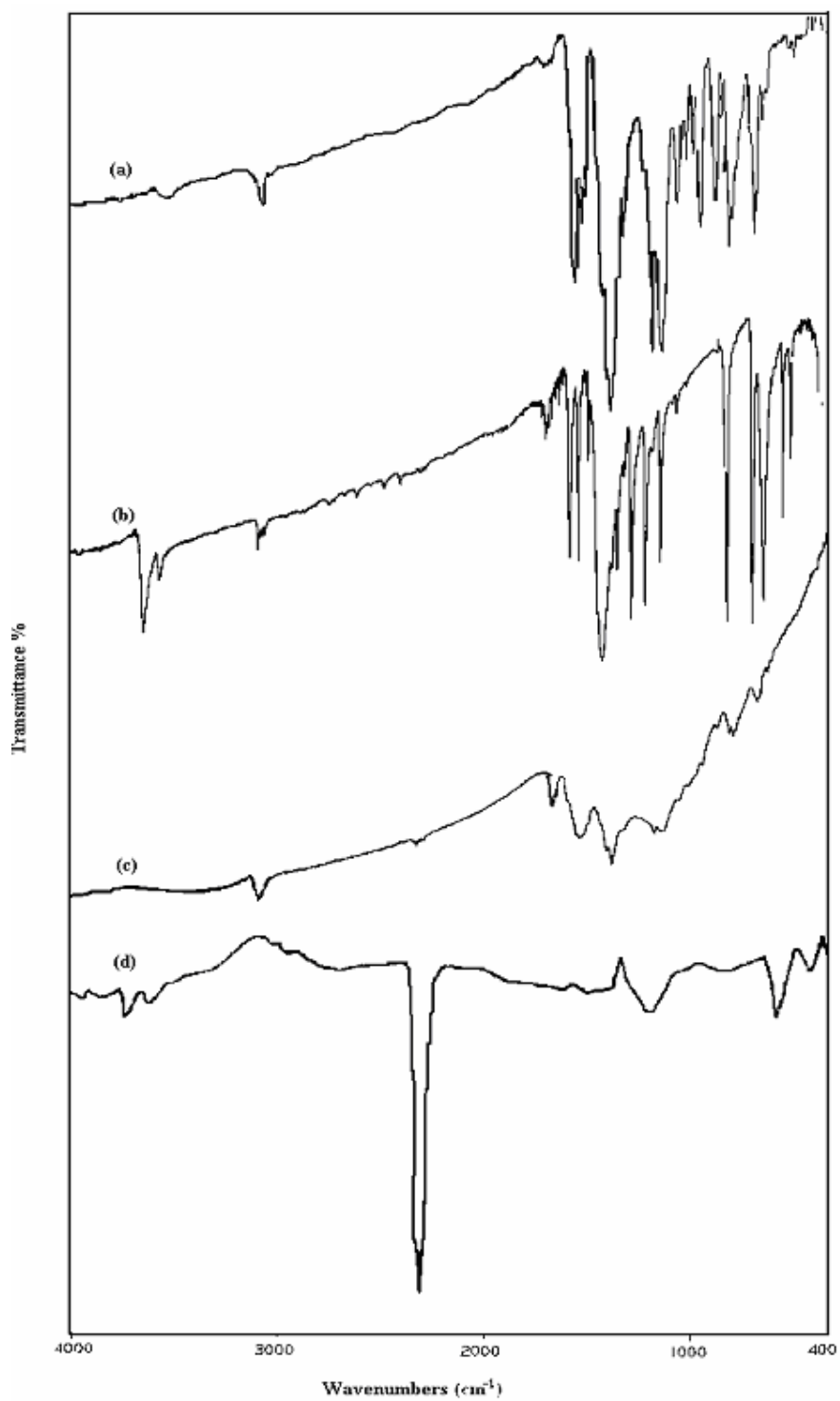


Figure 3.2.1 FTIR spectrum of (a) **P**, (b) **CLP**, (c) **CP** and (d) released gases during polymerization (TBP and LiOH).

The DSC thermograms of the **P** and **CLP** have glass transition temperature 173.03 and 208.87 °C respectively, indicating high rigidity of polymers whereas, glass transition temperature was not observed for **CP** (Figure 3.2.2).

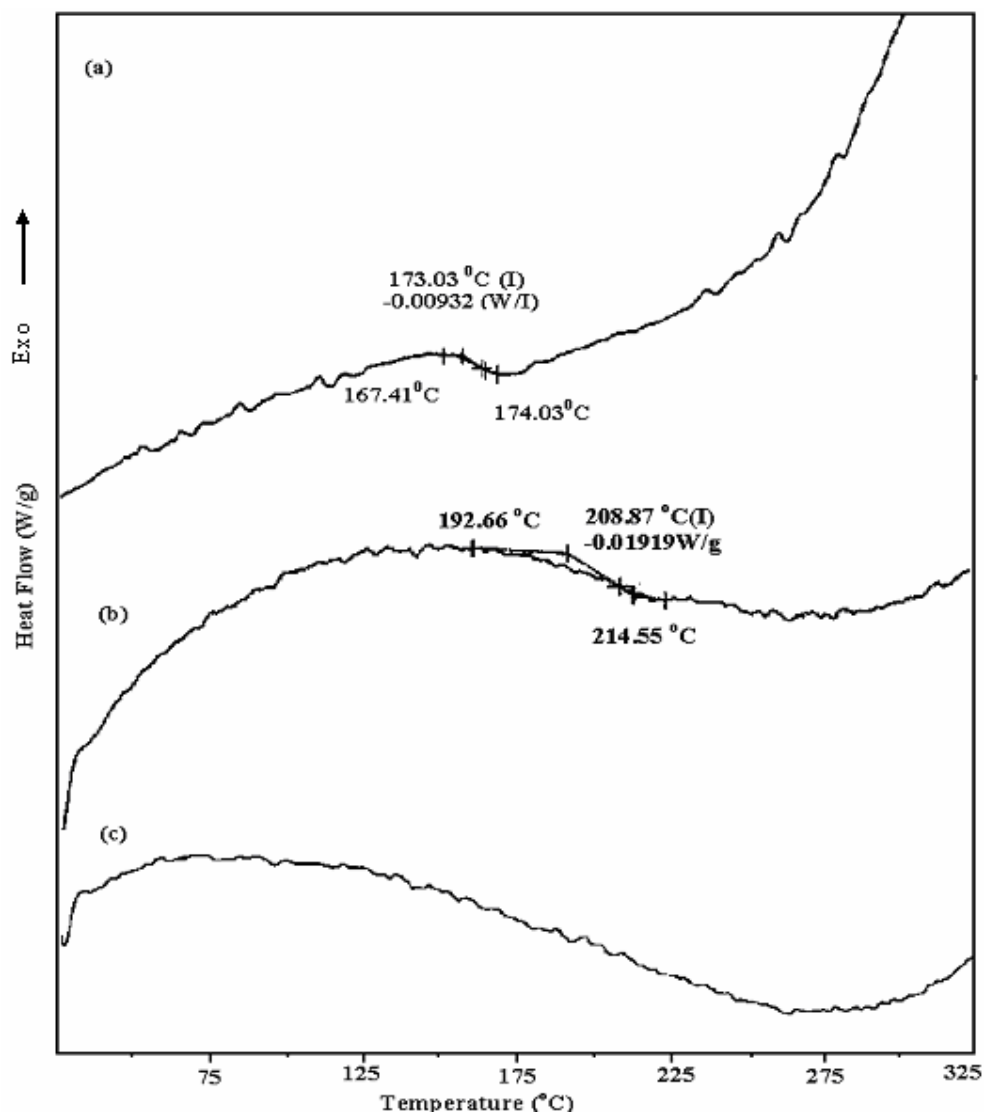


Figure 3.2.2 DSC thermograms of (a) **P**, (b) **CLP** and (d) **CP** (TBP and LiOH).

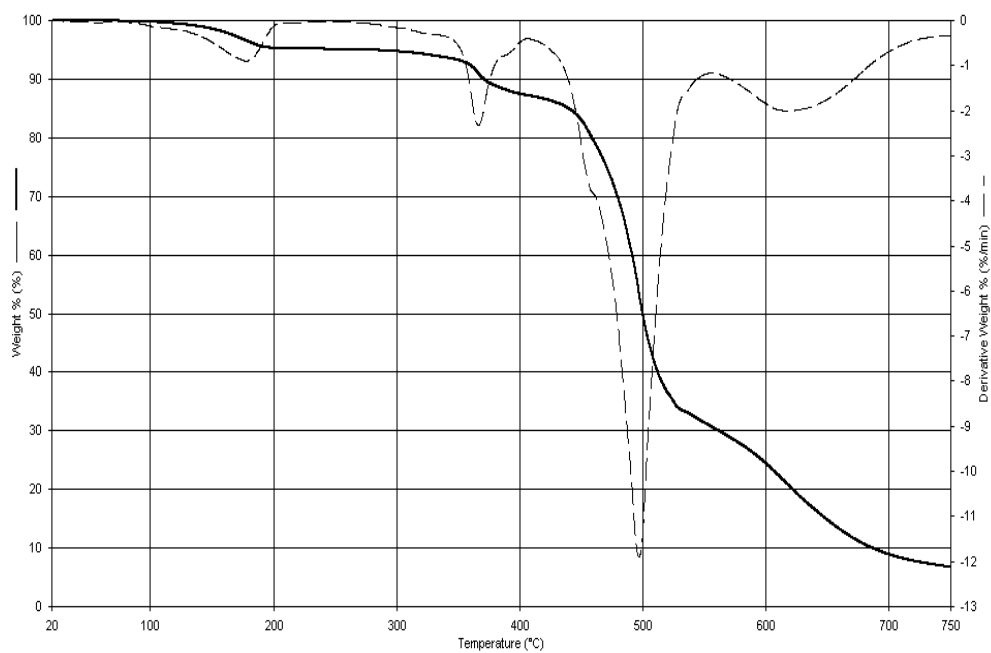
TGA weight loss curve and the corresponding derivative curves (DTG) for **P** were shown in Figure 3.2.3a. In situ FTIR spectra of the evolved gases during the thermal gravimetric analysis were very similar to these of **P** synthesized from sodium 2,4,6-bromophenolate (Figure 3.1.3 from b to f). **P** shows no weight loss up to 140 °C and was stable up to nearly 370 °C and then approximately 65 % of sample was lost when the temperature reached to 500 °C. Decomposition occurs in four stages with the small weight loss around 170 °C and 380 °C, main degradation around 490 °C and 620 °C. In the first and second stage of degradation with a weight loss of 5% and 7% respectively, the characteristic peaks of an aromatic groups (2974, 2880, 1380 cm^{-1}) were observed. For the main degradations around 490 °C and 620 °C, bands of CO_2 (2358 and 2309 cm^{-1}), CO (2100-2200 cm^{-1}), HBr (2300-2700 cm^{-1}), vinyl bromide (1460 and 2950 cm^{-1}) were observed.

The TGA and DTG curves showed that **CLP** was more stable than **P** (Figure 3.2.3b). Sharp weight loss (13 %) observed up to 120 °C followed by a slight decrease up to 200 °C due to the trapped water. 70 % **CLP** remained when the temperature reached to 750 °C which showed the stability of polymer. The generation of H_2O was observed over the whole range because of the trapped water in crosslinked region of polymers. In the beginning stage of degradation, the characteristic peaks of H_2O were observed with 18 % weight loss. In the second stage of degradation showed characteristic peaks of CO_2 (2358 and 2309 cm^{-1}). Then around 500 °C, peak due to CO (2100-2200 cm^{-1}) was observed. Finally beyond 700 °C, characteristic peaks of HBr (2300-2700 cm^{-1}) started to be observed.

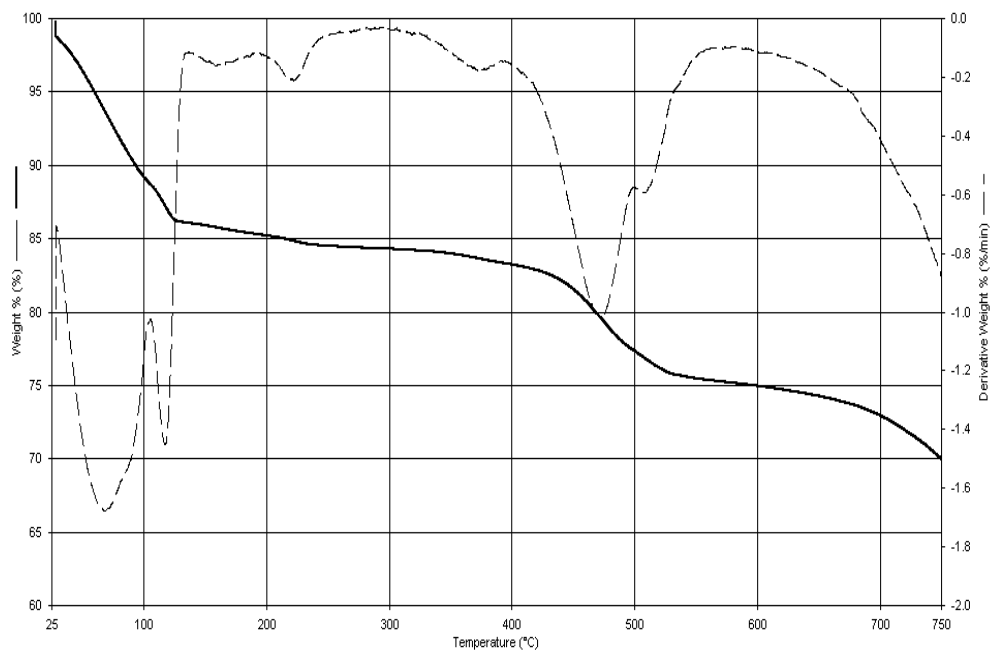
In the case of **CP**, the weight loss started from 450 °C, indicating a higher thermal stability and still having residues of 84 % beyond 750 °C (Figures 3.2.3c). The main decomposition occurs in two stages. In the first emission around 350 °C characteristic bands of CO_2 (2358 and 2309 cm^{-1}) and CO (2100-2200 cm^{-1}) were observed. In the second main weight loss which is beyond

450 °C, characteristic peaks of Br (2300-2700 cm^{-1}) were observed in addition to CO_2 and CO peaks.

a)



b)



c)

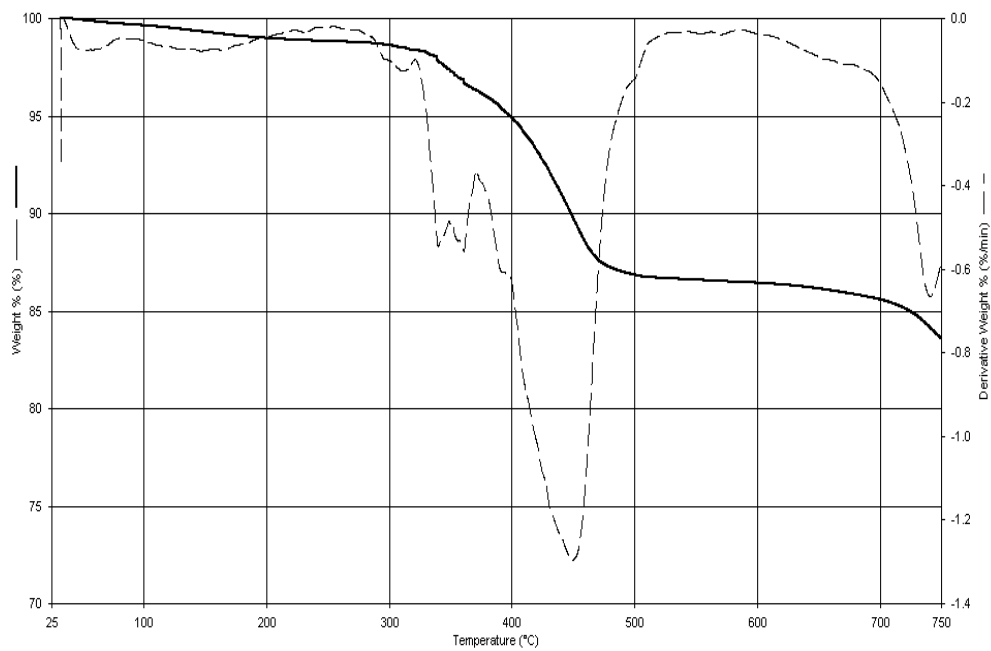


Figure 3.2.3 TGA thermograms of (a) **P** (b) **CLP** and (c) **CP** (TBP and LiOH).

The ^1H -NMR spectra of **P** showed the peak at 7.0 ppm due to protons of 2,6-dibromo-1,4-phenylene oxide (1,4-addition) and the smaller peak at 7.3 ppm due to protons of 2,4-dibromo-1,6-phenylene oxide unit (1,2 addition) and the broader peaks at higher field due to the presence of 1,2 and 1,4-addition on the same monomeric unit indicating 1,2- and 1,4-additions were taking place at equal rates (Figure 3.2.4). ^{13}C -NMR decoupled spectrum of **P** is displayed in Figure 3.2.5. The theoretical ^{13}C -NMR chemical shift data for five possible addition products were calculated by using appropriate tables. ^{13}C -NMR shift data showed that **P** correlated well with the structure (Figure 3.1.9c and d) indicating 1,2- and 1,4-addition at almost equal rate.

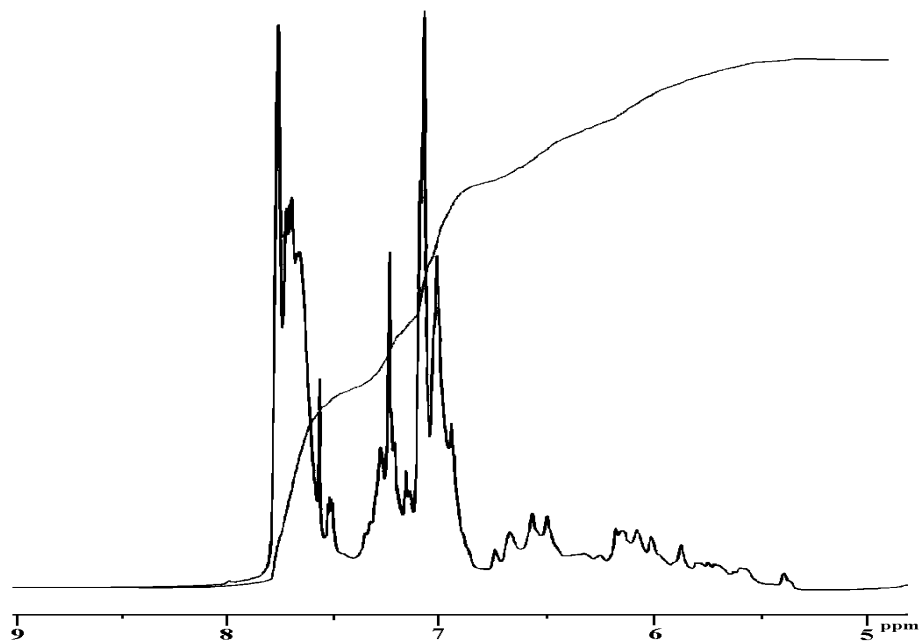


Figure 3.2.4 ^1H -NMR spectrum of **P** (TBP and LiOH).

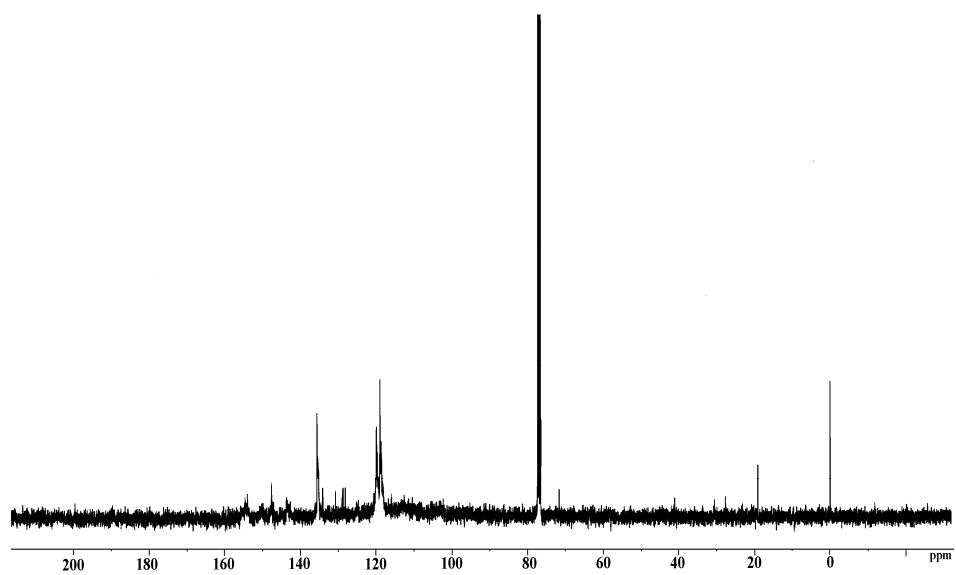


Figure 3.2.5 Proton-decoupled ^{13}C -NMR spectrum of **P** (TBP and LiOH).

Figure 3.2.6a showed the powder X-ray diffraction pattern of the unwashed **P**. The diffraction peaks are in good agreement with those of LiCO_3 crystals which can be indexed as the monoclinic structure of LiCO_3 (JCPDS card no 83-1454). **P** was washed with diluted HCl and hot water in order to remove LiCO_3 crystals trapped in the synthesized polymer. After that, a broad X-ray spectrum of polymer was observed indicated the presence of an amorphous polymer (Figure 3.2.6b).

Two and four probe conductivity measurements were performed on compacted disks of the polymers. The electrical conductivities of washed and unwashed **CP** fall in the range of 10^{-2} and 10^{-3} S cm^{-1} respectively whereas **CLP** and **P** were insulators. Conductivity of unwashed **CP** was higher than washed **CP**, indicating that LiCO_3 crystals decrease the conductivity. Very similar conductivity values were observed for **CP** which was synthesized at different reaction conditions (microwave- energy, time and water content).

ESR spectra of **CLP** and **CP** revealed the signals with g values of 2.0068 and 2.0017 respectively (Figure 3.2.7a and b) which were very close to g values of free electron (2.0023).

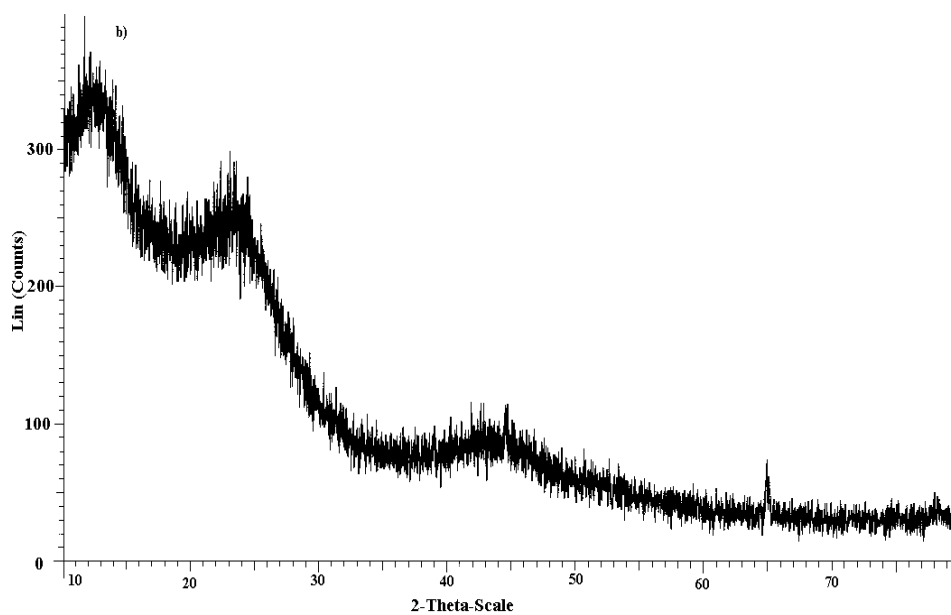
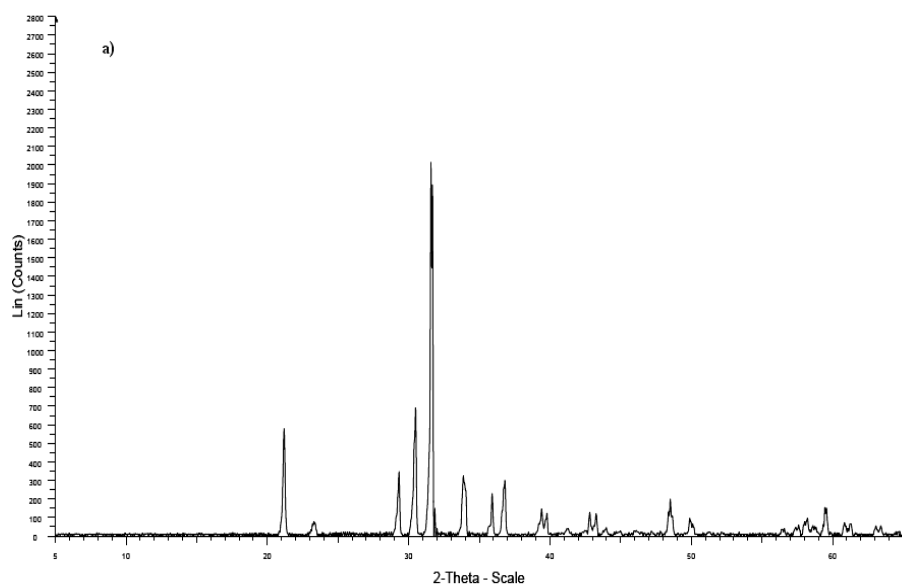
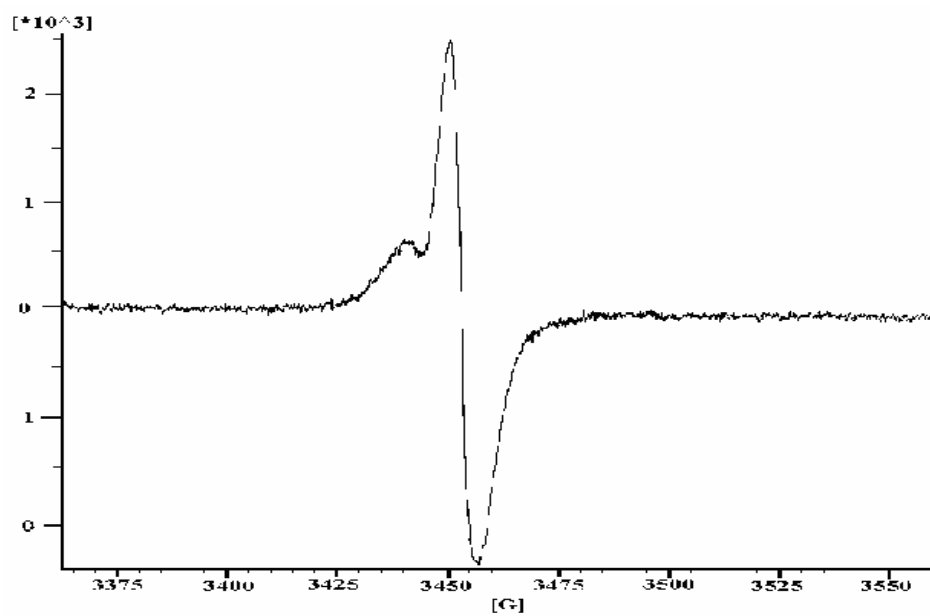


Figure 3.2.6 X-ray powder diffraction spectra of (a) unwashed CP and (b) washed CP (TBP and LiOH).

a)



b)

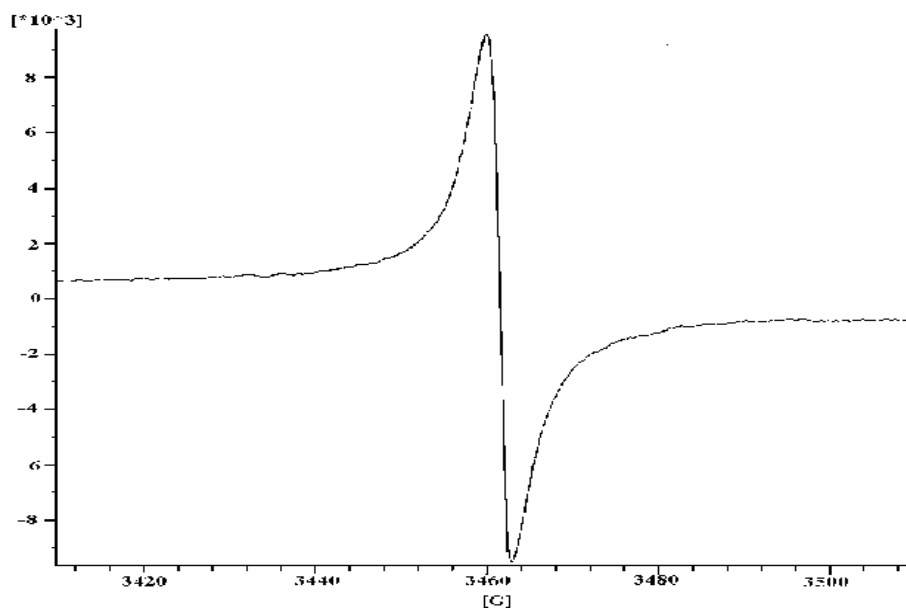


Figure 3.2.7 ESR Spectrum of (a) **CLP** and (b) **CP** at room temperature (TBP and LiOH).

The UV-Visible absorption spectra of synthesized polymers dissolved in toluene were shown in Figure 3.2.8. The spectra of **P** showed single absorption maxima around 270 nm which can be correlated to absorption of aromatics (Figure 3.2.8a). In addition, the formation of polarons was observed for the soluble part of **CLP** with the evolution of new broad band located around 470 nm, was related to the π - π^* transition and the formation of polarons (Figure 3.2.8b).

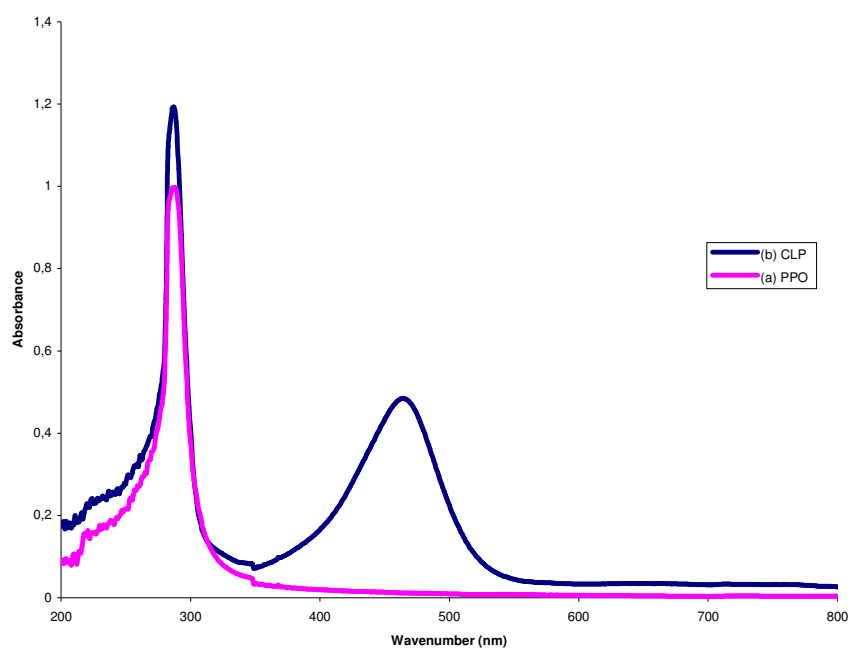
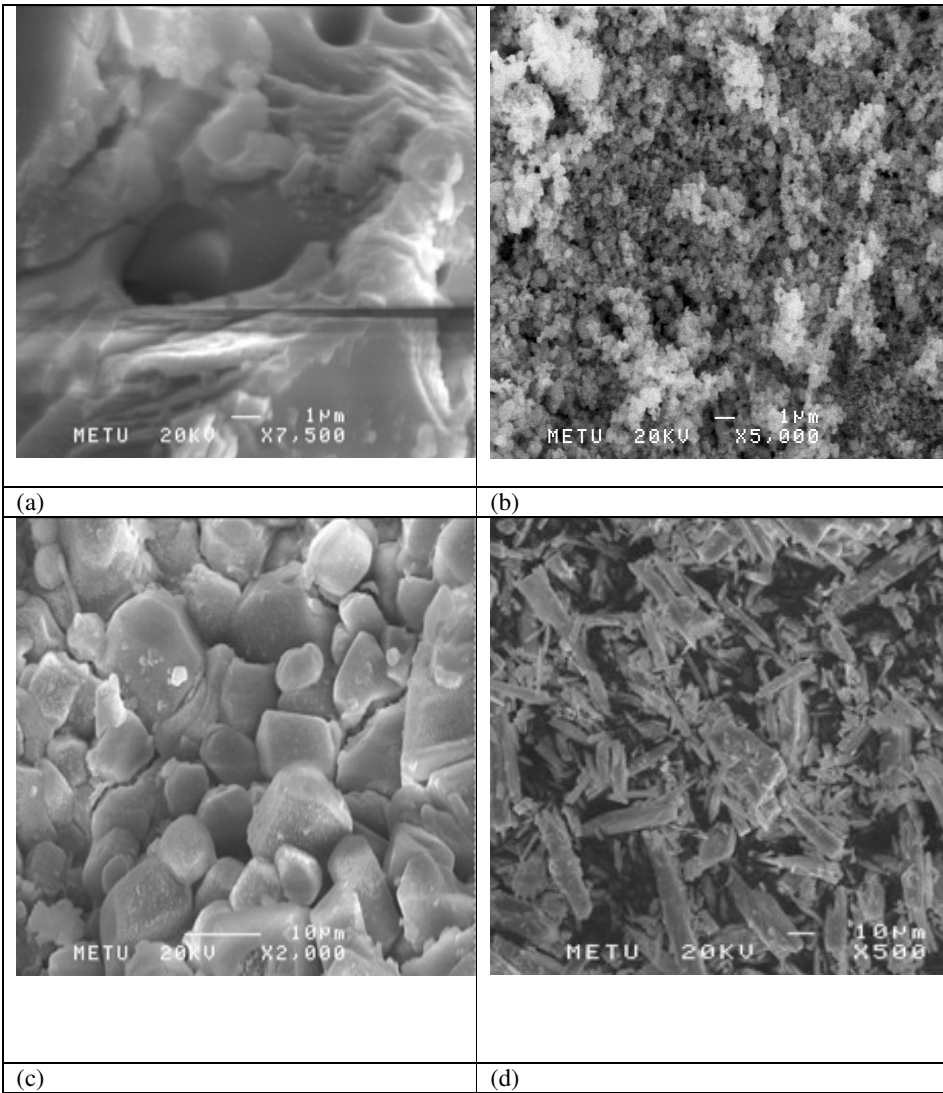


Figure 3.2.8 UV-Vis Spectrum of (a) **P** and (b) soluble part of **CLP** at room temperature (TBP and LiOH).

The scanning electron microscope images showed that polymers morphology were different. The existence of LiCO_3 was observed on the surface of the unwashed **P**, **CLP** and **CP** (Figure 3.2.9a, c and g, respectively), like observed in X-ray spectrum. The washed **P** (Figure 3.2.9b) had fine granular structure, significantly different from the washed **CLP** (Figure 3.2.9d, e and f) having dendrite like structures. However, sponge like structure was observed for washed **CP** (Figure 3.2.9h). The X-ray microanalysis system detected the existence of O, Br and C in all of washed **P**, **CP** and **CLP** samples.

The molecular weight of the **P** was determined as 1.123×10^5 g/mol by using light scattering. Radius of gyration and second virial coefficient of the **P** were determined as 1.856×10^2 nm and 1.298×10^{-7} mol.dm³/g² respectively.

Two and four probe conductivity measurements were performed on compacted disks of the polymers. The electrical conductivities of washed and unwashed **CP** fall in the range of 10^{-2} and 10^{-3} S cm⁻¹ respectively whereas **CLP** and **P** were insulators. No significant changes in the conductivities were observed in the **CP** which was synthesized at different reaction conditions (such as variations in microwave- energy, time and amount of water).



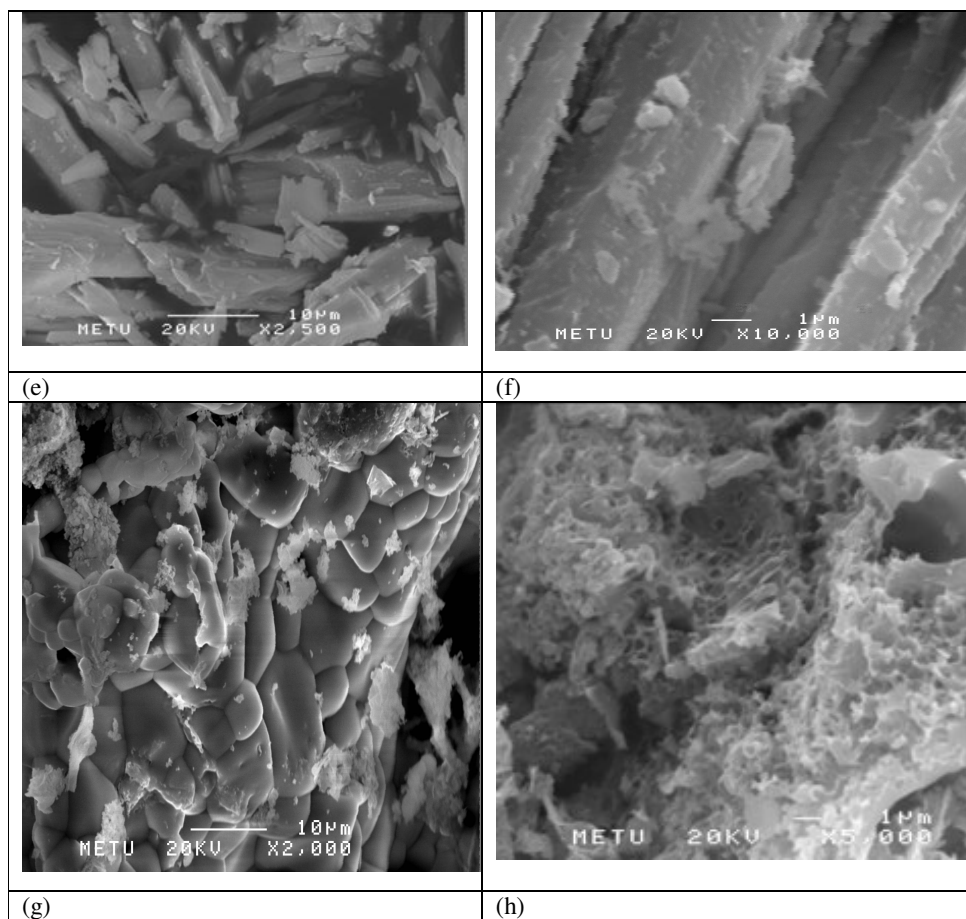


Figure 3.2.9 SEM micrographs of (a) Unwashed P (b) Washed P (c) Unwashed CLP (d, e and f) Washed CLP (g) Unwashed CP (h) Washed CP (TBP and LiOH).

3.3. Synthesis of Polymer with TBP and KOH

Microwave-assisted simultaneous novel synthesis of poly(dibromophenylene oxide) (**P**), Radical ion polymer (**RIP**) and conducting polymer (**CP**) were achieved from potassium 2,4,6-tribromophenolate. Polymerizations were performed by varying the time from 1 to 7 min, microwave energy from 70 to 900 watt and amount of water from 0.5 to 5 ml.

The effect of polymerization time, energy and amount of water on the % conversions and %weight losses were listed in Table 3.3.1. At 70 watt, in 0.5 and 5.0 ml water, the % conversion of **P** showed an increasing trend up to 30 % at the end of 5 minutes and remained almost constant whereas there were no changes in % conversion of **CP**. The synthesis of **P** and **CP** were achieved in 3 min at 70 watt whereas in 1 min in the range of 100-900 watt. In addition, **RIP** synthesis was only achieved in between 17 to 25 minutes in 5 ml water at 70 watt and at the end of 3 minutes in between 0.5 to 5 ml water at 350 watt. In the range of 100-900 watt, generally % conversion slightly increased for **P** whereas decreased for **CP** as the time increased. On the other hand, % conversion slightly increased for **P** while decreased for **CP** as the amount of water was increased (0.5-5.0 ml). Hence, the optimum condition for **P** and **CP** was 350 watt for 1 min in 5 ml water and 500 watt for 1 min in 0.5 ml water, having maximum values 39.2 and 27.9 % respectively.

Table 3.3.1 The effect of polymerization time, energy and amount of water (w)

	3min	3min	5min	5min	17min	25min
70watt	0.5 ml w	5 ml w	0.5 ml w	5 ml w	5 ml w	5 ml w
% P	18.1	20.7	29.5	30.2	29.6 ^(a)	29.6 ^(a)
% CP	10.8	9.3	11.0	10.9	-	-
	1.5min	1.5min	3min	3min	5min	5min
180watt	0.5 ml w	5 ml w	0.5 ml w	5 ml w	0.5 ml w	5 ml w
% P	20.5	23.7	23.5	24.0	26.7	29.5
% CP	12.8	13.1	11.3	11.9	11.0	10.9
	1min	1min	1.5min	1.5min	3min	3min
350watt	0.5 ml w	5 ml w	0.5 ml w	5 ml w	0.5 ml w	5 ml w
% P	31.5	39.2	32.7	32.9	31.9 ^(a)	35.0 ^(a)
% CP	25.6	25.0	23.1	24.3	22.6	21.3
	1min	1min	1.5min	1.5min	3min	3min
500watt	0.5 ml w	5 ml w	0.5 ml w	5 ml w	0.5 ml w	5 ml w
% P	30.0	33.9	30.6	30.8	-	-
% CP	27.9	26.0	25.8	18.4	-	-
	1min	1min	1.5min	1.5min	3min	3min
900watt	0.5 ml w	5 ml w	0.5 ml w	5 ml w	0.5 ml w	5 ml w
% P	29.9	30.2	31.5	31.8	-	-
% CP	19.5	19.1	18.3	15.4	-	-
(a) RIP synthesized instead of P						

3.3.2 Characterization

Elemental analysis results of all polymers correlate perfectly with the written stoichiometries as tabulated in Table 3.3.2.

Table 3.3.2 Elemental analysis results of **P**, **RIP** and **CP** (TBP and KOH) (experimental errors ± 0.5).

	% C		% H	
	Calc.	Found	Calc.	Found
P	29.12	29.51	1.111	0.986
RIP	29.20	29.26	1.273	1.204
CP	-	68.36	-	1.216

FTIR spectrum of **P** and **RIP** exhibit the characteristic absorptions at 850 cm^{-1} (out of plane C-H bending), $955\text{-}1040\text{ cm}^{-1}$ (C-O-C stretching), $1140\text{-}1210\text{ cm}^{-1}$ (C-O stretching), 1440 and 1580 cm^{-1} (C=C ring stretching), 3079 cm^{-1} (aromatic C-H stretching) and 3500 cm^{-1} (the phenolic end group) (Fig. 3.3.1a and b), respectively. FTIR spectrum of **CP** exhibits the peaks at $1460\text{-}1600\text{ cm}^{-1}$ (C=C stretching of both benzenoid and quinoid structures), 1710 cm^{-1} (C=O stretching), $1110\text{-}1280\text{ cm}^{-1}$ (C-O stretching), 3050 cm^{-1} (aromatic C-H stretching) and $730\text{-}760\text{ cm}^{-1}$ (C-Br stretching) (Fig. 3.3.1c). The FTIR spectrum of the evolved gas collected in a glass cell during polymerization, exhibits the peak at 2450 cm^{-1} (CO_2), 1270 (C=O stretching) (Fig. 3.3.1d).

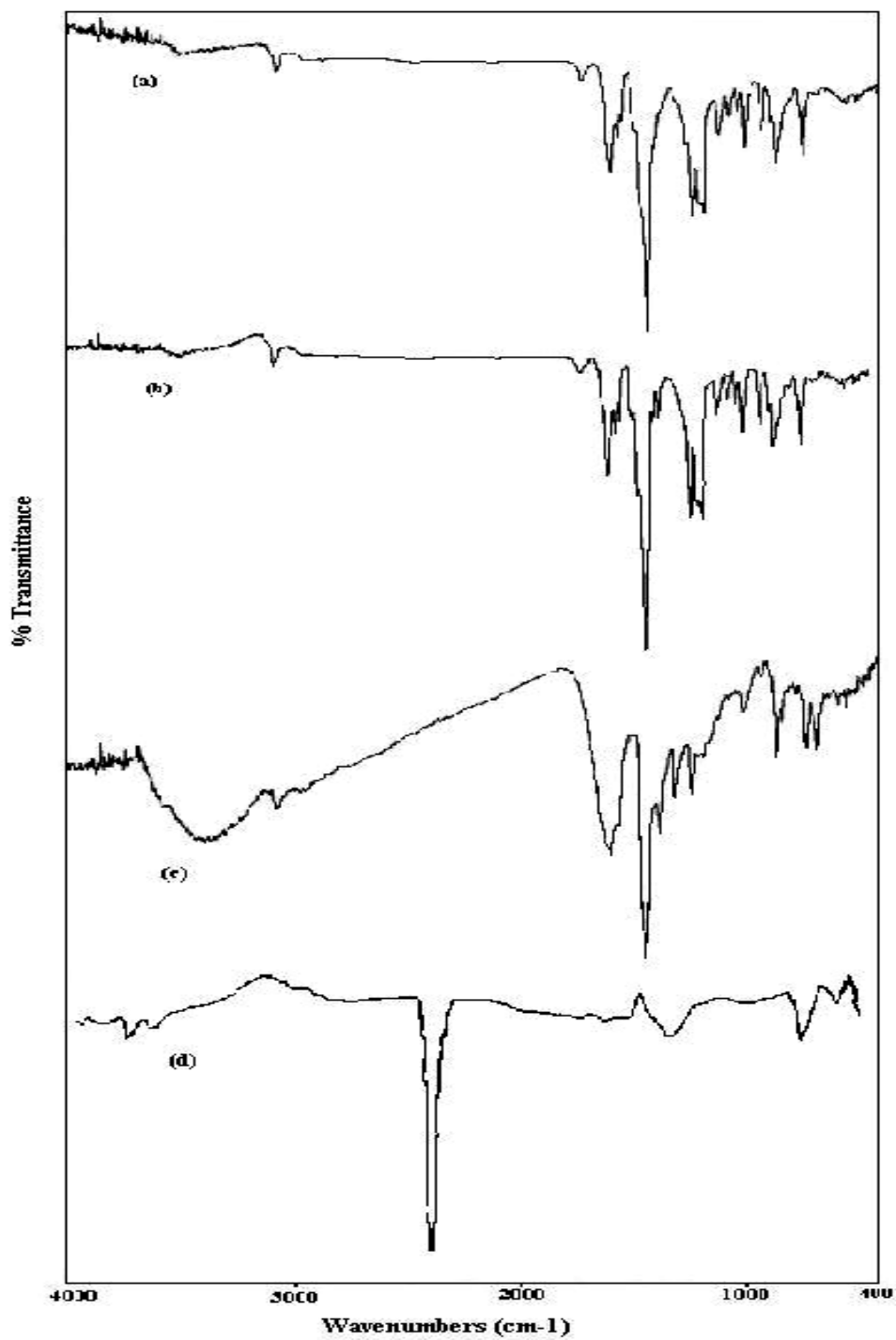


Figure 3.3.1 FTIR spectra of (a) **P**, (b) **RIP**, (c) **CP** and (d) evolved gases during polymerization (TBP and KOH).

The glass transition temperature of the **P** and **RIP** were observed at 171.05 and 209.67 °C respectively in the DSC thermogram, indicating high rigidity of polymers. However, the glass transition temperature was not observed for **CP** (Figure 3.3.2).

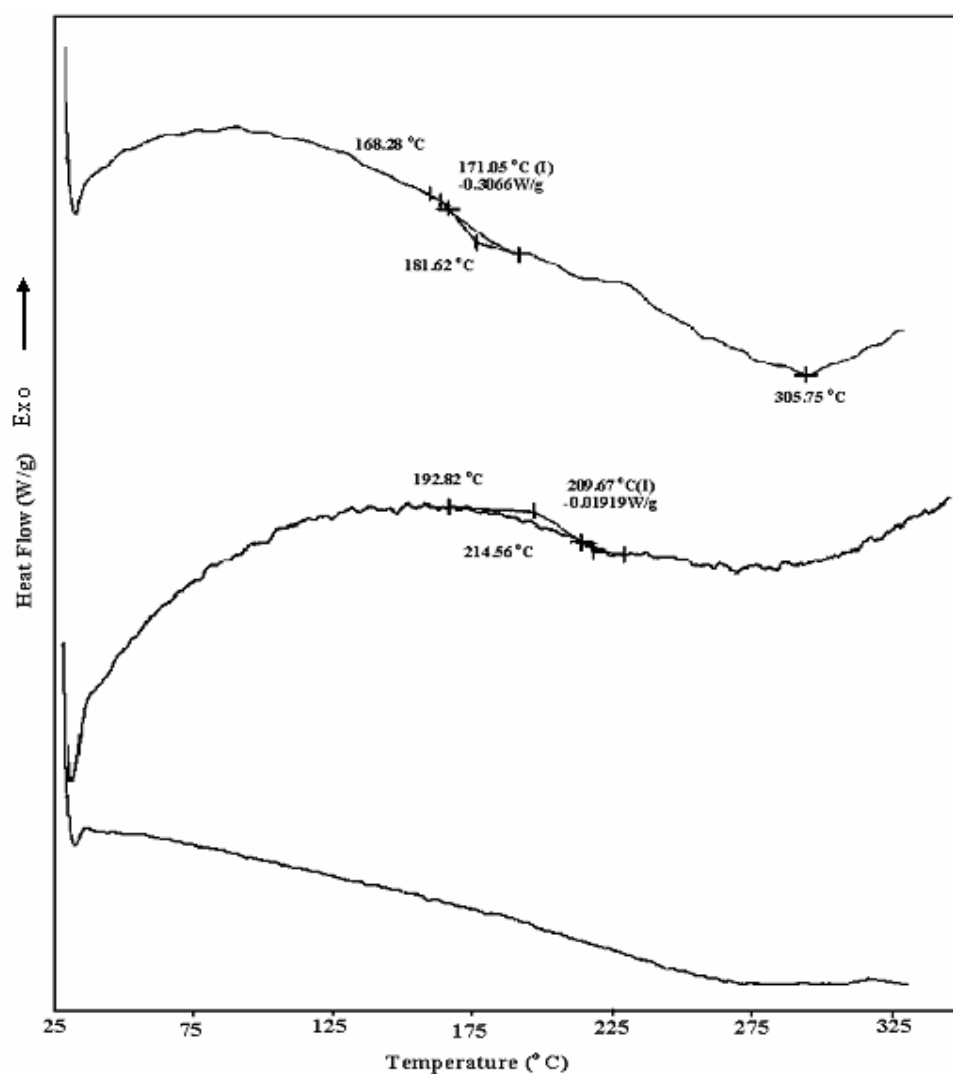
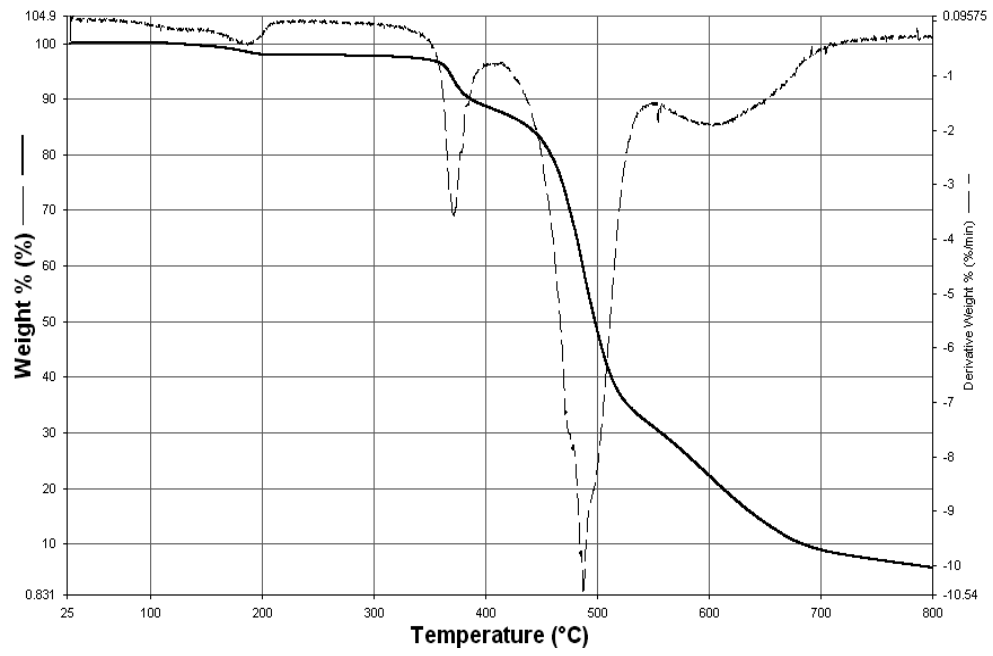


Figure 3.3.2 DSC thermograms of (a) **P**, (b) **RIP** and (c) **CP** (TBP and KOH).

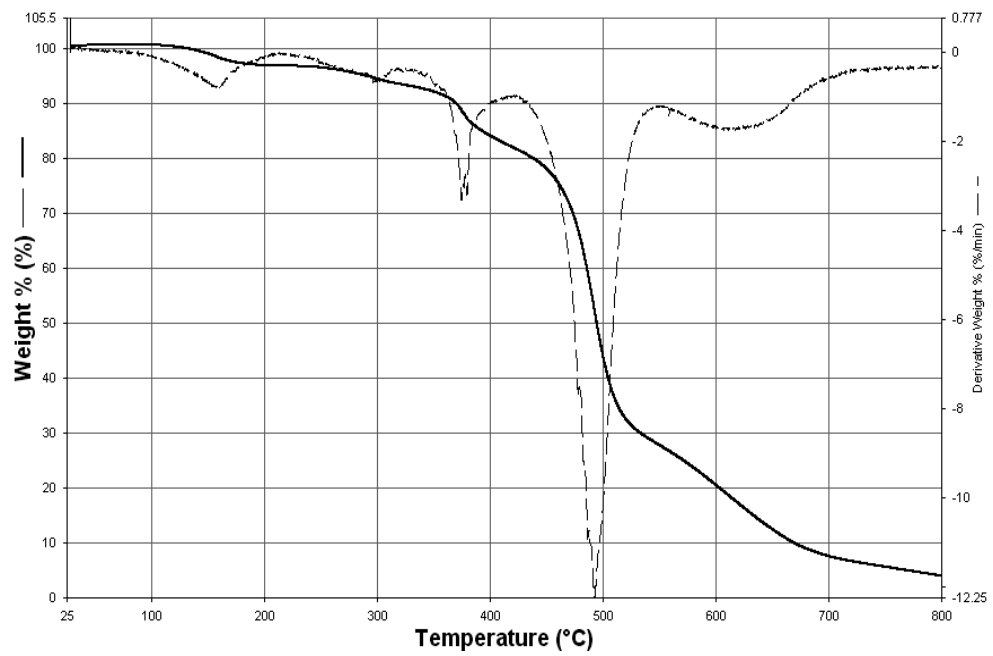
In the TGA thermogram, the **P** and **RIP** were stable up to nearly 360 °C and then approximately 98 % of sample was lost when the temperature reached to 800 °C (Figure 3.3.3a and b). Weight loss was not observed up to 190 °C and decomposition occurs in four stages with the small weight loss around 190 °C and 380 °C, main degradation around 480 °C and 620 °C. The characteristic peaks of aromatic group (2974, 2880, 1380 cm^{-1}) were observed in the first and the second stages of degradation with a weight loss of 2% and 8% respectively. The main degradations around 480 °C showed bands of CO_2 (2358 and 2309 cm^{-1}), CO (2100-2200 cm^{-1}), HBr (2300-2700 cm^{-1}), vinyl bromide (1460 and 2950 cm^{-1}). The fourth emission around 620 °C showed bands of CO_2 , CO and HBr.

However, thermal stability of **CP** was higher than other polymers. Significant the weight loss started from 500 °C having residues less than 65% beyond 800 °C (Figure 3.3.3c). The main decomposition occurs in two stages with maximum rate of degradation around 600 °C and 800 °C. Small degradation (5%) observed up to 500 °C. In the first emission around 600 °C, characteristic bands of CO_2 (2358 and 2309 cm^{-1}), CO (2100-2200 cm^{-1}) were observed. In the second main weight loss which is beyond 700 °C, characteristic peaks of HBr (2300-2700 cm^{-1}) were observed in addition to CO_2 and CO peaks.

a)



b)



c)

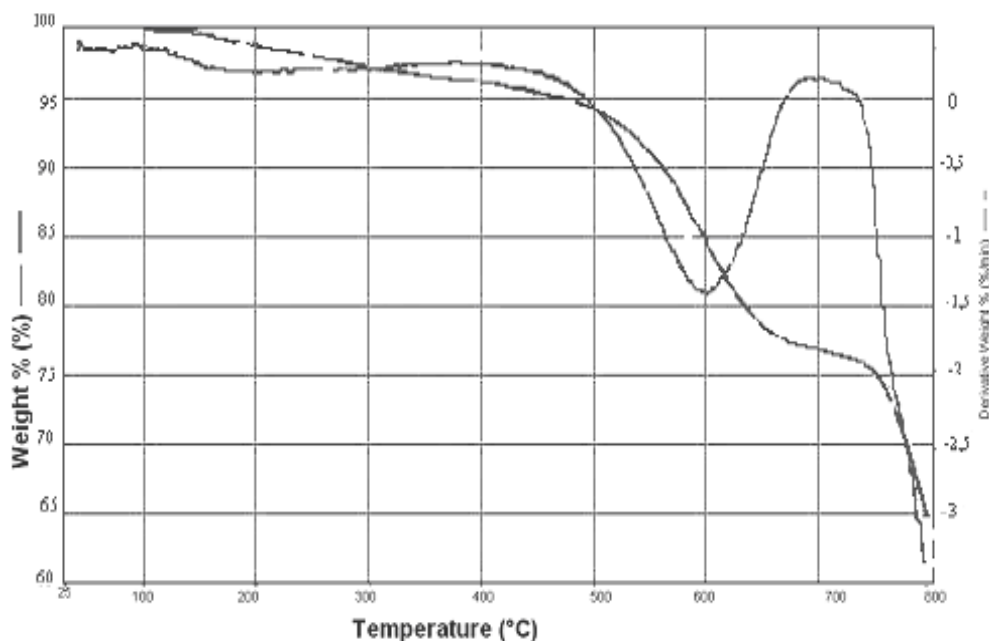


Figure 3.3.3 TGA thermograms of (a) **P**, (b) **RIP** and (c) **CP** (TBP and KOH).

The $^1\text{H-NMR}$ spectrum of **P** and **RIP** were characterized by the peak around 7.0 ppm due to protons of 2,6-dibromo-1,4-phenylene oxide (1,4-addition) and the small peak at 7.6 ppm due to protons of 2,4-dibromo-1,6-phenylene oxide unit (1,2 addition) and the boarder peaks at higher field due to the presence of 1,2 and 1,4-additon on the same monomeric unit (Figure 3.3.4a and b). $^{13}\text{C-NMR}$ decoupled spectra of **P** and **RIP** were displayed in Figure 3.3.5. The theoretical $^{13}\text{C-NMR}$ chemical shift data for five possible addition products were calculated by using appropriate tables. $^{13}\text{C-NMR}$ shift data showed that **P** and **RIP** correlated well with the branched structure indicating 1,2- and 1,4-addition at almost equal rate (Figure 3.1.9).

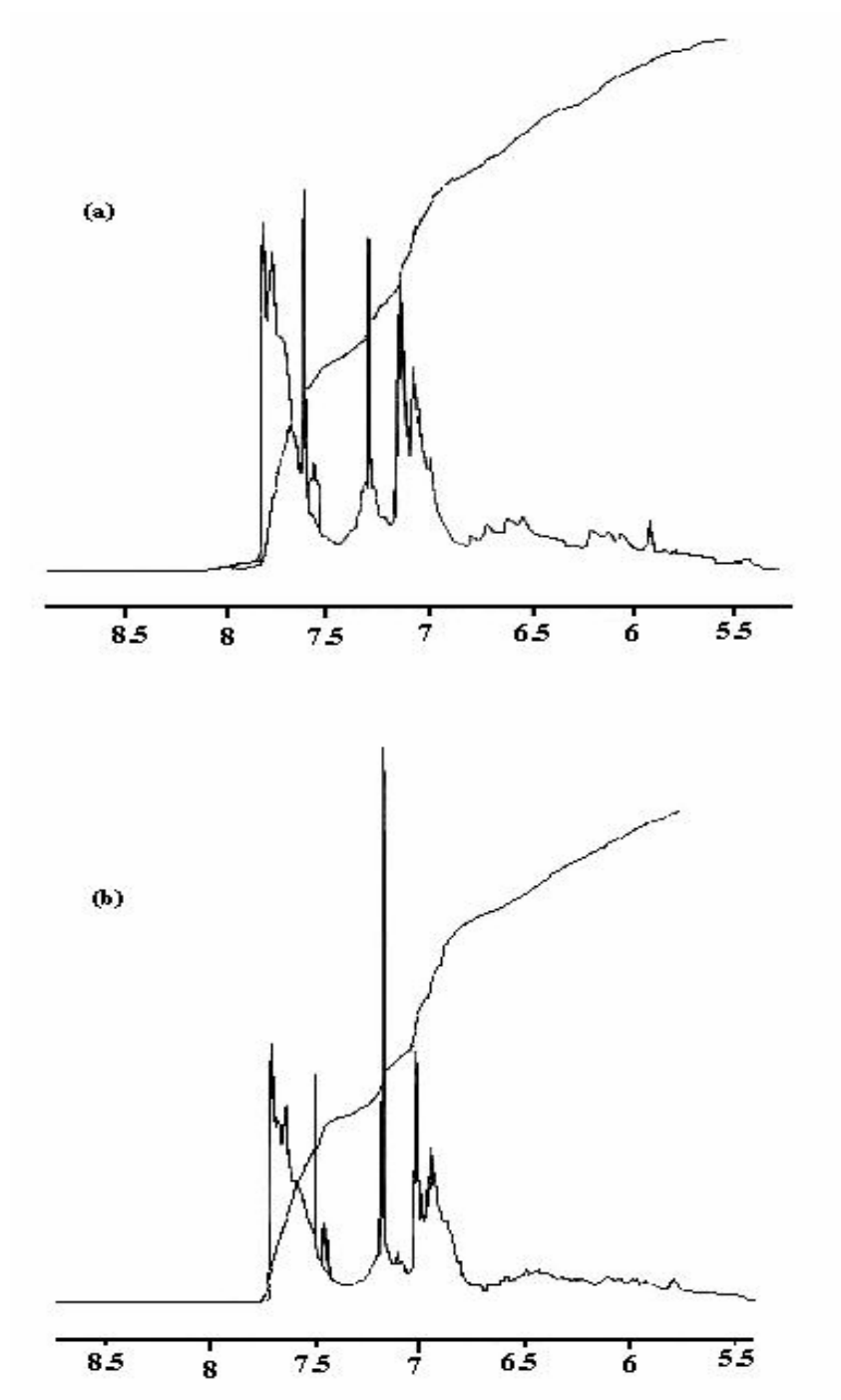


Figure 3.3.4 $^1\text{H-NMR}$ spectrum of (a) **P** and (b) **RIP** (TBP and KOH).

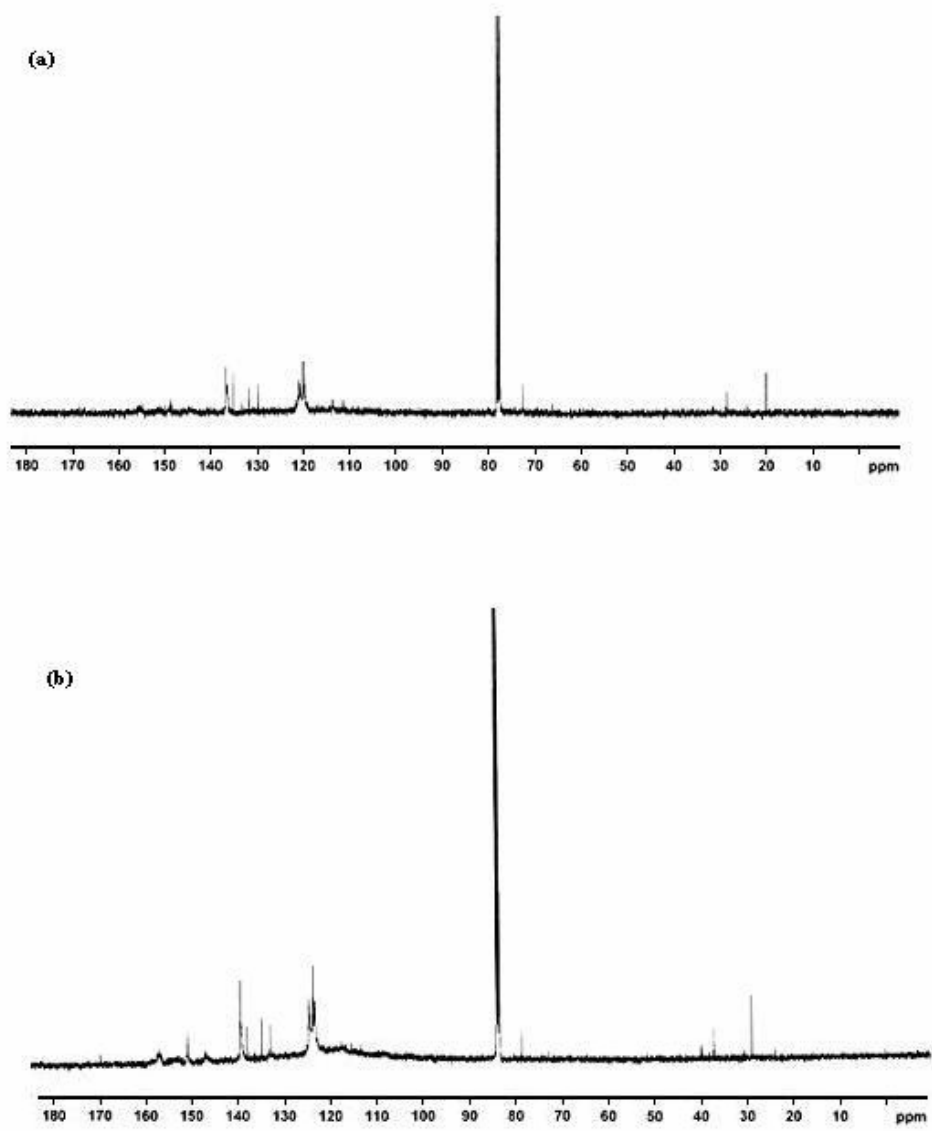


Figure 3.3.5 Proton-decoupled ^{13}C -NMR spectrum of (a) **P** and (b) **RIP** (TBP and KOH).

The powder diffraction X-ray spectra of unwashed **CP** contains three strongest line of d-spacing of NaBr (by product of the polymer synthesis) (Figure 3.3.6a) and washed **CP**, having a broad line, indicating an amorphous polymer (Figure 3.3.6b).

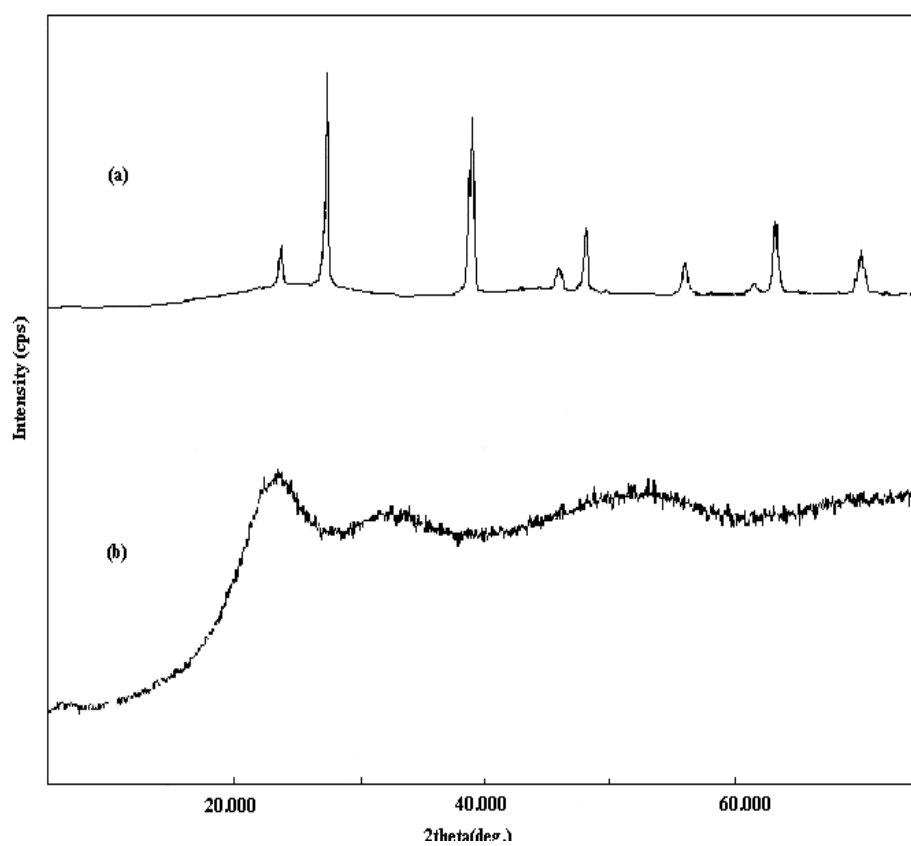


Figure 3.3.6 X-ray powder diffraction spectra of (a) unwashed **CP** and (b) washed **CP** (TBP and KOH).

The electrical conductivities of washed **CP**, unwashed **CP** and **RIP** were measured as 0.2, 1.34 and 2×10^{-5} S cm⁻¹ respectively whereas **P** was an insulator. Because of the doping effect of KBr, conductivity of washed **CP** was higher than unwashed **CP**. Conductivity values of **CP** which was synthesized at different reaction conditions (microwave- energy, time and water content) were very close to each other.

ESR spectrum of microwave-assisted **RIP** and **CP** products revealed the signals with g values of 2.00450 and 2.00244 respectively (Figure 3.3.7a and b) which were very close to the g values of free electron.

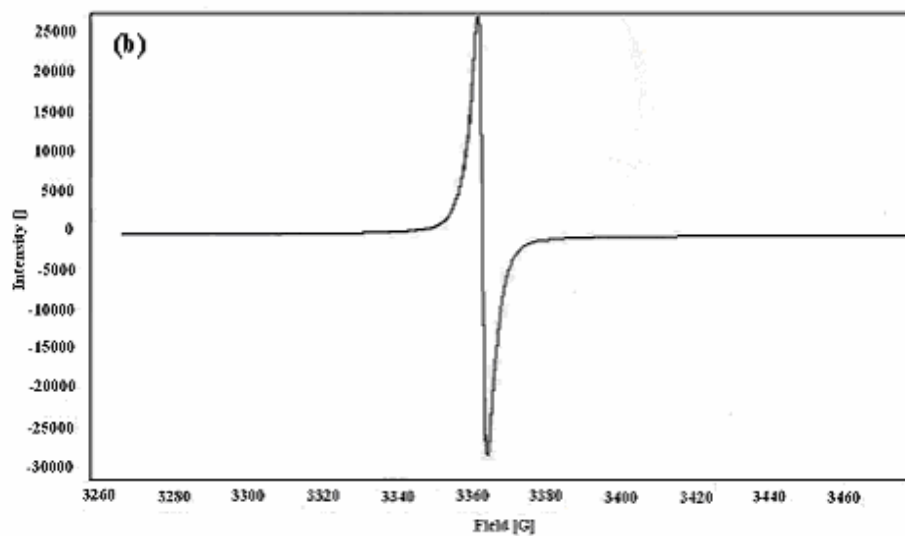
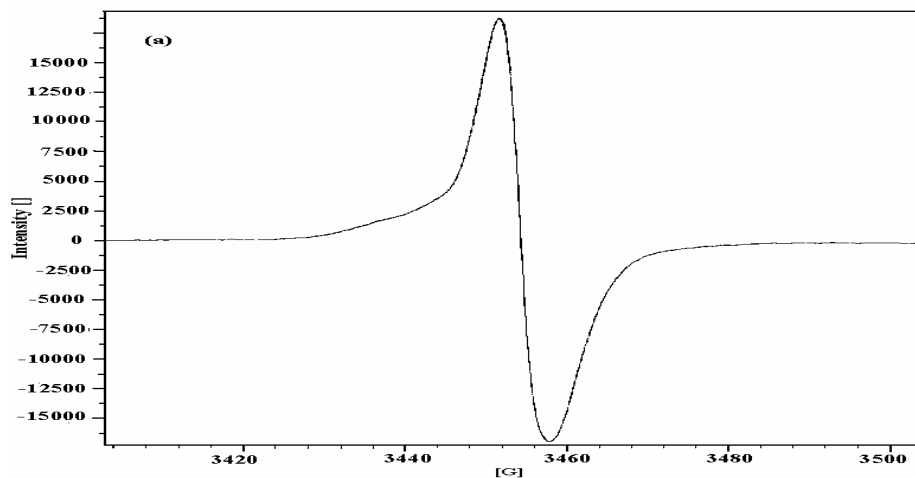
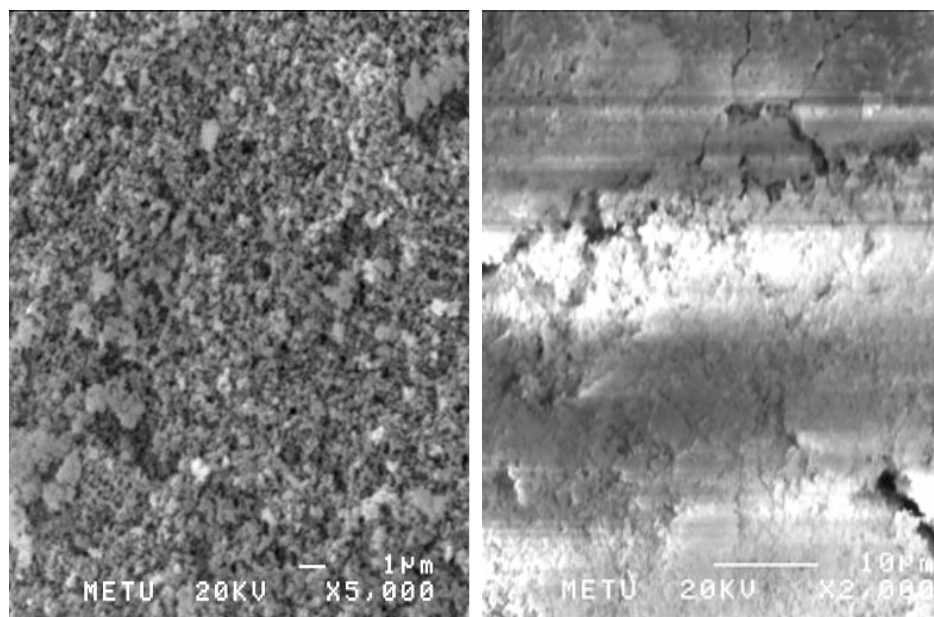


Figure 3.3.7 ESR Spectrum of (a) **RIP** and (b) **CP** at room temperature (TBP and KOH).

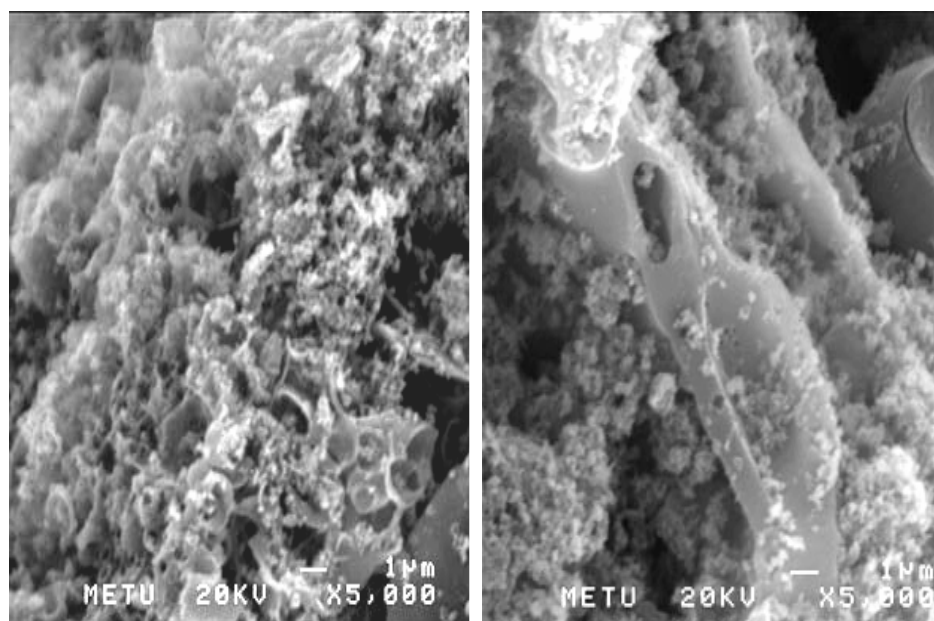
The UV-Visible absorption spectra of synthesized polymers dissolved in toluene were shown in Figure 3.1.12. The spectrum of monomer (TBP) and **P** show single absorption maxima around 270 nm which can be correlated to absorption of benzene ring K-band (Figure 3.1.12a and b). However, in the spectrum of **RIP** and soluble part of **CLP**, evolution of new broad band located around 470 nm were observed, which was related to the π - π^* transition and the formation of polarons (Figure 3.1.12c and d).

The surface morphology analyses of all type of polymers were done by scanning electron microscope. In Figure 3.3.8a, **P** had fine granular structure, significantly different from the **CP** having sponge like structures (Figure 3.3.8c and d) and tubular structures when magnified 5000 times and orange colored coarse surface of **RIP** was detected when magnified 2000 times (Figure 3.3.8b). The X-ray microanalysis system detected the existence of O, Br and C on all of **P**, **CP** and **RIP** whereas K detected on the unwashed **CP**.



(a)

(b)



(c)

(d)

Figure 3.3.8 SEM micrographs of (a) **P** (b) **RIP** and (c and d) **CP** (TBP and KOH).

3.4. Synthesis of Polymer with TIP and NaOH

Poly(diiodophenylene oxide) (**P**) and conducting polymer (**CP**) synthesized simultaneously with microwave-assisted polymerization of sodium 2,4,6 triiodophenolate in a very short time. Polymerizations at several time intervals (0.5-10 min), microwave energies (90-900 watt) and water contents (1-5 ml) were performed.

Table 3.4.1 listed the effect of time, energy and water amount on the % conversions and polymerizations. At 90 watt, the synthesis of **P** and **CP** were achieved 3 ml and 5 ml water at the end of 10 minutes respectively whereas in the range of 180-900 watt, the syntheses were in between 0.5 to 2 min. Both the % conversion of **P** and **CP** showed an increasing trend as the microwave energy and water content increased. The optimum condition for **P** and **CP** was 180 watt for 10 min in 5 ml water and 900 watt for 1 min in 1 ml water having maximum % conversion values 9.21 and 44.8 % respectively.

Table 3.4.1 The effect of polymerization time, energy and amount of water (w) on the % P and %CP (TIP and NaOH).

90 watt	5 min 1 ml water	10 min 3 ml water	10 min 5 ml water
%P	-	-	3,57
%CP	-	26,9	27,2
180 watt	2 min 1 ml water	5 min 3 ml water	10 min 5 ml water
%P	3,65	4,10	9,21
%CP	30,3	32,4	33,5
360 watt	1 min 1 ml water	3 min 3 ml water	5 min 5 ml water
%P	4,15	4,25	4,86
%CP	29,9	40,6	41,6
900 watt	0,5 min 1 ml water	1 min 3 ml water	1 min 5 ml water
%P	8,34	8,22	8,5
%CP	44,8	43,5	44,0

3.4.2 Characterization

Table 3.4.2 listed the results of the elemental analysis of all polymers. Results correlated perfectly with the written stoichiometries.

Table 3.4.2 Elemental analysis results of **P** and **CP** (TIP and NaOH) (experimental errors ± 0.5).

	% C		% H	
	Calc.	Found	Calc.	Found
P	21.49	21.94	1.32	0.91
CP	33.55	33.07	1.15	1.64

FTIR spectra of **P** exhibited the characteristic absorptions at 850 cm^{-1} (out of plane C-H bending), $955\text{-}1040\text{ cm}^{-1}$ (C-O-C stretching), $1140\text{-}1210\text{ cm}^{-1}$ (C-O stretching), 1440 and 1580 cm^{-1} (C=C ring stretching), 3079 cm^{-1} (aromatic C-H stretching) and 3500 cm^{-1} (the phenolic end group) (Fig. 3.4.1a). FTIR spectra of **CP** exhibited the peaks at $1460\text{-}1600\text{ cm}^{-1}$ (C=C stretching of both benzenoid and quinoid structures), 1710 cm^{-1} (C=O stretching), $1110\text{-}1280\text{ cm}^{-1}$ (C-O stretching), 3050 cm^{-1} (aromatic C-H stretching) and $730\text{-}760\text{ cm}^{-1}$ (C-Br stretching) (Figure 3.4.1b).

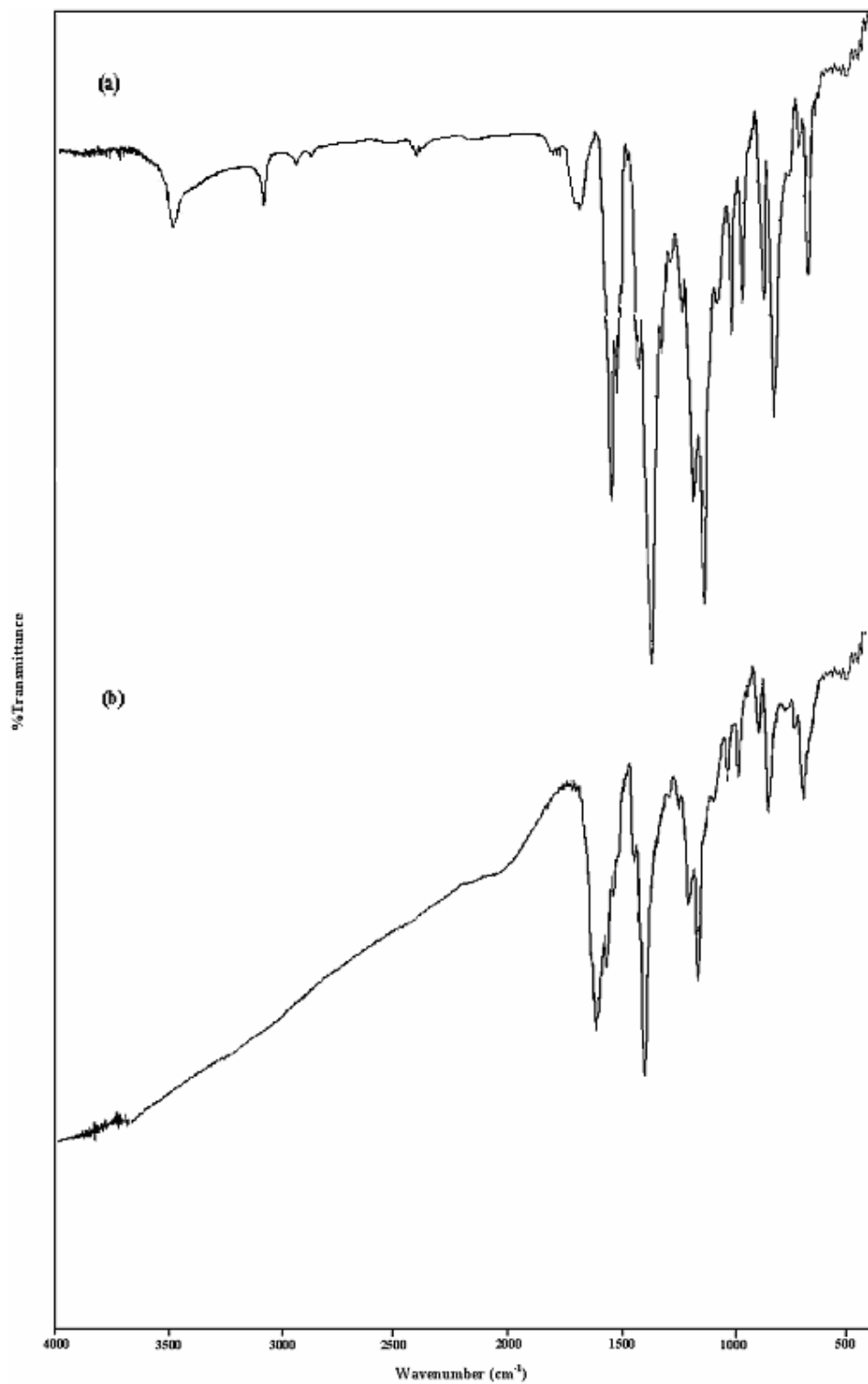


Figure 3.4.1 FTIR spectrum of (a) **P** and (b) **CP** (TIP and NaOH).

The thermal properties of the resulting polymers were studied with DSC and TGA under nitrogen atmosphere. The DSC thermogram of the **P** has glass transition temperature 214.90 °C, indicating high rigidity. The glass transition temperature was not observed for **CP** (Figure 3.4.2). In the TGA thermogram, the **P** was stable up to nearly 370 °C and then approximately 65 % of sample was lost when the temperature reached to 500 °C (Figure 3.4.3a). In the case of **CP**, the weight loss started from 200 °C, still having residues of 20 % beyond 750 °C indicating a higher thermal stability (Figures 3.4.3b).

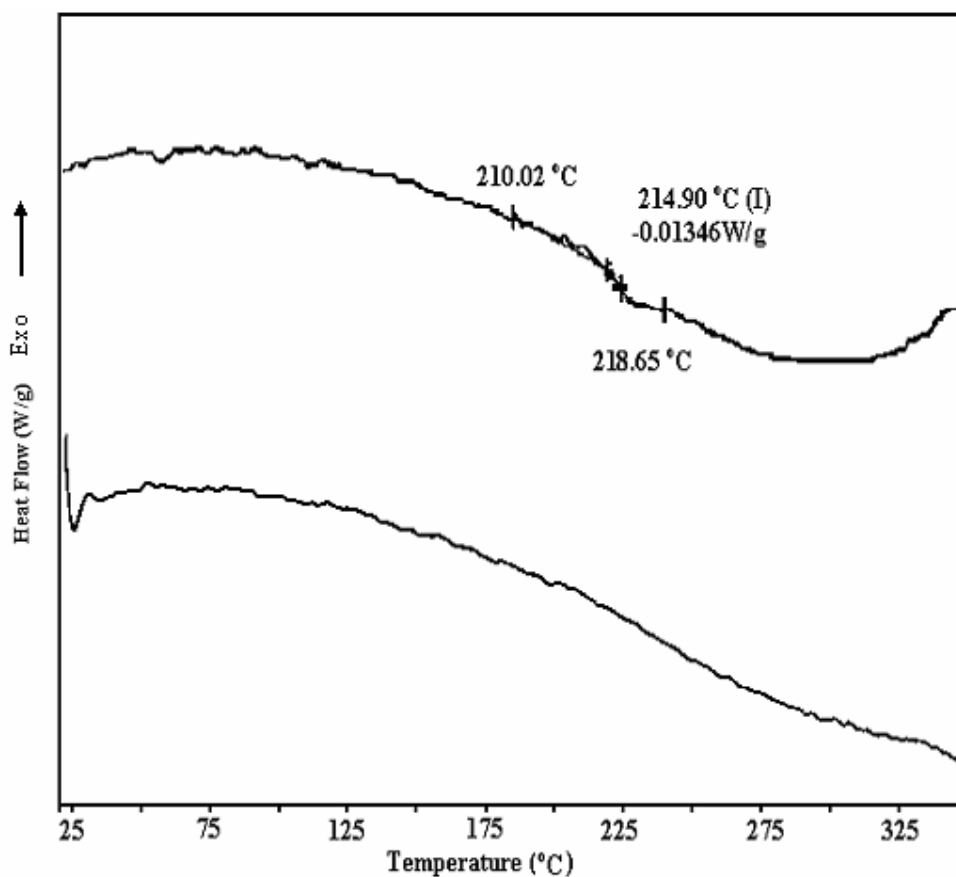
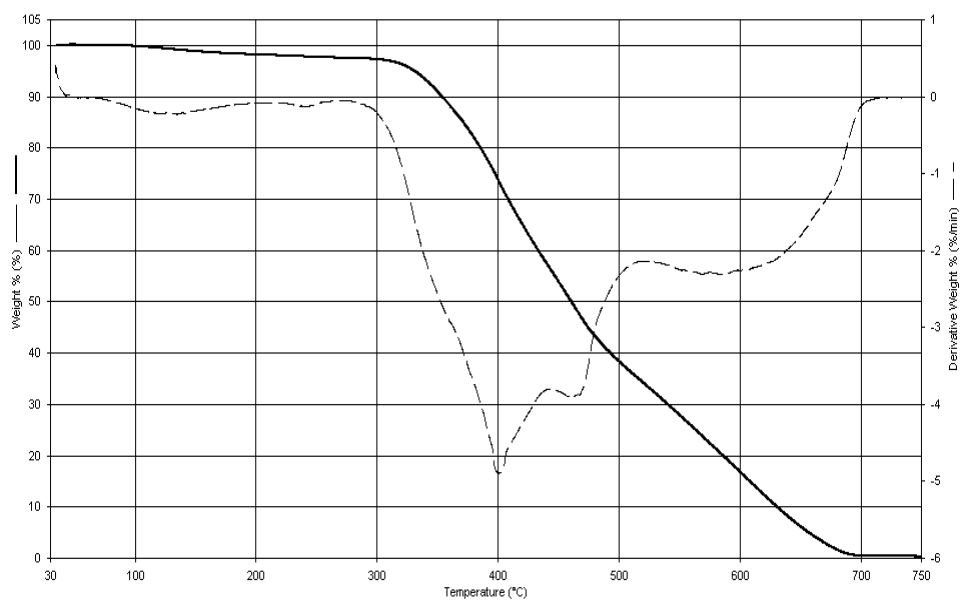


Figure 3.4.2 DSC thermograms of (a) **P** and (b) **CP** (TIP and NaOH).

a)



b)

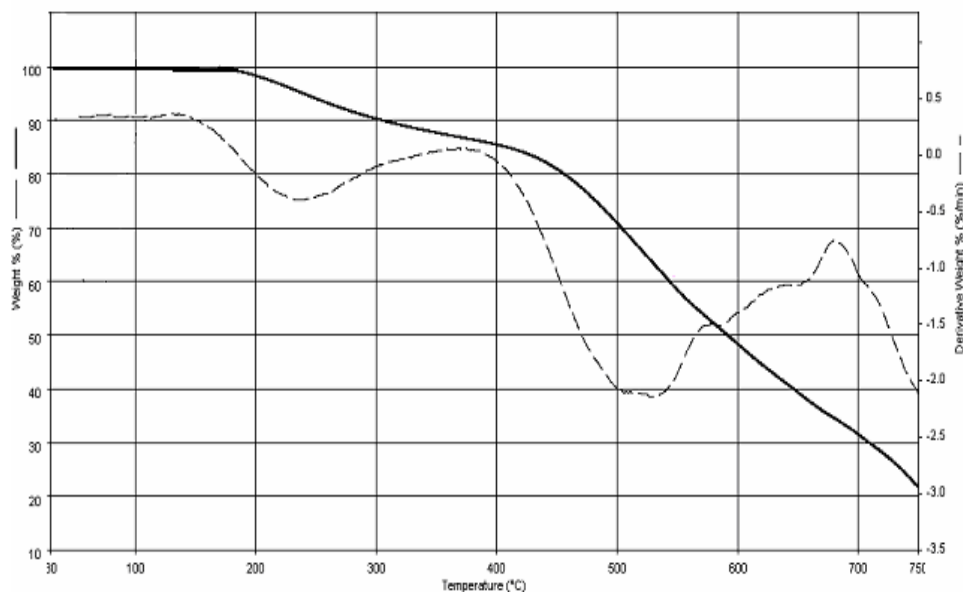


Figure 3.4.3 TGA thermograms of (a) **P** and (b) **CP** (TIP and NaOH).

The $^1\text{H-NMR}$ spectra of **P** was characterized by the peak at 7.3 ppm due to protons of 2,6-diiodo-1,4-phenylene oxide (1,4-addition) and the small peak at 8.2 ppm due to protons of 2,4-diiodo-1,6-phenylene oxide unit (1,2 addition) (Figure 3.4.4). Thus, it can be clearly observed that polymerization proceed mainly 1,4-additions. $^{13}\text{C-NMR}$ decoupled spectrum of **P** is displayed in Figure 3.4.5. The theoretical $^{13}\text{C-NMR}$ chemical shift data for five possible addition products were calculated by using appropriate tables. $^{13}\text{C-NMR}$ shift data showed that **P** correlated well 1,4-addition product (Figure 3.2.9a).

The powder diffraction X-ray spectra of both unwashed **CP** and washed **CP**, having a broad line, indicating an amorphous polymer (Figure 3.4.6). As a result, the electrical conductivities of both washed and unwashed **CP** have nearly the same values, measured around $3 \times 10^{-1} \text{ S cm}^{-1}$.

ESR spectra of microwave-assisted **CP** revealed the signal with g value of 2.0102 (Figure 3.4.7) which was very close to the g value of free electron.

The weight average molecular weight (\overline{M}_w) of the **P** was determined as $9.87 \times 10^4 \text{ g/mol}$ by the light scattering. This is the smallest molecular weight among the synthesized poly(dihalophenylene oxide) in this study.

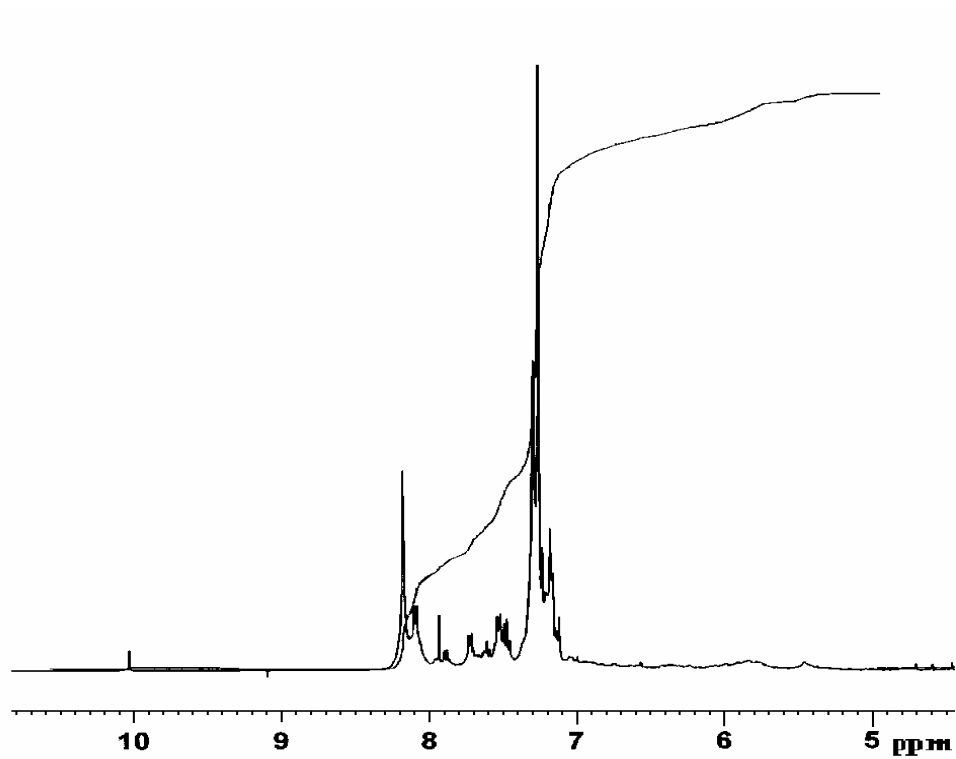


Figure 3.4.4 ^1H -NMR spectrum of **P** (TIP and NaOH).

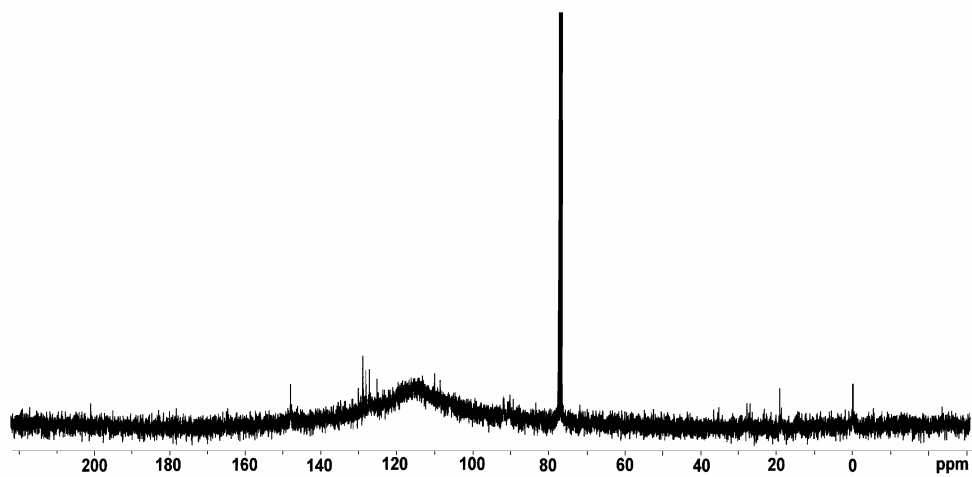


Figure 3.4.5 Proton-decoupled ^{13}C -NMR spectrum of **P** (TIP and NaOH).

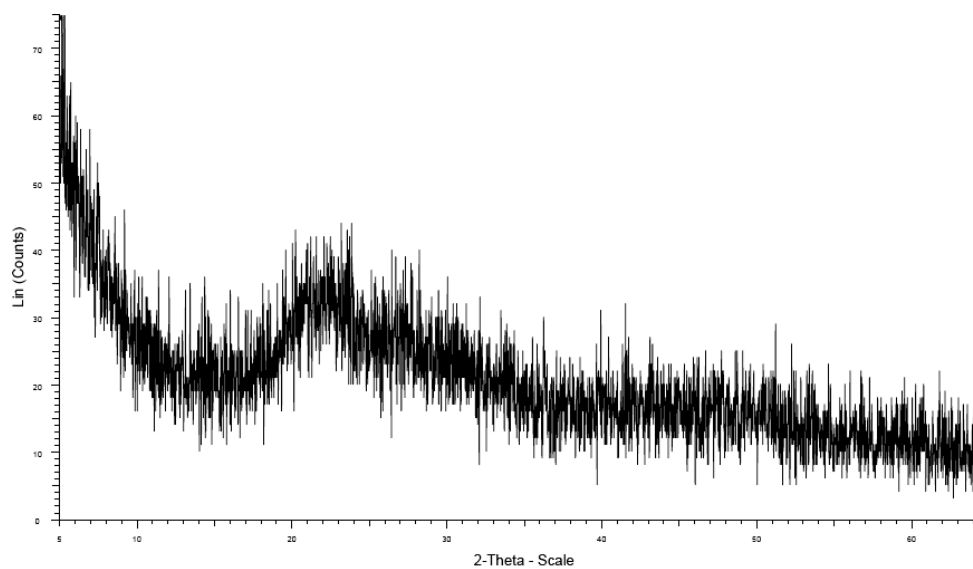


Figure 3.4.6 X-ray powder diffraction spectra of **CP** (TIP and NaOH).

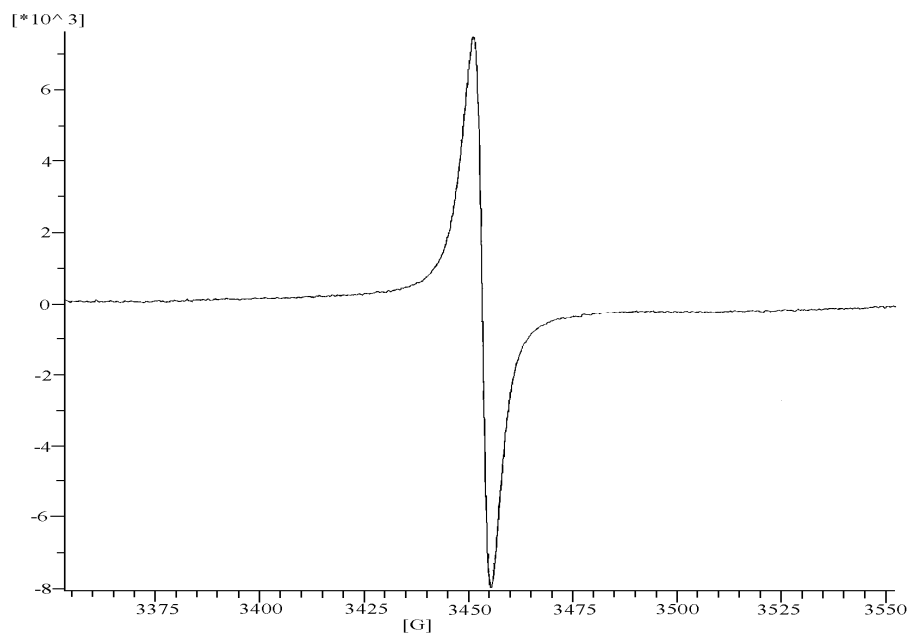
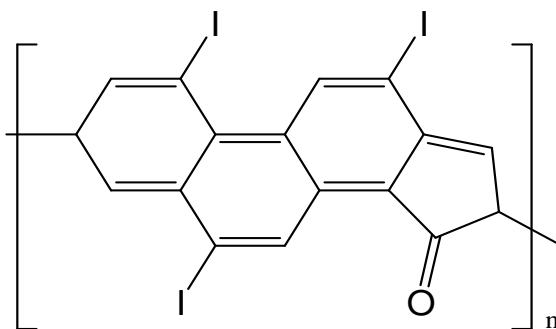


Figure 3.4.7 ESR Spectrum of (a) **CP** at room temperature (TIP and NaOH).

Differences in surface morphologies of polymers were evaluated scanning electron microscope (SEM) (Figure 3.4.8). The appreciable differences in the morphology of the **P** and **CP** were observed in the images. The **P** (Figure 3.4.8a) had fine granular structure, significantly different from the **CP** (Figure 3.4.8b, c, d, e) having, sponge like structures. The X-ray microanalysis system detected the existence of O, I and C in all of **P** and **CP** structures.

From the elemental analysis, powder diffraction X-Ray, TGA, DSC and FTIR results, the following structure was proposed for **CP**:



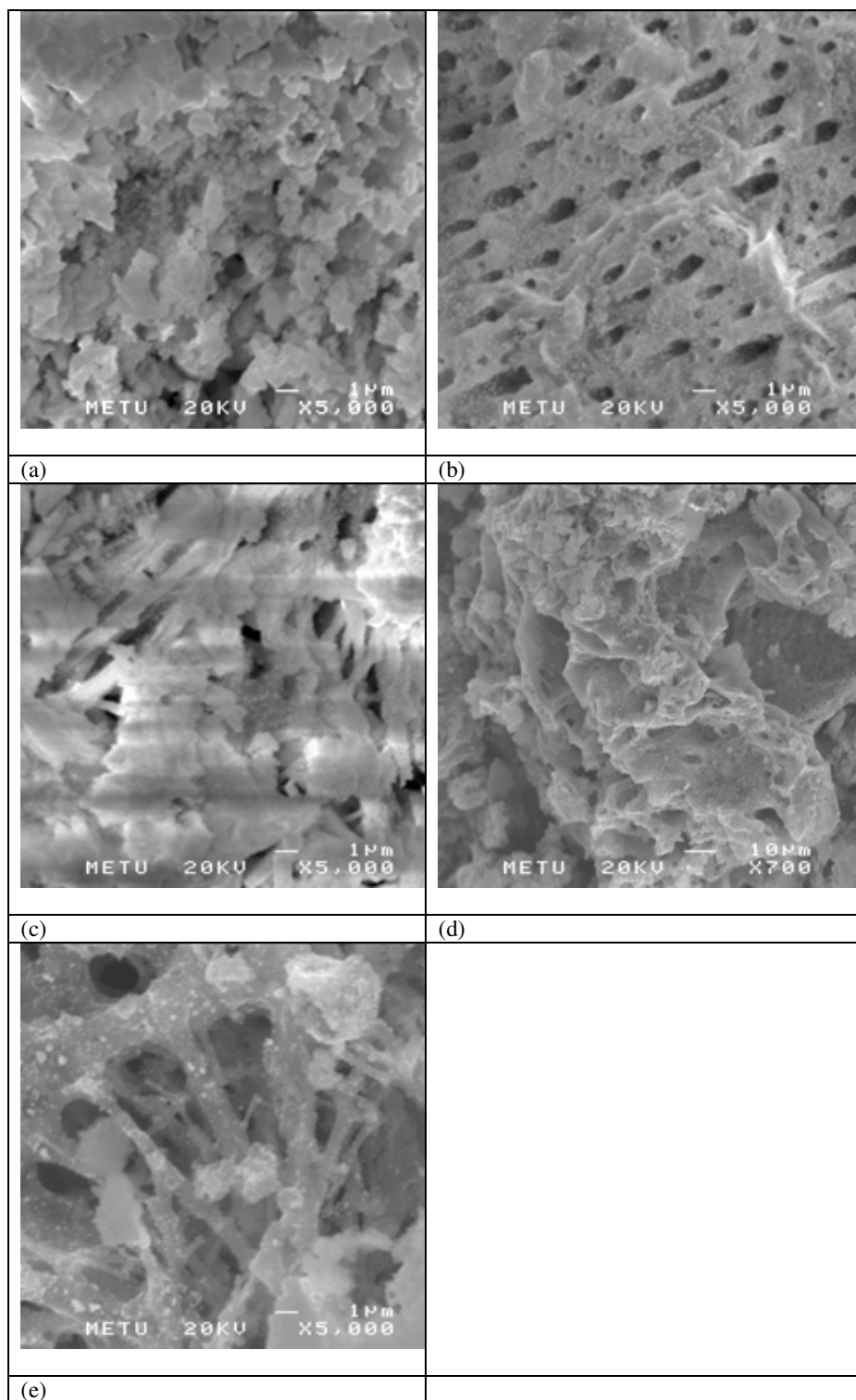


Figure 3.4.8 SEM micrographs of (a) P and (b, c, d, e) CP (TIP and NaOH).

Table 3.4.3 Summary Results of Experiments

		TBP-NaOH	TBP-LiOH	TBP-KOH	TIP-NaOH
Optimum Conditions	% P	2.6 70 watt, 5 min, 5 ml w	24.5 180 watt, 2 min, 1 ml w	39.2 350 watt, 1 min, 5ml	9.21 180 watt, 10 min, 5ml
	% CP	27.2 100 watt, 1 min, 0,5 ml	53.1 900 watt, 5 min, 3 ml w	27.9 500 watt, 1min, 0,5 ml	44.8 900 watt, 1 min, 1 ml
	% CLP	-	80.8 900 watt, 10 min, 5 ml	-	-
Tg	P	194.27 °C	173 °C	171 °C	214.9 °C
	RIP	214.99°C	-	209.7 °C	-
	CLP	-	208.9 °C	-	-
NMR		Both 1,4 and 1,2 addition	Both 1,4 and 1,2 addition	Both 1,4 and 1,2 addition	Mainly 1,4 addition
Mw	P	2.97×10^5 g/mol	1.123×10^5 g/mol	8.061×10^4 g/mol	9.87×10^3 g/mol
	RIP	1.2×10^4 g/mol	-	3.324×10^4 g/mol	-
ESR (g)	RIP	2.00552	-	2.00450	-
	CLP	2.00549	2.0068	-	-
	CP	2.00294	2.0017	2.00244	2.0102
Cond.	CP Washed	0,1	10^{-2}	0,2	3×10^{-1}
	CP Unwash	1	10^{-3}	1.34	3×10^{-1}
	RIP	1×10^{-4}	-	2×10^{-4}	-
Xray (unwashed CP)		NaBr	LiCO ₃	KBr	Amorph

CHAPTER 4

CONCLUSION

In this study, microwave-assisted synthesis of four different types of poly(dihalophenyleneoxide), (poly(dibromophenylene oxide) and poly(diiodophenylene oxide)) (**P**), conducting polymer (**CP**) and/or crosslinked polymer (**CLP**) and/or radical ion polymer (**RIP**), were achieved simultaneously from 2,4,6-bromophenolate or 2,4,6-iodophenolate in a very short time interval for the first time. Polymers were achieved either at constant microwave energy with different time intervals (1 - 20 min) or at constant time intervals with different microwave energy (70-900 watt) or in different water content (0.5 – 5 ml) at constant time intervals and microwave energy.

Poly(dihalophenylene oxide) and radical ion polymers were characterized by FTIR, ¹H-NMR, ¹³C-NMR, TGA/ FTIR, DSC, SEM, ESR, GPC, UV-Vis, light scattering and elemental analysis. Conducting and crosslinked polymers were characterized by FTIR, TGA/ FTIR, DSC, SEM, ESR, powder diffraction X-Ray and elemental analysis. The effects of heating time, microwave energy and amount of water on polymer synthesis on the % conversion were also investigated.

Microwave-assisted polymerization was achieved very rapidly (1 to 5 min) compared to previously used methods (3 to 48 hours). In addition, induction period for the polymerization was very short (less than 3 min at 70 watt and 1 min at higher watts) when compared to the syntheses in solution or in solid state.

The conclusion of this study will be discussed under four topics. Each topic includes the results related to the synthesis and the characterization of the polymers which were synthesized with different starting materials.

In the synthesis of polymers from sodium 2,4,6-tribromophenolate, poly(dibromophenylene oxide) (**P**) and conducting polymer (**CP**) and/or crosslinked polymer (**CLP**), and/or radical ion polymers (**RIP**) were achieved simultaneously. The optimum conditions to obtain the highest % conversion of **P** and **CP** were 70 watt for 5 min in 5 ml water and 100 watt for 1 min in 0.5 ml water having maximum values of 23.6 and 27.2 % respectively.

In the synthesis of polymers from lithium 2,4,6-tribromophenolate, poly(dibromophenylene oxide) (**P**) and conducting polymer (**CP**) and/or crosslinked polymer (**CLP**) were achieved simultaneously. The optimum conditions to obtain the highest % conversion of **P**, **CP** and **CLP** were at 180 watt for 2 min in 1 ml water, 900 watt for 5 min in 3 ml water, 900 watt for 10 min in 5 ml water having maximum values 24.5, 53.1 and 80.8 % respectively.

In the synthesis of polymers from potassium 2,4,6-tribromophenolate poly(dibromophenylene oxide) (**P**), Radical ion polymer (**RIP**) and conducting polymer (**CP**) were achieved. The optimum conditions to obtain the highest % conversion of **P** and **CP** were 350 watt for 1 min in 5 ml water and 500 watt for 1 min in 0.5 ml water, having maximum values 39.2 and 27.9 % respectively.

In the synthesis of polymers from sodium 2,4,6 triiodophenolate poly(diiodophenylene oxide) (**P**) and conducting polymer (**CP**) were achieved. The optimum conditions to obtain the highest % conversion of **P** and **CP** were 180 watt for 10 min in 5 ml water and 900 watt for 1 min in 1 ml water having maximum values 9.21 and 44.8%, respectively.

In this synthesis, polymerization proceed through 1,2- and 1,4-addition at almost equal rate for poly(bromophenylene oxide), mainly 1,4-addition for poly(diiodophenylene oxide) whereas mainly 1,2-addition for poly(dichlorophenylene oxide) [69].

For the first time, the highest \overline{M}_w value of **P** (2.97×10^5 g/mol), was achieved at 70 watt in 5 ml at the end of 5 min from sodium 2,4,6-tribromophenolate. The synthesized **P** from lithium 2,4,6-tribromophenolate, potassium 2,4,6-tribromophenolate, sodium 2,4,6 triiodophenolate and sodium 2,4,6-trichlorophenolate have the molecular weights 1.123×10^5 , 8.061×10^4 , 9.87×10^4 and 1.8×10^4 g/mol respectively. Hence, \overline{M}_w of the poly(dibromophenylene oxide) synthesized by using microwave is greater than both synthesized by electro-initiation and thermal decomposition methods. The **RIP** synthesized from sodium 2,4,6-tribromophenolate and potassium 2,4,6-tribromophenolate have the molecular weight of 1.2×10^4 and 3.324×10^4 g/mol respectively. The \overline{M}_w of **P** has always higher than the \overline{M}_w of **RIP**.

The direct synthesis of highly conducting polymers was achieved in the absence of applied doping process in a very short time sequence with microwave-assisted polymerization. The washed **CP** synthesized from sodium 2,4,6-tribromophenolate, lithium 2,4,6-tribromophenolate, sodium 2,4,6 triiodophenolate and sodium 2,4,6-trichlorophenolate have conductivity values 0.1, 0.01, 0.3 and 0.2 S cm⁻¹ respectively. The highest conductivity values for unwashed and washed **CP** were achieved 1.34 and 0.2 S cm⁻¹ respectively for potassium 2,4,6-tribromophenolate polymers.

The powder diffraction X-ray spectra of unwashed **CP** contained always peaks of by products (NaBr, KBr and LiCO₃) and washed **CP**, having a broad line, indicating an amorphous polymer.

High Tg value of polymers indicated their high rigidity.

ESR spectrum of **RIP**, **CLP** and **CP** products revealed the signals very close to the g values of free electron.

Analysis of the surface morphologies of all types of polymers indicated fine granular, sponge like, dendrite and coarse surface structures for **P**, **CP**, **CLP** and **RIP** respectively.

The effects of monomer (TBP or TIP) and metal-hydroxides (NaOH, LiOH or KOH) on polymer synthesis and on the % conversion were;

- In the comparison of optimum % conversions of **P** were:

TBP-KOH > TBP-LiOH > TBP-NaOH > TIP-NaOH

- In the comparison of optimum % conversions of **CP** were:

TBP-KOH > TIP-NaOH > TBP-LiOH \geq TBP-NaOH

- In the comparison of optimum % conversions of **CLP** were:

TBP- LiOH > TBP-NaOH

- In the comparison of optimum \bar{M}_w of **P** were:

TBP-NaOH > TBP-LiOH > TBP-KOH > TIP-NaOH

-In the comparison of conductivity of unwashed and washed **CP** were:

TBP-KOH > TBP-NaOH > TBP-LiOH > TIP-NaOH

TIP-NaOH > TBP-KOH > TBP-NaOH > TBP-LiOH

REFERENCES

- [1] Lidström, P., Tierney, J., Wathey, B. and Westman, J., *Tetrahedron*, 57, 9225, 2001.
- [2] Buffler, C.R., *Microwave Cooking and Processing*, Van Nostrand Reinhold, New York, 1993.
- [3] Login, G.R. and Dvorak, A. M., *The Microwave Tool Book. A Practical Guide for Microscopists*, Boston, 1994.
- [4] Metaxas, A.C., Meredith, R.J., *Industrial Microwave Heating*, London, 1983.
- [5] Bose, A.K., Manhas, M.S., Ganguly, S.N., Sharma, A.H., Banik, B.K. and Bimal, K., *Synthesis*, 11, 2002.
- [6] Mingos, D.M.P. and Baghurst, D.R., *Chem Soc. Rev.*, 1, 20, 1991.
- [7] Gedye, R.N., Smith, F.E. and Westaway, K.C., *Can. J., Chem.*, 17, 66, 986.
- [8] Giguere, R.J., Bray, T.L., Duncan, S.M. and Majetich, G., *Tetrahedron Lett.*, 27, 4945, 1986.
- [9] Majetich, G. and Hicks, R., *Radiat. Phys. Chem*, 45, 567, 1995.
- [10] Yeganeh, H., Tamami, B., Ghazi, I., *European Polymer Journal*, 40, 2059, 2004.
- [11] Jullien, H.B., Delmotte, M. In: Salomone J.C., editor. *Polymeric Material Encyclopedia*, vol.3. Boca Raton, FL: CRC Press, 2253, 1996.
- [12] Fini, A. and Breccia, A., *Pure Appl. Chem.*, 71, 573, 1999.
- [13] Bogdal, D., Penczek, P., Pielichowski, J. and Prociak, A., *Adv. Polym. Sci.*, 163, 193, 2003.
- [14] Abramovitch, R.A., *Org. Prep. Proc. Int*, 23, 685, 1991.
- [15] Laurent, R., Laporterie, A., Dubac, J., Berlan, J., Lefeuvre, S. and Audhuy, M., *J. Org. Chem.*, 57, 7099, 1992.
- [16] Caddick, S., *Tetrahedron*, 51, 10403, 1995.

- [17] Wiesbrock, F., Hoogenboom, R. and Schubert, U.S., *Macromol. Rapid Commun.*, 25, 1739, 2004.
- [18] Perreux, L. and Loupy, A., *Tetrahedron*, 57, 2001, 2001.
- [19] Herman, F.M., Norman, G.G. and Norbert, M.B., *Encyclopedia of Polymer Science and Technology*, John Wiley & Sons, 10, 1969.
- [20] Concise, *Encyclopedia of Polymer science and Engineering*, John Wiley and Sons, 870, 1068, 1990.
- [21] Blanchard, H.S., Finkbeiner, H. L. and Russell, G.A., *J. Polym. Sci*, 58, 469, 1962.
- [22] Abramovitch, R.A., *Org. Prep. Proc. Int*, 23, 685, 1991.
- [23] Solomons, T.W.G., *Organic chemistry*, John Willey & Sons Inc, 6th Edition, 963, 966, 1996.
- [24] Vogt, L. H. Jr., Wirth, J. G. and Finkbeiner, H. L., *J. Org. Chem.*, 34(2), 273, 1969.
- [25] Hunter, W.H., Olson, A. O. and Daniels, E.A., *J. Am. Chem. Soc.*, 38, 1761, 1916.
- [26] Hunter, W.H. and Joyce, F.E., *J. Am. Chem. Soc.*, 39, 2640, 1917.
- [27] Hay, A. S., *J. Polym. Sci.*, 58, 581, 1962.
- [28] Hunter, W.H., Dahlen, M.A., *J. Am. Chem. Soc.*, 54, 2456, 1932.
- [29] Staffin, G. D., Price, C. C., *J. Am. Chem. Soc.*, 82, 3632, 1960.
- [30] Hay, A. S., *J. Polym. Sci.*, 58, 581, 1962.
- [31] Harrod, J. F., *Can. J. Chem.*, 47 (4), 637, 1969.
- [32] Harrod, J.F., Van Gheluwe, P., Kısakürek, D. and Shaver, A., *Macromolecules*, 14, 565, 1981.
- [33] Harrod, J.F. and Shaver, A., *Macromolecules*, 15, 676, 1982.
- [34] Türker, L., Kısakürek, D., Şen, Ş., Toppare, L. and Akbulut, U., *J. Polym. Sci. Phys. Ed.*, 26, 2485, 1988.
- [35] Saçak, M., Akbulut, U., Kısakürek, D., Türker, L. and Toppare, L., *J. Polym. Sci.Chem. Ed.*, 27, 1599, 1 989.
- [36] Şen, Ş., Kısakürek, D., Türker, L., Toppare, L. and Akbulut, U., *New Polym. Mat.*, 1(3), 177, 1989.

- [37] Yiğit, S., Kısakürek, D., Türker, L., Toppare, L. and Akbulut, U., *Polymer*, 30, 348, 1989.
- [38] Saçak, M., Akbulut, U., Kısakürek, D. and Toppare, L., *Polymer*, 30, 928, 1989.
- [39] Akbulut, U., Saçak, M., Kısakürek, D. and Toppare, L., *J. Mol. Sci. Chem.*, A26(12), 1623, 1989.
- [40] Akbulut, U., Saçak, M., Kısakürek, D. and Toppare, L., *Br. Polym. J.*, 22, 65, 1990.
- [41] Toppare, L., Türker, L., Yiğit, S., Kısakürek, D. and Akbulut, U., *Eur. Polym. J.*, 26(3), 255, 1990.
- [42] Kısakürek, D. and Yiğit, S., *Eur. Polym. J.*, 27(9), 955, 1991.
- [43] Şen, Ş., Kısakürek, D. and Toppare, L., *J. Macromol. Sci. Pure and Appl. Chem.*, A30 (6, 7), 481, 1993.
- [44] Şen, Ş., Kısakürek, D., *Polymer*, 34(19), 4146, 1993.
- [45] Pulat, M., Önal, A. M., Kısakürek, D., *New Polym. Mat.*, 4(2) 111, 1994.
- [46] Aras, L., Şen, Ş., Kısakürek, D., *Polymer*, 36(15), 3013, 1995.
- [47] Şen, Ş. and Kısakürek, D., *Polymer*, 34(19), 4146, 1993.
- [48] Aras, L., Şen, Ş. and Kısakürek, D., *Polymer*, 36(15), 3013, 1995.
- [49] Yaman, Ş., M. Baştürkmen, D. Kısakürek D, *Polymer* 46 (2005) 678.
- [50] Kısakürek, D., Şen, Ş., Aras, L., Türker, L. and Toppare, L., *Polymer*, 32 (7), 1323, 1991.
- [51] Kısakürek, D., Aras, L. and Şanlı, O., *METU J. Pure and Appl. Sci.*, 23(2), 49, 1990.
- [52] Pulat, M., Şanlı, O. and Kısakürek, D., *Polish J. Chem.*, 68, 453, 1994.
- [53] Şanlı, O. and Kısakürek, D., *Macromol. Chem.*, 193, 619, 1992.
- [54] Kısakürek, D. and Şanlı, O., *Macromol. Chem.*, 190, 1843, 1989.
- [55] Kısakürek, D. and Türker, L., *Br. Polym. J.*, 21, 367, 1989.
- [56] Kısakürek, D., Binboğa, N. and Harrod, J. F., *Polymer*, 28, 1767, 1987.
- [57] Baştürkmen, M. and Kısakürek, D., *Polymer*, 34(3), 625, 1993.
- [58] Şentürk, Ö. and Kısakürek, D., *Polym- Plast Technol. Eng.*, 42, 373, 2003.
- [59] Çelik, B.G. and Kısakürek, D., *e-Polymers*, 073, 2006.

- [60] Çelik, B.G. and Kısakürek, D., *Designed Monomers and Polymers*, 9, 663, 2006.
- [61] Baştürkmen, M., İşçi, H. and Kısakürek, D., *Polym. Int. J.*, 30, 387, 1993.
- [62] Şanlı, O., Pulat, M. and Kısakürek, D., *Eur. Polym. J.*, 31(12), 1255, 1995.
- [63] Akbaş, M., Bilir, M. and Kısakürek, D., *Macromol. Chem. Phys.*, 199, 169, 1997.
- [64] Aslan, A., M. S. Thesis, 1996.
- [65] Baştürkmen, M., Ph.D. Thesis, 1997.
- [66] Kesici, N., M.S.Thesis, 1997.
- [67] Molu, L.K., Kısakürek, D., *J. Appl. Polym. Sci.*, 86, 2232, 2002.
- [68] Çakmak, O., Baştürkmen, M., Kısakürek, D., *Polymer*, 45, 5451, 2004.
- [69] Çelik, B.G. and Kısakürek, D., *J. Appl. Polym. Sci.*, 102, 5427, 2006.
- [70] Çelik, B.G. and Kısakürek, D., *Designed Monomers and Polymers*, in press.
- [71] Kumar, D. and Sharma, R.C., *Eur Polym J.*, 34, 1053, 1998.
- [72] Gerard, M., Chaubey, A., Malhotra, B.D., *Biosens Bioelectron*, 17, 345, 2002.
- [73] DePaoli, M.A., Waltman, R.J., Diaz, A.F. and Bargon, J., *J. Polym. Sci. Polym. Chem. Ed.*, 23, 1687, 1985.
- [74] Billingham, N.C. and Calvert, P.D., *Electrically Conducting Polymers- Advances in Polymer Science*, 90:1-104, 1989.
- [75] Chiang, C.K., Fincher, C.R., Park, Y.W., Heeger, A.J., Shirakawa, H., Louis, E.J. and MacDiarmid, A.G., *Phys. Rev. Lett.*, 39, 1098, 1977.
- [76] Skotheim, T.A., Elsenbaumer, R.L. and Reynolds, J.R., *Handbook of Conducting Polymers*, Marcel Dekker: New York, 1998.
- [77] Skotheim, T.A., *Handbook of Conducting Polymers*, Marcel Dekker: New York, 1986.
- [78] Chandrasekhar, P., *Conducting Polymers, Fundamentals and Applications*, Kluwer Academic Publishers: Boston, 1999.
- [79] Nalwa, H.S., *Handbook of Conducting Organic Conductive Molecules and Polymers*, John Wiley and Sons: New York, 1987.

- [80] Heeger, A.J., *Chem. Int. Ed.*, 40, 2591, 2001.
- [81] Ito, T., Shirakawa, H. and Ikeda, S., *J. Polym. Sci. Polym. Chem. Edu.*, 12, 11, 1974.
- [82] Heeger, A.J., Kivelson, S., Schrieffer, J. and Su, W.P., *Rev. Mod. Phys.*, 60, 781, 1988.
- [83] Chiang, C.K., Fincher, C.R., Park, Y.W., Heeger, A. J., Shirakawa, H., Louis, E.J., Gau, S.C. and McDiarmid, A.G., *Phys. Rev. Lett.*, 39, 1089, 1977.
- [84] Shirakawa, H., Louis, E.J., Heeger, A.J. and Chiang, C.K., *J. Chem. Soc., Chem. Commun.*, 578, 1977.
- [85] Bredas, J.L. and Silbey, R., *Conjugated Polymers*, 141, 210, 1991.
- [86] Wise, D. L., Wnek, E. G., Trantolo, J. D., Cooper, T. M., Gresser, D. J., *Electrical and Optical Polymer Systems*, Marcell Dekker, New York, (1998).
- [87] Skotheim, T.A. (ed.), *Handbook of Conducting Polymers*, Vol 1 and 2, Marcel Dekker, New York, (1986).
- [88] Springborg, M., *Synt. Met.*, 85, 1037, (1997).
- [89] Kauay, Y., S. Kagoshima, H. Nagasawa, *Synth. Met.*, 9, 369, (1984).
- [90] Shirakawa, H., S. Ikeda, *J. Polym.*, 2, 231, (1971).
- [91] Chen, S.A. and Tsai, C.C., *Macromolecules*, 26, 2234, 1993.
- [92] Mort, N.F., Davis, E.A., *Electronic Processes in Non-Crystalline Materials*, Clarendon Press, Oxford, 1979.
- [93] Hoier, S.N., Park S.M., *J. Phys. Chem.*, 96, 5188, 1992.
- [94] Bredas, J.L., Street, G.B., *Acc. Chem. Res.*, 18, 309, 1985.
- [95] Yoshino, K., Hayashi, R. and Sugimoto, R., *Jpn. J. Appl. Phys.*, 23, 899, 1984.
- [96] Toshima, N. and Hara, S., *Prog. Polym. Sci.*, 20, 155, 1995.
- [97] Yano, J. and Kitani, A., *Synth. Met.*, 69, 117, 1995.
- [98] Dodabalapur, A., Torsi, L. and Katz, H.E., *Science*, 268, 270, 1995.
- [99] Gustafson, J.C., Inganas, O. and Andersson, A.M., *Synth. Met.*, 62, 17, 1994.

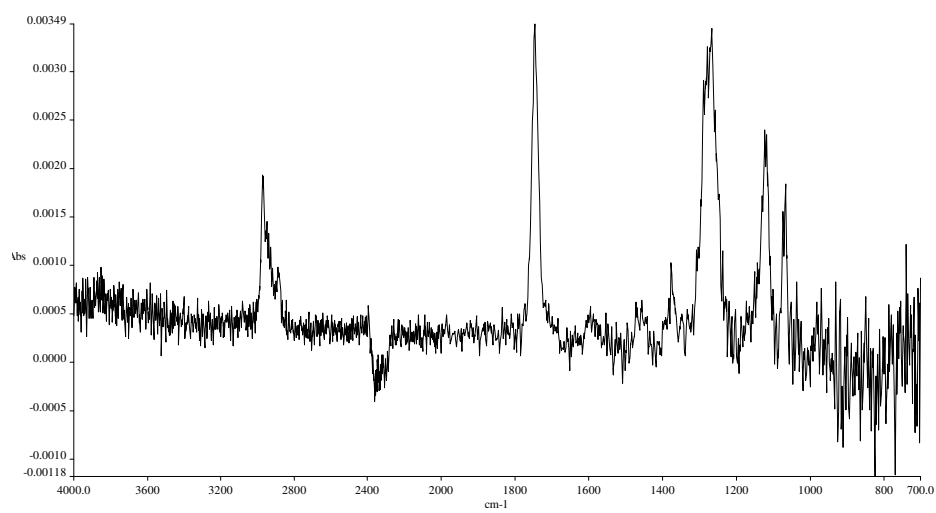
- [100] Kraft, A., Grimsdala, A.C. and Holmes, A.B., *Angew. Chem. Int. Ed.*, 37,402,1998
- [101] Ferraris, J.P., Eissa, M.M., Brotherson, I.D. and Loveday, D.C., *Chem. Mater.*, 10, 3528, 1998.
- [102] Heywang, G. and Jonas, F., *Adv. Mater.*, 4, 116, 1992.
- [103] Bartlett, P.N. and Whitaker, R.G., *J. Electroanal. Chem.*, 224, 37, 1987.
- [104] Foulds, N.C. and Lowe, C.R., *J. Chem. Soc. Faraday Trans.*, 82, 1259, 1986.
- [105] Schuhmann, W., *Microchim. Acta.*, 121, 1, 1995.
- [106] Novak, P., Muller, K., Santhanam, K.S.V. and Hass, O., *Chem. Rev.*, 97, 207, 1997.
- [107] Otero, T.F. and Grande, *Handbook of Conducting Polymers*, 2nd ed., Marcel Dekker, New York, (1998).
- [108] McQuade, D.T., Pullen, A.E. and Swager, T.M., *Chem. Rev.* 100, 2537, 2000.
- [109] Pernaut, J. and Reynolds, J.R., *J. Phys. Chem. B.*, 104, 4080, 2000.
- [110] Sankaran, B., Reynolds, J.R., *Macromolecules*, 30, 2582, 1997.
- [111] Sapp, S.A., Sotzing, J.R. and Reynolds, J.R., *Chem. Mater.*, 10, 2101, 1998.
- [112] IUPAC, Glossary of Basic Terms in Polymer Science, A. D. Jenkins, P. Kratochvíl, R. F. T. Stepto, and U. W. Suter, *Pure Appl. Chem.*, 68, 2287 1996.
- [113] Walker, K.A., Markoski, L.J., Deete, G.A., Spilman, G.E., Martin, D.C. and Jeffrey S. Moore, J.S., *Polymer*, 35, 5012,1994.
- [114] McGinnes,D., *Kirk-Othmer Encyclopedia of Chemical Technology*, 3rd edition, Wiley Interscience, Newyork, 607-624, 1982.
- [115] Hoboken, N.J.: *Encyclopedia of Polymer Science and Technology*, 3rd edition Wiley-Interscience, c2003-c2004.
- [116] Stevens, P.M., *Polymer Chemistry*, 85, 86
- [117] Dusek, K. and M. Duskova, M., *Prog. Polym. Sci.*, 25, 1215, 2000.
- [118] Dusek, K., Network formation. In: Meijer HEH, editor. *Processing of*

Polymers, Material Science and Technology, vol. 13. Weinheim: Verlag Chemie, 401, 1997.

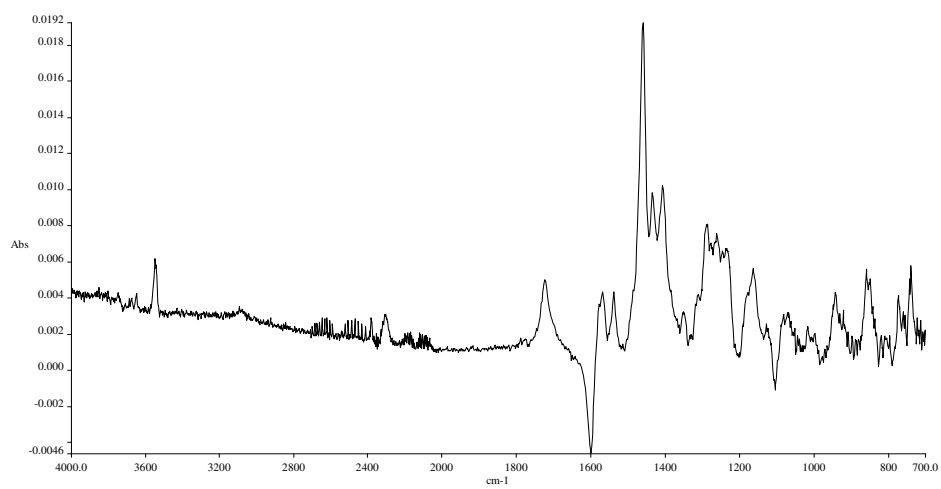
[119] Wang, Z., Jiang, D.D., McKinney, M.A. and Wilkie, C.A., *Polym. Degrad. Stab.* 64, 387, 1999.

APPENDIX A

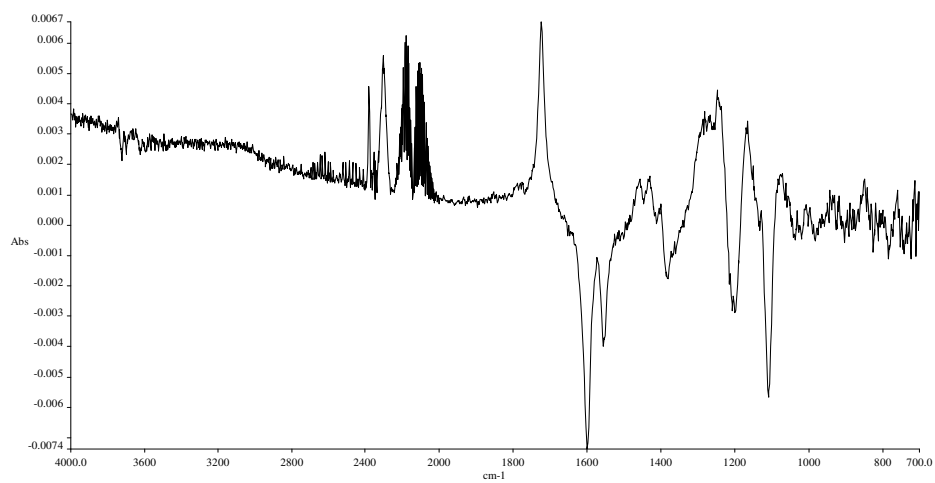
a)



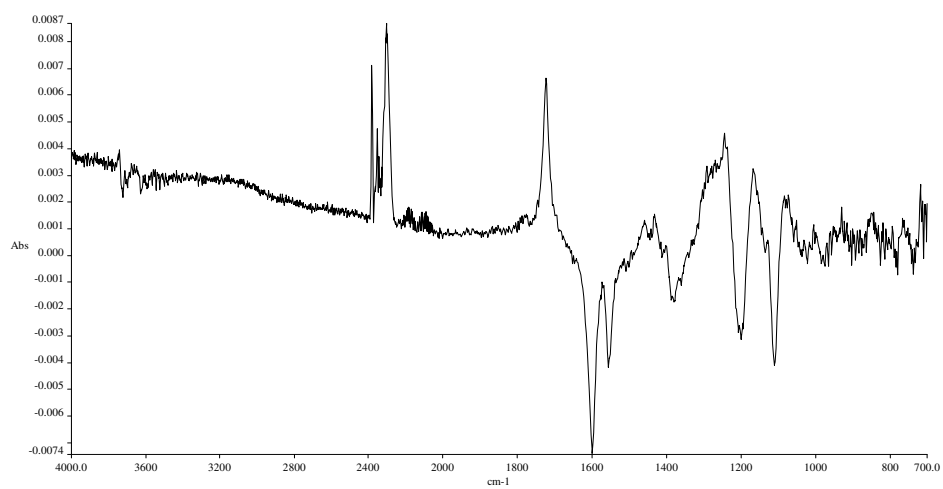
b)



c)



d)



e)

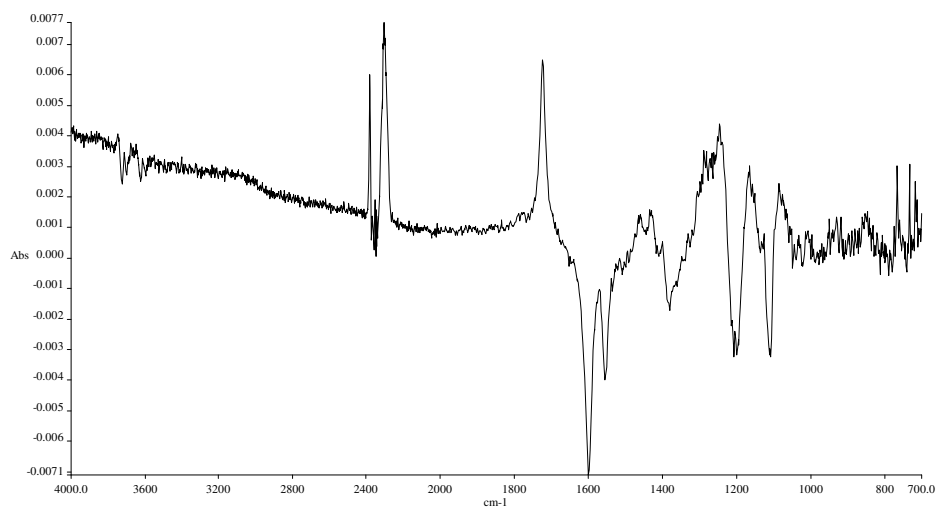
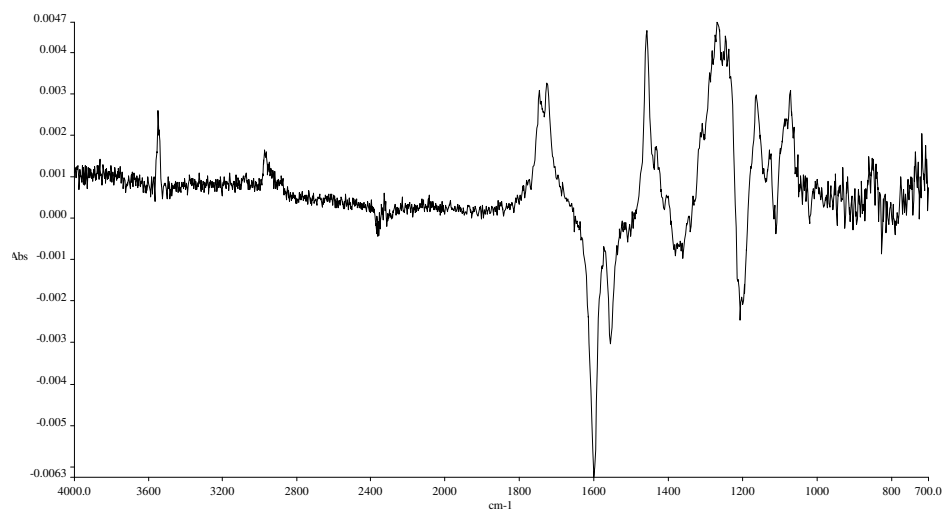
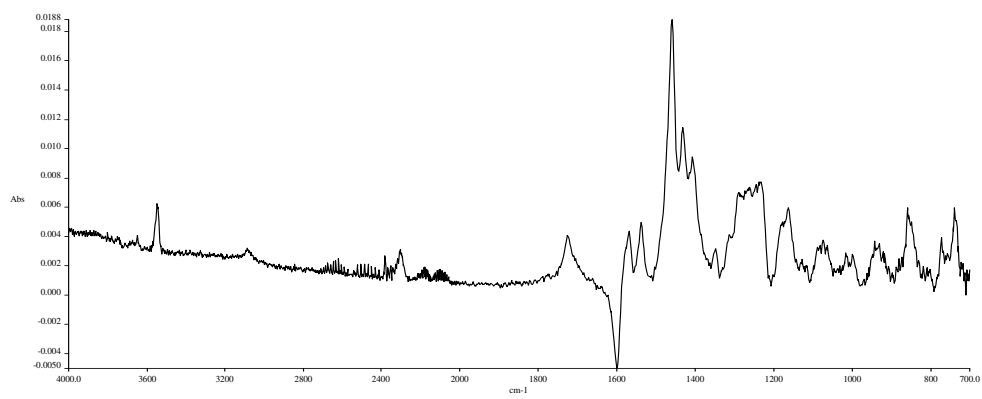


Figure A 1. In situ FTIR spectrum of evolved volatile components during TGA of **P** synthesized from sodium 2,4,6-tribromophenolate at (a) 177 °C (b) 497 °C (c) 629 °C (d) 707 °C (e) 805 °C

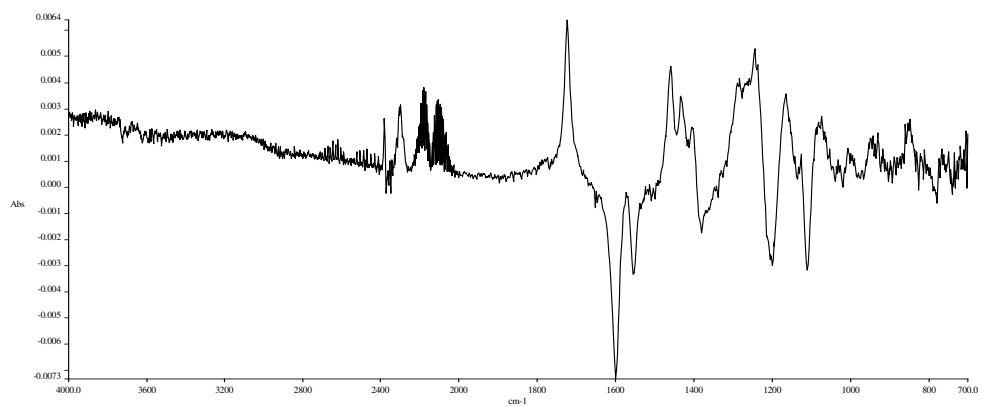
a)



b)



c)



d)

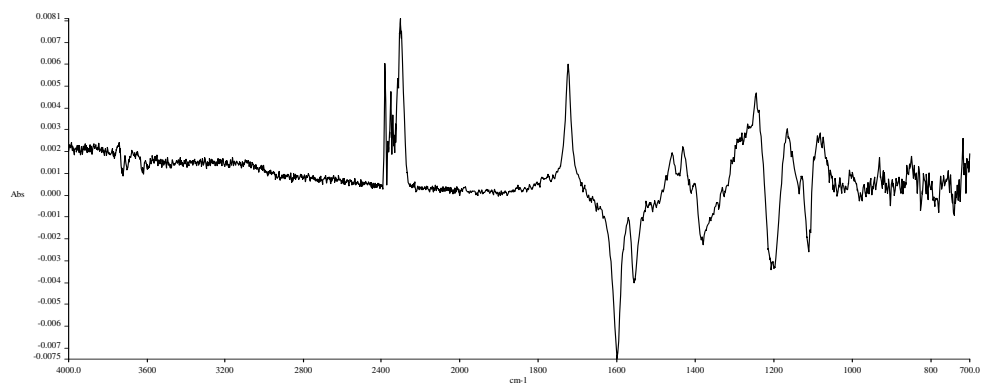
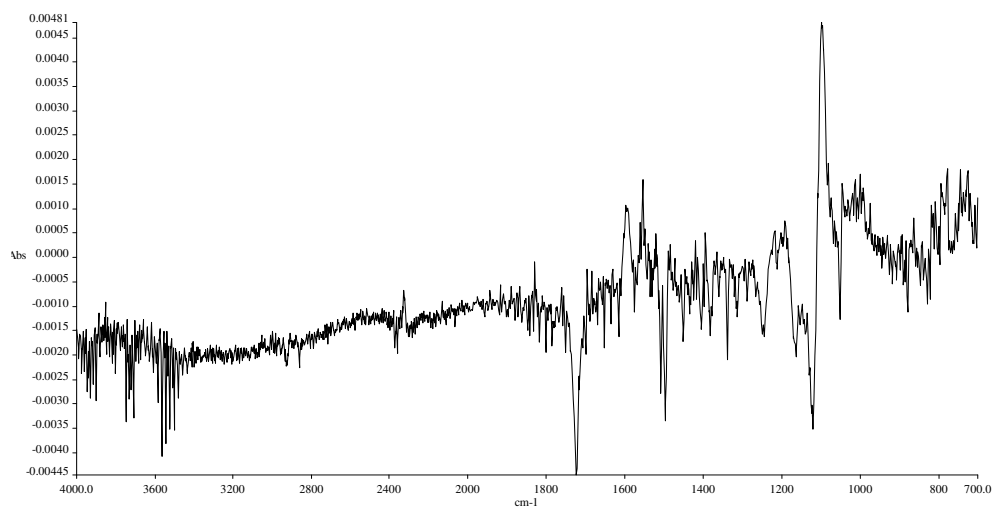
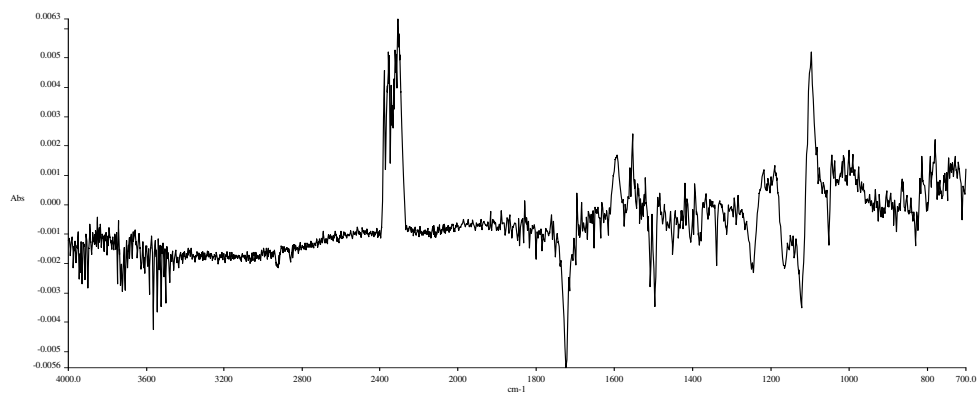


Figure A 2. In situ FTIR spectrum of evolved volatile components during TGA of **RIP** synthesized from sodium 2,4,6-tribromophenolate at (a) 156 °C (b) 493 °C (c) 594 °C (d) 803 °C.

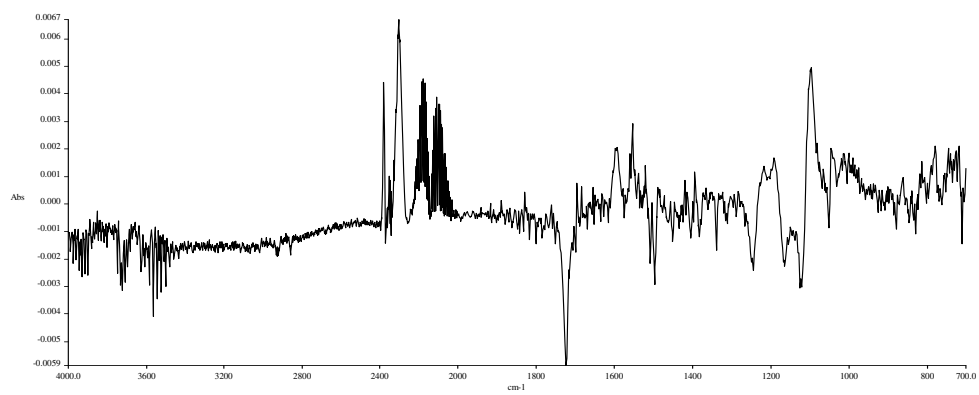
a)



b)



c)



d)

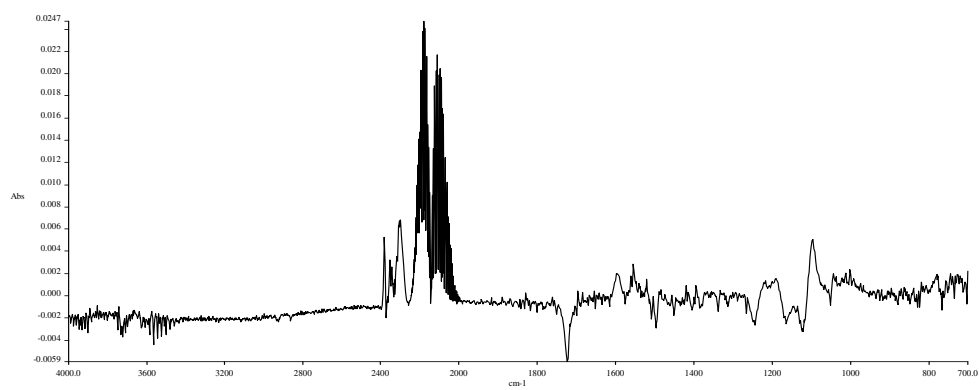
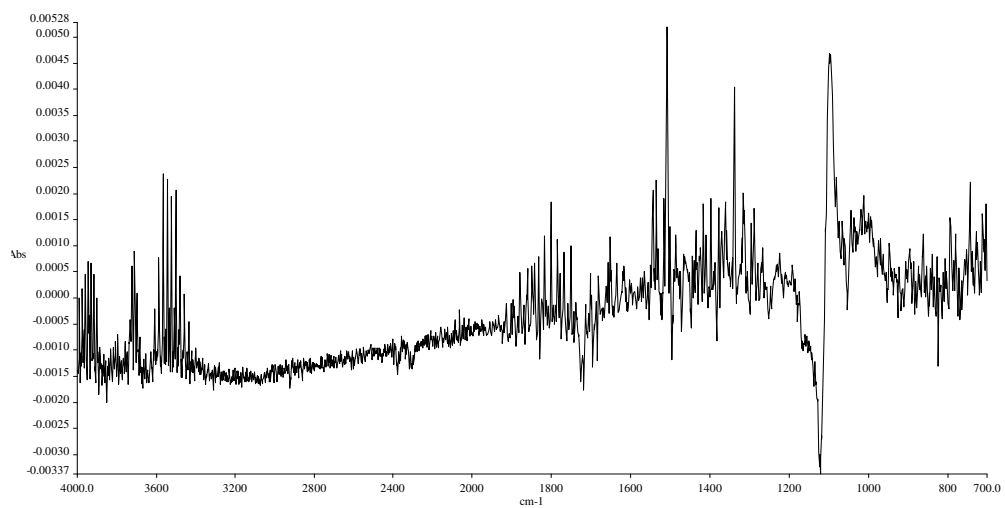
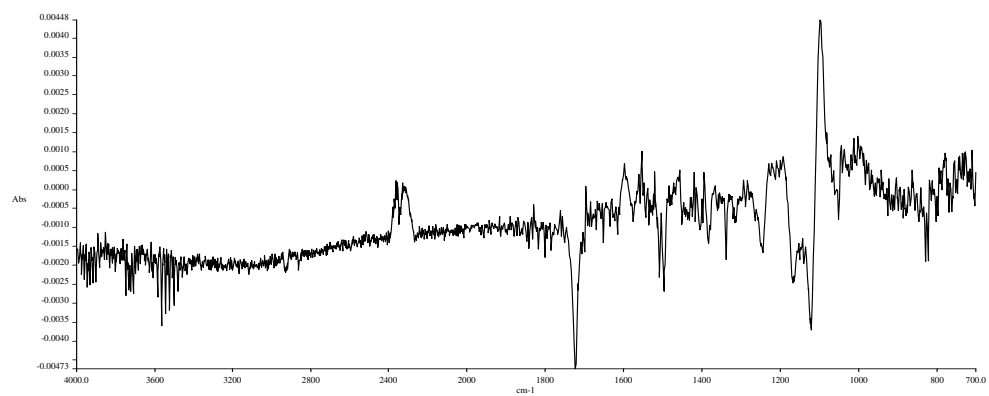


Figure A 3. In situ FTIR spectrum of evolved volatile components during TGA of CP synthesized from sodium 2,4,6-tribromophenolate at (a) 185 °C (b) 421 °C (c) 664 °C (d) 803 °C.

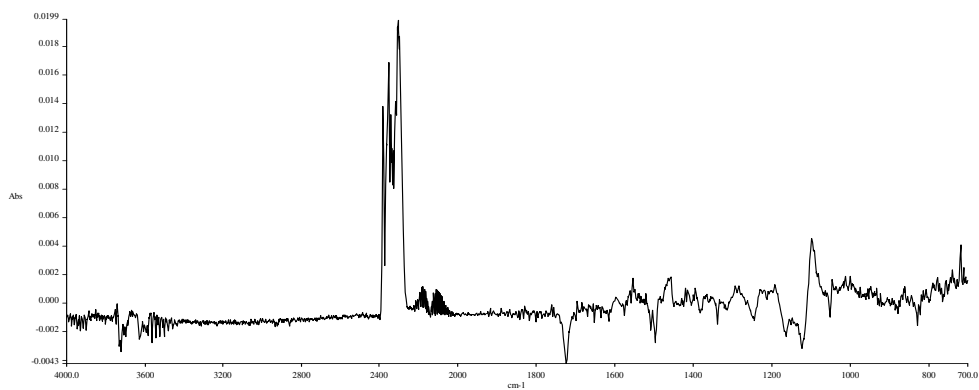
a)



b)



c)



d)

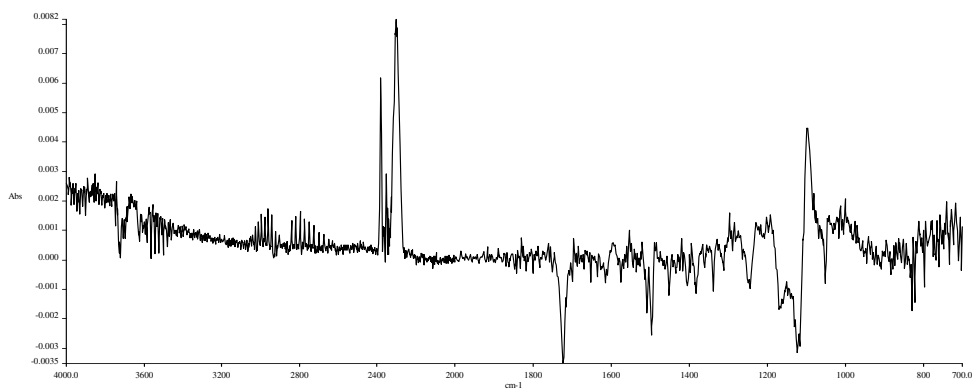


Figure A 4. In situ FTIR spectrum of evolved volatile components during TGA of CLP synthesized from sodium 2,4,6-tribromophenolate at (a) 45 °C (b) 397 °C (c) 562 °C (d) 767 °C.

CURRICULUM VITAE

PERSONAL INFORMATION

Surname, Name: Çelik, Güler
Nationality: Turkish (TC)
Date and Place of Birth: 12 January 1976, İzmir
Marital Status: Married
Phone: +90 312 815 43 00
Email: guler.celik@taek.gov.tr

EDUCATION

Degree	Institution	Year of Graduation
MS	METU Chemistry	2001
BS	METU Chemistry Education	1998
High School	Karataş High School, İzmir	1993

WORK EXPERIENCE

Year	Place	Enrollment
2006-Present	TAEK	Chemist
1999-2006	METU Department of Chemistry	Research Assistant

FOREING LANGUAGES

Advanced English

PUBLICATIONS

1. Çelik, B.G. and Kısakürek, D., *e-Polymers*, 073, 2006.
2. Çelik, B.G. and Kısakürek, D., *Designed Monomers and Polymers*, 9, 663, 2006.
3. Çelik, B.G. and Kısakürek, D., *J. Appl. Polym. Sci.*, 102, 5427, 2006.
4. Çelik, B.G. and Kısakürek, D., *Designed Monomers and Polymers*, in press.